

USING THE NEURAL NETWORK ALGORITHMS TO ESTIMATE THE  
THERMAL STRESSES OF POWER ELECTRONIC DEVICES AS FUNCTION  
OF DESIGN PARAMETERS

A THESIS SUBMITTED TO  
THE BOARD OF GRADUATE PROGRAMS  
OF  
MIDDLE EAST TECHNICAL UNIVERSITY, NORTHERN CYPRUS CAMPUS

BY

NEMER NASSIR ALI ODEH

IN PARTIAL FULFILLMENT OF THE REQUIREMENTS  
FOR  
THE DEGREE OF MASTER OF SCIENCE  
IN ELECTRICAL AND ELECTRONICS ENGINEERING PROGRAM

AUGUST 2021



Approval of the Board of Graduate Programs

---

(Title and Name)

Chairperson

I certify that this thesis satisfies all the requirements as a thesis for the degree of Master of Science

---

(Title and Name)

Program Coordinator

This is to certify that we have read this thesis and that in our opinion it is fully adequate, in scope and quality, as a thesis for the degree of Master of Science.

---

(Title and Name)

Supervisor

**Examining Committee Members** (first name belongs to the chairperson of the jury and the second name belongs to supervisor)

(Title and Name, Jury Chair)      Affiliation/Prog. \_\_\_\_\_

(Title and Name, Jury Chair)      Affiliation/Prog. \_\_\_\_\_

(Title and Name, Jury Chair)      Affiliation/Prog. \_\_\_\_\_

**I hereby declare that all information in this document has been obtained and presented in accordance with academic rules and ethical conduct. I also declare that, as required by these rules and conduct, I have fully cited and referenced all material and results that are not original to this work.**

Name, Last name : Nemer, Odeh

Signature :

## **ABSTRACT**

# **USING THE NEURAL NETWORK ALGORITHMS TO ESTIMATE THE THERMAL STRESSES OF POWER ELECTRONIC DEVICES AS FUNCTION OF DESIGN PARAMETERS**

Odeh, Nemer

Master of Science, Electrical and Electronics Engineering Program  
Supervisor: Asst. Prof. Dr. Canraş Batunlu

August 2021, 117 pages

The demand for high power rating applications is increasing rapidly. The essential components needed to fulfill these demands are power electronic devices and circuits such as IGBTs, diodes, rectifiers, inverters, and DC-DC converters. However, these components usually are sensitive to parameter changes and can face significant failures if we don't examine our system component's reliability well. The traditional approaches to calculating the failure-tolerant capability in power electronic systems are redundancy designs, which select the individual components in the circuits with sufficient thermal and electrical stress margin, thus expecting their low failure rates and, consequently, high reliability of the overall reliability system.

This work will try to involve neural network technology in reliability topics by building a model that can estimate the device's thermal stress as a function of the design parameters and predict the remaining lifetime. The solar and wind profiles of a solar-wind hybrid renewable system, which would be constructed in METU-NCC campus, will be used to estimate the junction temperature of discrete IGBTs automatically and use this estimation to enhance the lifetime of the inverters by using a controller that prevents the system from working under high frequencies when possible extreme junction temperatures may occur, the thing that can lead to a four-times reduction in the lifetime consumption of power electronics inverters.

**Keywords:** reliability analysis, power electronics, neural networks, artificial intelligence, thermal networks.

## ÖZ

# GÜC ELEKTRONİĞİ CİHAZLARININ TERMAL STRES PARAMETRELERİNİ SİNİR AĞI ALGORİTMALARINDA KULLANARAK ÖMÜR SÜRESİ TAHMİNİ MODELLEMESİ

Odeh, Nemer  
Yüksek Lisans, Elektrik ve Elektronik Mühendisliği  
Tez Yöneticisi: Dr. Öğr. Üyesi Canraş Batunlu

Ağustos 2021, 117 sayfa

Yüksek güç uygulamalarındaki artan talebe bağlı olarak, güç elektroniği cihazları ve devreleri, bu talepleri karşılamak için günden güne yeni teknolojiler barındırmak zorundadırlar. IGBT'ler, diyonotlar, doğrultucular, invertörler ve DC dönüştürücüler bu bileşenlere verilebilecek cihaz örnekleridir. Bu cihazlar, genellikle değişen çalışma ortamı parametrelerine duyarlı olup, bu değişkenlerin tasarım sırasında dikkate alınmaması büyük bozulmalara neden olabilir.

Bundan dolayı, sistem bileşenlerinin güvenilirliğini iyi incelenmelidir. Geleneksel yaklaşımalarla güç elektroniği sistemlerinde arıza toleranslı yeteneğini hesaplamak artık zorlaşmıştır. Tasarımlar ve devrelerdeki münferit bileşenlerin yeterli düzeyde seçilmesi, termal ve elektriksel stres marji analizleri, düşük arıza oranlarını mümkün kılabilir. Bu çalışmada, bir model oluşturulup, sinir ağı teknolojisi kullanımı ile bir güvenilirlik analizi yapılmıştır.

Tasarım parametrelerinin bir fonksiyonu olarak, cihazların termal stresini ve kalan ömrünü tahmin edebilecek şekilde bir model geliştirilmiştir. Bu model, işletim sisteminin rüzgar profilini Kullanacak ve ODTÜ-KKK' nde kurulacak güneş-rüzgar hibrit yenilenebilir sistem yerleşkesi için bir ömür süresi analizi çalışmasını mümkün kılacaktır.

**Anahtar Kelimeler:** güvenilirlik analizi, güç elektroniği, sinir ağları, yapay zeka, termal ağlar.

To my wife

For her unconditional love, patience and inspiration

## **ACKNOWLEDGMENTS**

I would like to give my first and foremost appreciation to my supervisor, Assist. Prof. Dr. Canras Batunlu for his encouragement, powerful and expert advices through every step of my research and master studies. His constant trust and assistance inspired me in the most important moments making the right decision, and I'm glad that I have worked with him.

I would also like to acknowledge Middle East Technical University Northern Cyprus Campus, Campus Research Funds BAP-FEN-2 and sBAP- FEN-12-D-1 which provided financial support for solar and wind measurement stations, this acknowledge mainly goes for Assoc. Prof. Dr. Murat Fahrioglu, the coordinator of EEE department at MATU NCC and Assoc. Prof. Dr. Onur Taylan from the mechanical engineer department at METU NCC.

I am also grateful to the members of faculty of electrical and electronics engineering for all their support and the things they taught me: Prof. Dr. Ali Muhtaroglu , Assoc. Prof. Dr. Cem Direkoglu, Instructor Dr. Gurtag Yemiscioglu, and Assoc. Prof. Dr. Tayfun Nesimoglu.

My special thanks goes to my loving wife without whom this achievement was not possible, I also want to thank all my friends and teaching assistants at METU NCC for providing a pleasant environment to pursue my research studies during TA duties.

## TABLE OF CONTENTS

ABSTRACT .....	v
ÖZ .....	vi
ACKNOWLEDGMENTS .....	viii
TABLE OF CONTENTS.....	ix
LIST OF TABLES .....	xii
LIST OF FIGURES .....	xiii
CHAPTERS	
1 INTRODUCTION AND BACKGROUND .....	1
1.1 Background .....	1
1.2 Electricity Generation .....	3
1.2.1 Electricity Generation from Solar Energy .....	3
1.2.2 Electricity Generation from Wind Energy .....	7
1.2.3 Electricity Generation from Hybrid Wind & Solar Energy .....	10
1.3 Electrical Power Converters.....	10
1.3.1 Rectifiers .....	11
1.3.2 Inverters .....	12
1.3.3 Choppers .....	15
1.3.4 AC to AC Converters.....	18
1.4 Filters.....	18
1.4.1 Active Filters.....	18
1.4.2 Passive Filters .....	19
1.4.3 Hybrid Filters .....	20
1.5 Thermal Power Loss Modeling of Power Electronics Converters.....	20

1.6	Reliability Modeling and Lifetime Analysis .....	22
1.7	Neural Networks Models .....	23
1.8	Problem Statement.....	24
1.9	Thesis Organization .....	25
<b>2</b>	<b>LITERATURE REVIEW .....</b>	<b>27</b>
2.1	Condition Monitoring of Power Electronics Circuits .....	27
2.2	Lifetime Analysis for Discrete IGBT Devices .....	28
2.3	Using Neural Networks Algorithms in the Lifetime Analysis of Discrete IGBT Devices.....	32
2.4	Using the Artificial Intelligence in Automating and Enhancing the Reliability Designs of Discrete IGBTs .....	34
2.5	Gap in the Literature .....	37
<b>3</b>	<b>METHODOLOGY .....</b>	<b>39</b>
3.1	Solar Panel Modelling .....	39
3.2	Wind Turbine Modelling .....	40
3.3	DC to DC Converter Modelling for Input Power Regulation.....	41
3.4	Wind Maximum Power Point Tracking.....	42
3.5	2-Levels Power Inverter Modelling .....	43
3.6	Thermal Network of Discrete IGBT Modelling .....	43
3.7	Neural Network Modelling .....	45
3.8	Inverter Control Modelling .....	46
3.9	Passive Filter Modelling .....	47
3.10	Overall Design and Methodology .....	48
<b>4</b>	<b>RESULTS AND DISCUSSION .....</b>	<b>51</b>

4.1	Power Generated from Solar Panels.....	51
4.2	Power Generated from Wind Turbine Model .....	52
4.3	Generated Power from the Hybrid Combination of Solar and Wind Power Plants	54
4.4	DC-Link Voltage.....	55
4.5	Junction Temperature Calculation using Thermal Modelling.....	56
4.5.1	DC-Link Voltage Effect on the Junction Temperature .....	57
4.5.2	Carrier Frequency Effect on the Junction Temperature.....	58
4.5.3	Ambient Temperature Effect on the Junction Temperature.....	59
4.6	Neural Networks Training Criteria.....	60
4.7	Lifetime Analysis Results .....	63
4.8	Carrier Frequency and Filtering Effects on the Output Signal Quality....	64
5	CONCLUSION AND FUTURE WORK.....	68
5.1	Conclusion.....	68
5.2	Future Work .....	68
	REFERENCES .....	71
	APPENDICES .....	74
A.	Generated Dataset for ANN1 .....	74
B.	Generated Dataset for ANN2 .....	85

## **LIST OF TABLES**

Table 2.1. Forecast result of (Rosmaliati, 2018) for predicting the transformer lifetime using Nguyen Widrow neural networks.....	34
Table 4.1. Comparison between simulated and predicted results using some mission profiles operating points done by (Taylan,2018) .....	62
Table 4.2. Financial summary of 2 solutions that can enhance the output voltage quality of an inverter .....	66

## LIST OF FIGURES

Figure 1-1. Net consumption of electricity worldwide in select years from 1980 to 2018.....	1
Figure 1-2. General structure of power system.....	2
Figure 1-3. Energy sources cubes .....	4
Figure 1-4. Earths orbital distance from the sun.....	4
Figure 1-5. Air Mass definition.....	5
Figure 1-6. An example for the solar constant energy distribution inside the atmosphere .....	5
Figure 1-7. Photoelectric effect.....	6
Figure 1-8. Equivalent circuit of a real solar cell.....	6
Figure 1-9. I-V characteristics of the solar cell equiavlent circuit in addition to the power curve.....	7
Figure 1-10. Generalized global wind patterns .....	8
Figure 1-11. Wind turbine rotor .....	8
Figure 1-12. Typical wid turbine power output with steady wind speed.....	9
Figure 1-13. Direct drive permanent magnet synchronous generator wind turbine energy conversion principle scheme.....	9
Figure 1-14. A basic solar/wind hybrid energy system .....	10
Figure 1-15. Block diagram of a rectifier .....	11
Figure 1-16. Half-wave rectifier concept.....	11
Figure 1-17. Full-wave bridge rectifier concept .....	12
Figure 1-18. One leg switch mode inverter.....	13
Figure 1-19. PWM technique concept .....	13
Figure 1-20. Square wave switching.....	14
Figure 1-21. Single phase half bridge inverter.....	15
Figure 1-22. Step-down converter .....	16
Figure 1-23. Output voltage ripple of a step-down converter.....	16

Figure 1-24. Step-up DC-DC converter .....	16
Figure 1-25. Step-up converter output voltage ripple.....	17
Figure 1-26. Buck-boost converter.....	17
Figure 1-27. Topology of (regenerative) voltage-source inverter AC/DC-AC converter.....	18
Figure 1-28. Active filters based on op-amps .....	19
Figure 1-29. Passive low pass filter.....	19
Figure 1-30. Single-phase hybrid filter (including two passive filters) as a combination of (a) passive-series and passive-shunt filters, (b) passive-shunt and passive-series filters.....	20
Figure 1-31. Equivalent thermal model of Cauer network .....	21
Figure 1-32. Equivalent thermal model of Foster network .....	21
Figure 1-33. Equivalent thermal model of eighth-order system using Cauer network .....	22
Figure 1-34. Equivalent thermal model Foster networks .....	22
Figure 1-35. A simple neural network.....	24
Figure 2-1. Schematic diagram of training the NN .....	27
Figure 2-2. Actual and estimated values of the normalized output voltage ripple of a power electronics circuit under normal operating conditions (Mohagheghi, 2009). .....	28
Figure 2-3. Scheme of lifetime consumption study made by (Albarbar and Batunlu in 2018).....	29
Figure 2-4. Lifetime curves for Albarbar and Batunlu study in 2018 .....	29
Figure 2-5. Proposed reliability prediction procedure for power electronic systems (Wang, 2009).....	30
Figure 2-6. Structural details of an IGBT module (Wang, 2009). .....	30
Figure 2-7. Cycle to failure models for different layers of the IGBT device (Wang, 2009).....	30
Figure 2-8. Reliability prediction process of the design for reliability (DfR) approach for power electronic systems, where $\beta x$ is the lifetime (Yang, 2008)....	31

Figure 2-9. The flowchart of the improved fireworks algorithm (Pang, 2009). ....	32
Figure 2-10. The general topology of the GNN model (Pang, 2009). ....	33
Figure 2-11. The comparison of prediction value using GM (1, 5) dimension with actual value of an electrical relay (Pang, 2009). ....	33
Figure 2-12. Backpropagation network architecture (Rosmaliati, 2018).....	34
Figure 2-13. Flow diagram of the proposed artificial intelligence by (Dragicevic, 2018) based design optimization of the power electronic system. ....	35
Figure 2-14. The relation between yearly lifetime consumption with the size of inductors according to the (Dragicevic, 2018) study.....	36
Figure 2-15. Flow diagram of the mission profile-based lifetime evaluation of PV inverters considering the PV panel degradation done by (Sanwongwanich, 2017)	36
Figure 3-1. Structure of solar panel model. ....	39
Figure 3-2. PV characteristics for the solar panel model under two different ambient temperatures. ....	40
Figure 3-3. Generated power by the solar model from 500 W/m <sup>2</sup> irradiance input. .....	40
Figure 3-4. Structure of wind turbine model that uses PMSG.....	41
Figure 3-5. Turbine power characteristics .....	41
Figure 3-6. Structure of 100 Vdc DC-to-DC converter .....	42
Figure 3-7. Structure of wind MPPT .....	42
Figure 3-8. Structure of 2-levels 6 IGBTs inverter.....	43
Figure 3-9. Foster thermal network of a discrete IGBT .....	44
Figure 3-10. Power loss model for a discrete IGBT .....	44
Figure 3-11. Structure of ANN1 .....	45
Figure 3-12. Structure of ANN2 .....	45
Figure 3-13. Proposed neural network model that controls the carrier frequency for the inverter to keep the temperature below pre-defined limit.....	46
Figure 3-14. Structure of the inverter controller .....	46
Figure 3-15. Structure of PWM generator model .....	47
Figure 3-16. Structur of the low-pass passive filter modelling.....	47

Figure 3-17. The overall design of the proposed system.....	49
Figure 3-18. Proposed methodology to enhance the lifetime reliability of power electronics devices .....	49
Figure 4-1. 0 W Power generated from the solar panels at 0 W/m <sup>2</sup> irradiance. ....	51
Figure 4-2. 3000 W Power generated from the solar panels at 500 W/m <sup>2</sup> irradiance. ....	52
Figure 4-3. 10000 W Power generated from the solar panels at 1000 W/m <sup>2</sup> irradiance. ....	52
Figure 4-4. 0 W generated from the wind turbine under 0 m/s wind speed .....	53
Figure 4-5. 2750 W generated from the wind turbine under 9 m/s wind speed .....	53
Figure 4-6. 10000 W generated from the wind turbine under 18 m/s wind speed ..	53
Figure 4-7. Generated power when the solar panel is on and the wind turbine is off .....	54
Figure 4-8. Generated power when the solar panel is off and the wind turbine is on .....	54
Figure 4-9. Generated power when both plants are on.....	55
Figure 4-10. DC-link voltage when the solar panel is on and the wind turbine is off .....	55
Figure 4-11. DC-link voltage when the solar panel is off and the wind turbine is on .....	56
Figure 4-12. DC-link voltage when both plants are on but the solar panel has the dominant energy production.....	56
Figure 4-13. Junction temperature response for the 200 V Vdc case.....	57
Figure 4-14. Junction temperature response for the 508 V Vdc case.....	57
Figure 4-15. Junction temperature response for the 2000 Hz carrier frequency case .....	58
Figure 4-16. Junction temperature response for the 10000 Hz carrier frequency case .....	58
Figure 4-17. Junction temperature response for the 0 C ambient temperature case	59

Figure 4-18. Junction temperature response for the 20 C ambient temperature case .....	59
Figure 4-19. Generating the dataset for ANN1 .....	60
Figure 4-20. Generating the dataset for ANN2.....	61
Figure 4-21. Training stage of ANN1 .....	61
Figure 4-22. Training stage of ANN2.....	62
Figure 4-23. Yearly mission profiles of solar irradiance, wind speed, and ambient temperature from the REDAR search group at METU NCC .....	63
Figure 4-24. Relation between the frequency and the yearly lifetime consumption .....	64
Figure 4-25. 3 phase output voltage for 2000 Hz carrier frequency, 36 mH and 8 uF LC filter components .....	64
Figure 4-26. 3 phase output voltage for 2000 Hz carrier frequency, 36 mH and 25 uF LC filter components .....	65
Figure 4-27. 3 phase output voltage for 15000 Hz carrier frequency, 36 mH and 8 uF LC filter components .....	66
Figure 5-1. 3 phase output voltage within a battery integrated system for 15000 Hz carrier frequency, 36 mH and 8 uF LC filter component.....	69



# CHAPTER 1

## INTRODUCTION AND BACKGROUND

### 1.1 Background

Global electricity consumption has increased rapidly in the recent years, according to the U.S. Energy Information Administration, 2021, the global electricity consumption has jumped from 7323 billion kWh in 1980 to 23398 billion kWh in 2018 as shown in Figure 1-1 and it is expected to be increased more and more in the coming years.

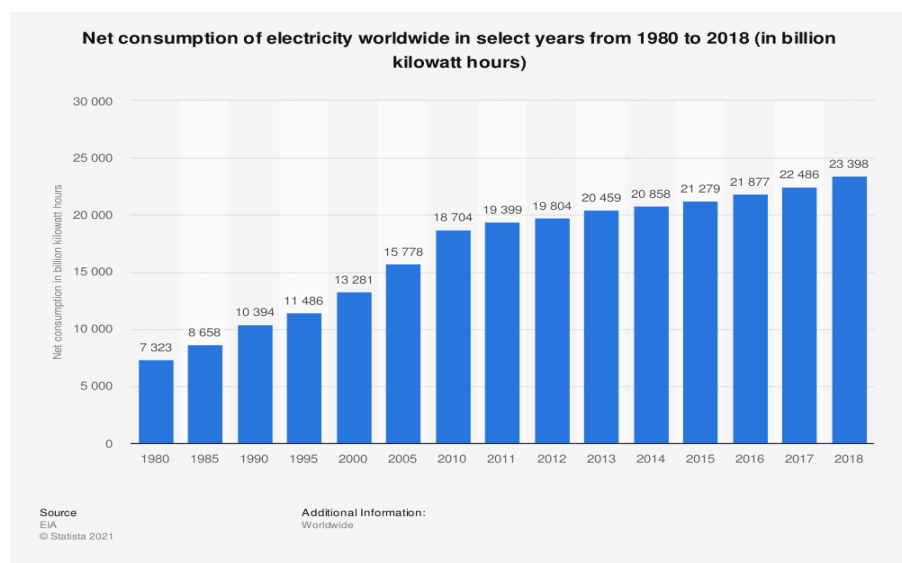


Figure 1-1. Net consumption of electricity worldwide in select years from 1980 to 2018

The main reason for this upward trend can be referred to the industrial activity and advances in both developing and developed countries, however, there were several implied factors that managed to help increasing the electricity demand, like the ease of transporting this type of energy from the source (power generators) to the

consumers (loads) using very tight and efficient electrical transmitting and distribution systems.

In Figure 1-2 we can see the general structure of an electrical power system, where the electricity is produced through a power plant, then it goes through a step-up transformer in order to increase the transmitted voltage and reduce the transmitted current and hence, reducing the transmission power loss, and after the energy passes through the transmission system, it goes through several step-down transformers (depending on the load demand) in order to restore most of the generated power back and consume it.

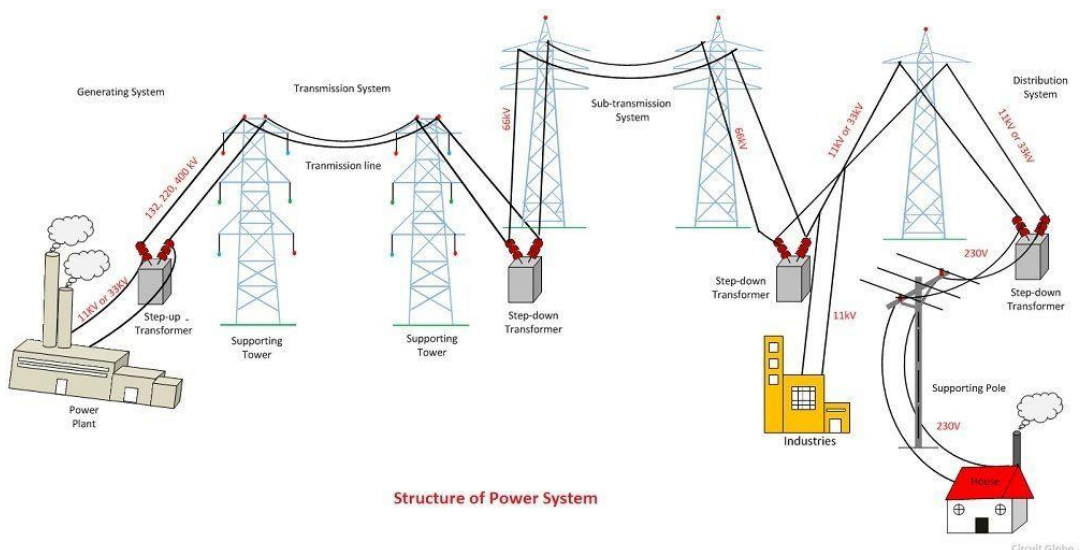


Figure 1-2. General structure of power system

In general, all power system components are designed to deal with the energy as a sine-waveform, because in this type of waveforms we can have the highest energy efficiency possible due to its unique periodic characteristics. Luckily, most of the traditional and most used thermal power plants which use coal, natural gas, heating oil and biomass as a fuel source can automatically generate the electricity in this periodic waveform, however, due to the shortage and the unfavorable effects in these sources, the recent trend of electricity generation is moving towards the renewable sources electricity generation, which mainly use the sun, wind and water as the electricity source, but in these type of generators and due to their rapid fluctuation, they can't produce the energy in the required form directly, and hence,

a solution is required. The most common solution here is to rectify the variable generated power from the renewable source using power rectifiers and after that we can use a sine wave inverter, which can produce a multiple step sinusoidal AC waveform from the dc source. These converters (the rectifier and the inverter) are constructed from semi-conductor power electronic devices, mainly Diodes and IGBTs, which are usually the most expensive components that can be placed in an electrical power system, and hence, they need to work under conditions where we can extend their life time and reduce their operation and maintenance costs in order to enhance the feasibility of the renewable electricity production.

From this point of view, we were inspired to study the reliability of power electronic devices in our work and try to find solutions in order to enhance their lifetime. In order to do so, we used the neural network algorithms (NN) as a tool that helped us to minimize the life span calculations time and complexity, and we used the solar-wind hybrid renewable system placed in the METU-NCC campus as our case study.

## **1.2 Electricity Generation**

As stated earlier, we are focusing in our work on the renewable power plants, mainly the solar and wind power generators, so a brief background on these types of generators in addition to their hybrid combination is discussed in this section.

### **1.2.1 Electricity Generation from Solar Energy**

The sun can be considered as a vast nuclear power plant of the fusion variety and by far the largest energy resource (Gilbert M. Masters, 2004). Annually,  $3.9 \times 10^{24}$  J which is about  $1.08 \times 10^{18}$  kWh of solar energy reaches the surface of the Earth. This is about ten thousand times more than the annual global primary energy demand and much more than all available energy reserves on earth as demonstrated in Figure 1-3.

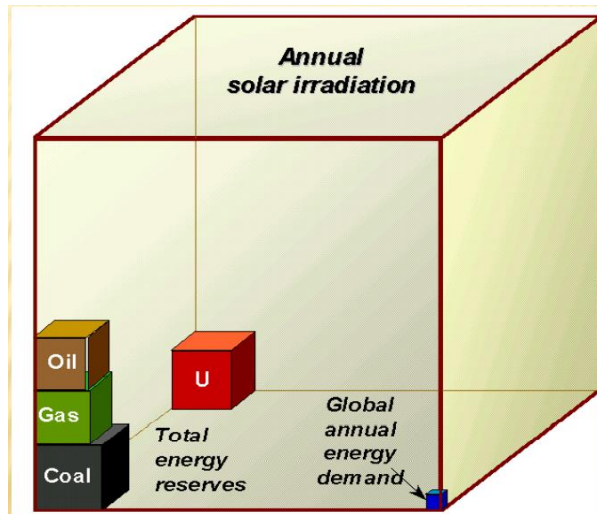


Figure 1-3. Energy sources cubes

The irradiance of the sun at the earth's atmosphere varies between 1325 W/m<sup>2</sup> and 1420 W/m<sup>2</sup> because the distance between the sun and Earth is not constant throughout the year as shown in Figure 1-4.

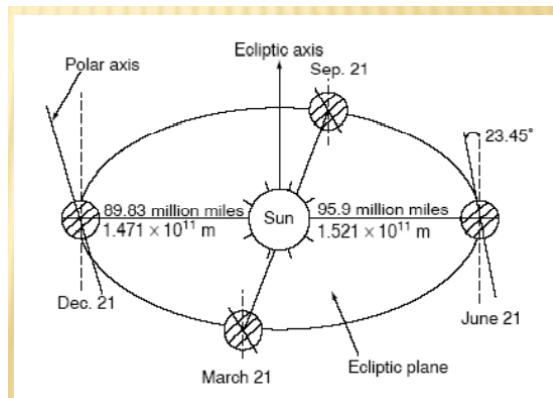


Figure 1-4. Earth's orbital distance from the sun

the average value of this irradiance is called the solar constant  $I_0$  and it is equal to 1367 W/m<sup>2</sup>, which in turn is divided into reflected or scattered solar irradiance by the earth's atmosphere, absorbed irradiance by the air, diffused solar irradiance by the impurities in the air (like clouds), and the direct solar irradiance that reaches the horizontal earth surface. The main factor that determines how the solar constant is divided between all the above-mentioned irradiance forms is the air mass (AM) factor, which is the ratio of the path length of the sun's rays through the atmosphere

when the sun is at a given angle ( $\theta$ ) to the zenith, to the path length when the sun is at its zenith, i.e.,  $AM = L/d = 1/\sin\alpha_s = 1/\cos \theta$ , see Figure 1-5.

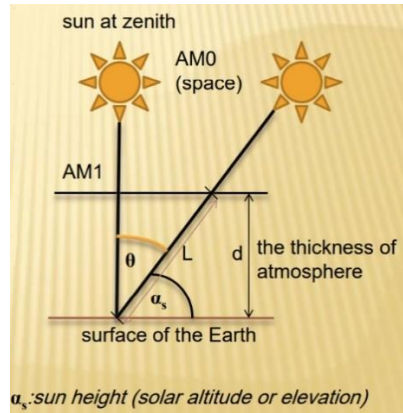


Figure 1-5. Air Mass definition

An example on the solar constant distribution is shown in Figure 1-6 , where the AM outside the atmosphere is equal to 0 and inside the atmosphere is equal to 1 since the the sun is placed vertically on the earth's surface.

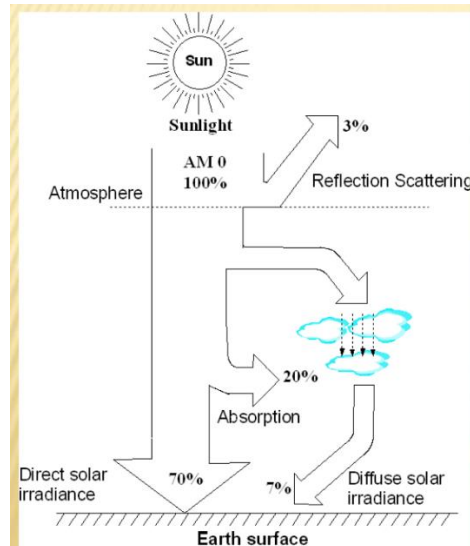


Figure 1-6. An example for the solar constant energy distribution inside the atmosphere

The total (global) irradiance on the earth's surface is equal to the sum of the direct irradiance and the diffuse irradiance on the surface:

$$I_G = I_{dir} + I_{diff}$$

The most common way to convert the global solar irradiance into electricity is by using the photovoltaic (PV) solid-state devices, which are constructed mainly to build a p-n junction, or an equivalent, such as a Schottky junction, to enable the photoelectric effect, which states that when no photons (solar irradiance) impinge on the junction, the p-n junction dissipates power. But when photons are present, the photon-induced current flows opposite to the passive direction. Therefore, current leaves the positive terminal, which means that the device is generating power, see Figure 1-7

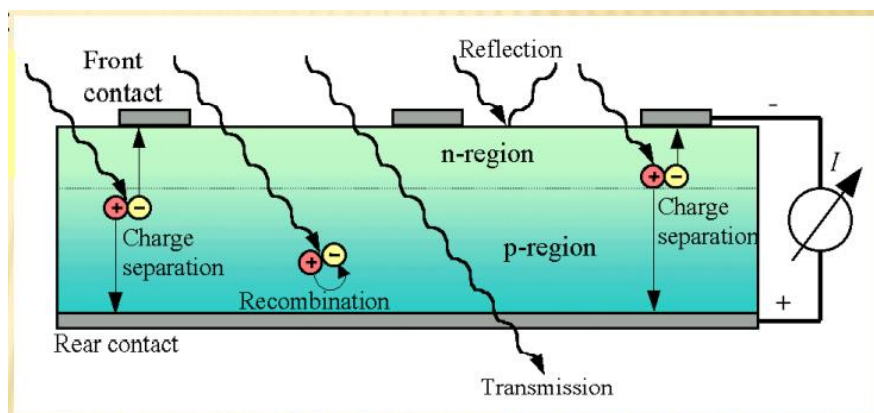


Figure 1-7. Photoelectric effect

This concept allows us to consider an illuminated solar cell as a current source provided with a parallel diode, however, series resistances  $R_s$  (losses in contacts or bulk) and shunt or parallel resistances  $R_p$  (conduction over the surfaces between front and backside, current conduction through junction via defects,...) should also be considered when building the PV cells, this leads to the final equivalent circuit shown in Figure 1-8 which allows us to simulate the solar energy production process.

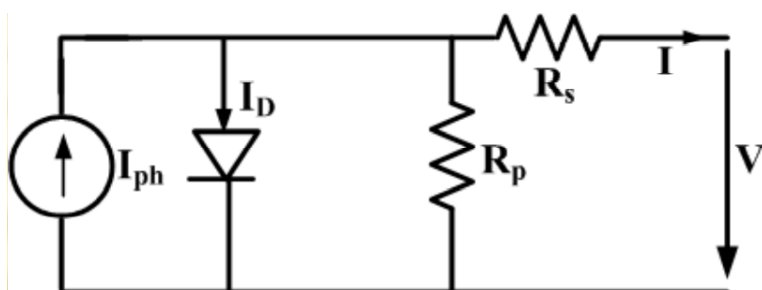


Figure 1-8. Equivalent circuit of a real solar cell

The main target in a solar cell is to produce the maximum energy possible from the solar irradiance, this can be determined using the generated current-voltage (I-V of the equivalent circuit) characteristic curve shown in Figure 1-9 . As we can see from the curve, the maximum power point occurs when the product  $V_{mp} \times I_{mp}$  is at its maximum value, and hence, all the solar plants are designed to follow this point.

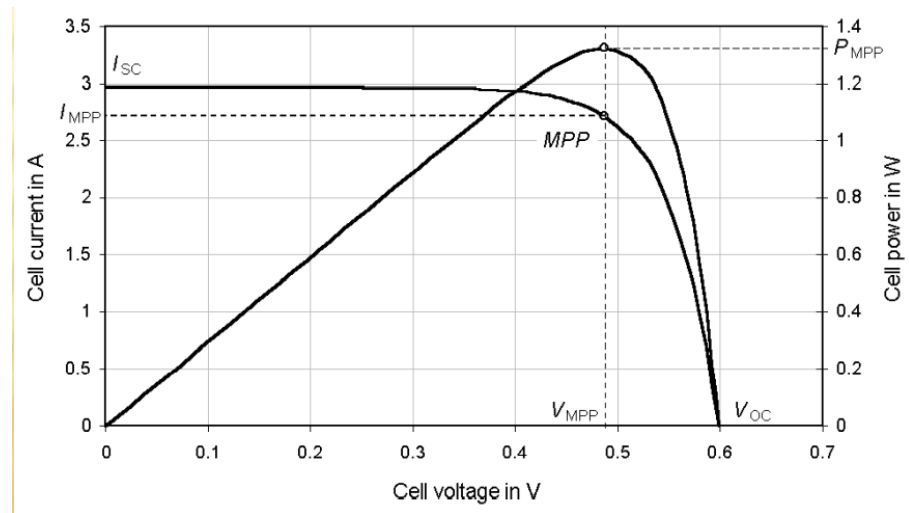


Figure 1-9. I-V characteristics of the solar cell equivalent circuit in addition to the power curve

### 1.2.2 Electricity Generation from Wind Energy

The main reason for air motion (wind) is the variation of the earth's heat caused by solar radiation and earth's rotation, and thus, wind can be considered as a result of indirect solar energy conversion.

Differences in solar radiation absorption at the surface of the Earth and transference back to the atmosphere create differences in atmospheric temperature, density, and pressure, which in turn create forces that move air from one place to another. On the other hand, the earth's rotation gives rise to semi permanent global wind patterns such as trade winds, westerlies, easterlies, and subtropical and polar jet, see Figure 1-10.

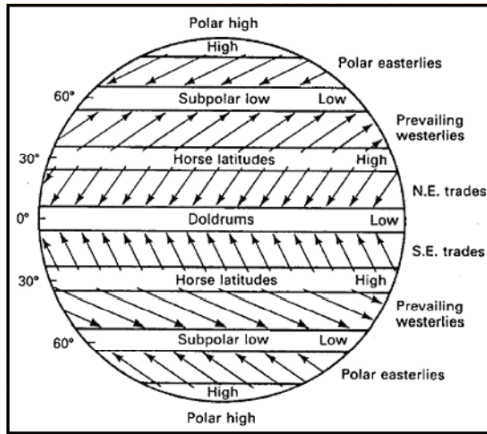


Figure 1-10. Generalized global wind patterns

The importance of wind electricity production is evident in being the cheapest source of renewable energy and is even less expensive than new coal and nuclear power plants. Wind power has grown at around 25% per year for the past few years, and global installation is predicted to reach 240 GW by 2012 in order to be the fastest growing renewable and manage to keep up to the task of producing serious amounts of electricity (Vaughn Nelson, 2009).

Figure 1-11 shows a wind turbine rotor, from this figure we can describe the generated power from the rotor as:

$$P_T = \frac{1}{2} C_p \rho A v^3$$

Where  $C_p$  is called the power coefficient and it is defined to be the percentage of power in the wind that is converted into mechanical energy, the maximum limit of this coefficient is called the Betz limit and it is equal to 0.5926,  $\rho$  is the air density,  $A$  is the cross sectional area, and  $v$  is the wind speed.

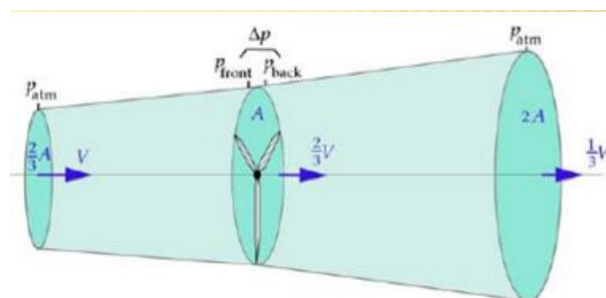


Figure 1-11. Wind turbine rotor

A typical wind speed vs power curve is shown in Figure 1-12, the reason behind this behavior is to follow the energy conservation principle and protect the wind turbine rotor at high wind speeds (higher than cut out speed). The turbine starts to generate the power after the cut in wind speed and reaches the rated output power at the rated wind speed, this results in the wind farms being designed and placed in a location where the rated wind speed is likely to exist in order to generate the available rated power most of the times.

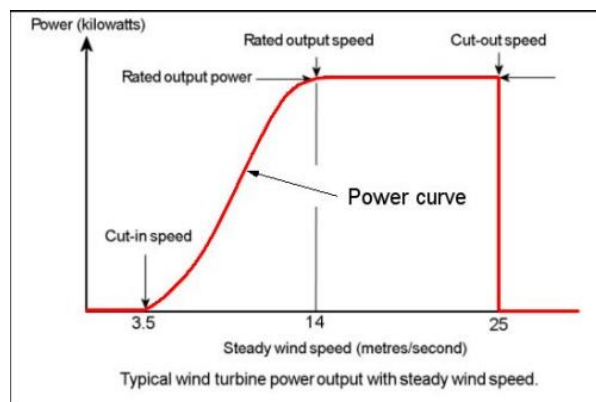


Figure 1-12. Typical wind turbine power output with steady wind speed

The generated power from wind turbine is in the form of mechanical torque, and hence, an electrical generator is used to convert this torque to electricity, permanent magnet synchronous generator (PMSG) is one of the most used and efficient generators in wind farms, the resulted electrical waveform is then followed to an AC/DC converter in order to rectify it, and after that, a DC/AC converter is used to convert the electrical energy into a suitable sinusoidal waveform for the grid. This wind production circuit is shown in Figure 1-13 (Ulutaş, Alper & DURU, Tarık, 2019) where both the rectifier and the converter are controlled by the system parameters.

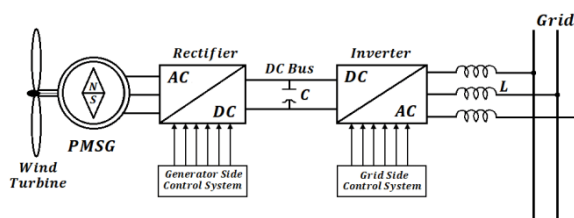


Figure 1-13. Direct drive permanent magnet synchronous generator wind turbine energy conversion principle scheme.

### 1.2.3 Electricity Generation from Hybrid Wind & Solar Energy

Combining wind electricity production with solar electricity production offers many several advantages over either single system, for example, in much of the United States, wind speeds are low in the summer when the sun shines brightest and longest. On the other hand, the wind is strong in the winter when less sunlight is available. Because the peak operating times for wind and solar systems occur at different times of the day and year, hybrid systems are more likely to produce power when you need it (U.S. Department of Energy, 2021).

In order to connect the hybrid solar & wind sources into the grid, an AC/DC converter for the wind generator and a DC/AC converter for the solar panel followed by a DC/AC converter for the combined energy are needed to match and control the generated power with the grid characteristics. An example for such a basic solar/wind hybrid energy system is shown in Figure 1-14.

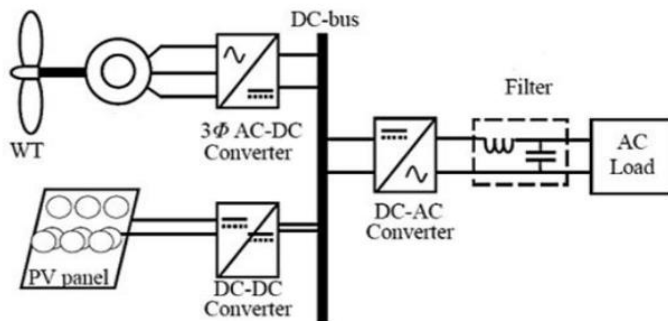


Figure 1-14. A basic solar/wind hybrid energy system

### 1.3 Electrical Power Converters

Mainly, there are 4 types of electrical power electronic converters; from AC to DC (rectifier), from DC to AC (inverter), from DC to DC (chopper), and from AC to AC. In this section we will go through each one of these power converters and explain the principle behind it in a nutshell.

### 1.3.1 Rectifiers

In most of the power electronic applications, the input power to the devices is characterized by a sine wave ac voltage which has 50 or 60 Hz line frequency supplied by the electricity grid (Ned Mohan, 2003). The most common way to convert this ac voltage into dc is to use uncontrolled diode rectifiers as demonstrated in Figure 1-15 where the power can only flow from utility ac side into the dc side.

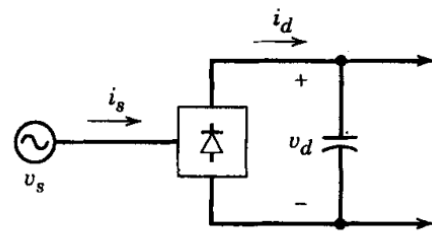


Figure 1-15. Block diagram of a rectifier

The diode rectifiers can be basically constructed to work in two manners; single phase half-wave rectifier, and single phase full-wave bridge rectifier.

#### 1.3.1.1 Single Phase Half-Wave Rectifier

Figure 1-16 shows a basic positive half wave rectifier, where it allows the positive input sine wave cycle to pass and prevent the negative one to go through, a capacitor should be added in parallel in order to obtain the desired dc output and ideally the output should be ripple free.

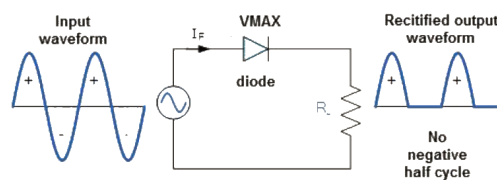


Figure 1-16. Half-wave rectifier concept

### 1.3.1.2 Single Phase Full-Bridge Rectifier

Figure 1-17 shows a typical full-wave bridge rectifier, where 4 diodes are used to allow the positive input cycle to pass and invert the negative input cycle to achieve only positive cycles at the output, after that a capacitor is added to achieve the required dc voltage.

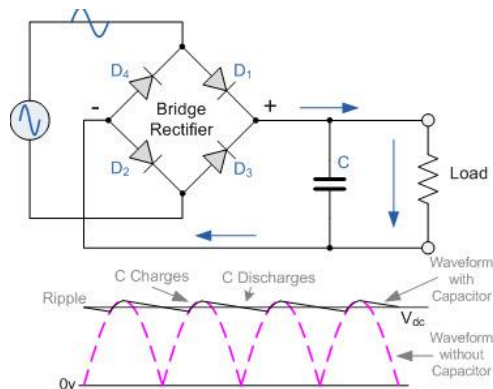


Figure 1-17. Full-wave bridge rectifier concept

### 1.3.2 Inverters

The main usage of the switch-mode dc-ac inverters are in the uninterruptable ac power supplies (UPS) applications such as ac motor drives, where the main goal is to produce a sinusoidal ac output that are controlled in both the magnitude and the frequency. The reason behind calling such devices as inverters is because the power flow is reversible (from dc side to the ac side). Mainly, there are two categories for the inverters; voltage source inverters (VSIs) and current source inverters (CSIs), however, the CSIs are used only for very high power ac motor drives, where the dc input to the inverter is a dc current source which limits the applications of the CSIs significantly, and hence, we will not discuss it in this section. The VSIs can be further divided into the following three general categories; pulse width modulated (PWM) inverters, Square wave inverters, and single phase inverters with voltage cancellation.

### 1.3.2.1 Pulse Width Modulated Inverters

Figure 1-18 shows a typical one leg switch mode inverter, where the input magnitude is fixed, and hence, the inverter should control both the magnitude and frequency of the ac output.

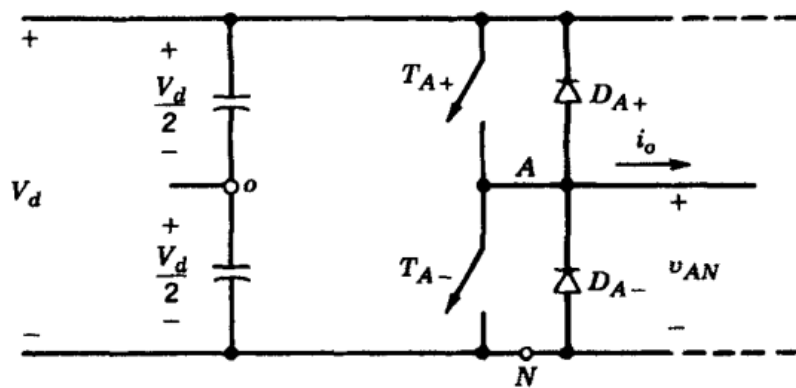


Figure 1-18. One leg switch mode inverter

In PWM technique, the output can be controlled by establishing a sinusoidal ac voltage reference ( $V_{ref}$ ) and compare it with a high frequency triangular carrier wave ( $V_c$ ), see Figure 1-19, if  $V_{ref}$  is higher than  $V_c$  then the upper switch of the one leg switch inverter is turned on and the output voltage becomes  $V_{dc}/2$ , while if  $V_{ref}$  is lower than  $V_c$  then the lower switch of the one leg switch inverter is turned on and the output voltage becomes  $-V_{dc}/2$ , after that, a filter to extract the fundamental wave is added and the controlled ac output voltage is produced.

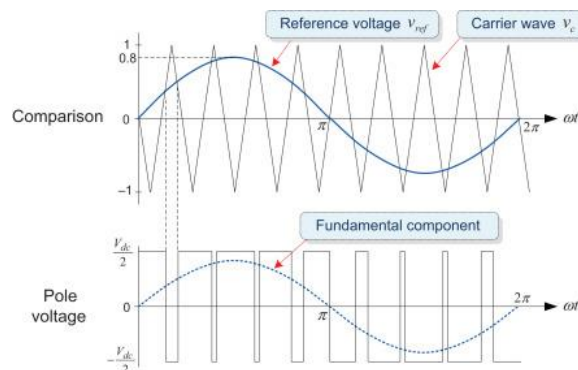


Figure 1-19. PWM technique concept

### 1.3.2.2 Square Wave Inverters

In the square wave inverters we assume that the dc input magnitude is controlled already, and hence, only the output frequency of the sinusoidal wave form should be controlled, this can be done by letting each switch of the inverter leg of Figure 1-18. One leg switch mode inverteron for one half-cycle ( $180^\circ$ ) of the desired output frequency, which results in an output voltage waveform ( $V_{AO}$ ) as shown in Figure 1-20, which is then filtered to extract the fundamental sinusoidal output wave form.

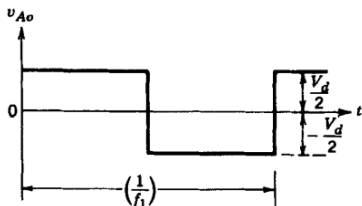


Figure 1-20. Square wave switching

### 1.3.2.3 Single Phase Inverters with voltage cancellation

In case of inverters with single phase output, it is possible to control the magnitude and the frequency of the inverter output voltage, even though the input to the inverter is a constant dc voltage and the inverter switches are not pulse-width modulated (and hence the output voltage waveshape is like a square wave). Therefore, these inverters combine the characteristics of the previous two inverters. The idea here is to use two equal and sufficiently large capacitors in series across the dc input and their junction is at a midpotential, with a voltage of  $V_d/2$  across each capacitor, see Figure 1-21. This results in the potential at point o remains essentially constant with respect to the negative dc bus N. Therefore, this circuit configuration is identical to the basic one-leg inverter discussed in detail earlier, where the output voltage ( $V_o$ ) is equal to the pole voltage ( $V_{AO}$ ) as in the square wave inverter case.

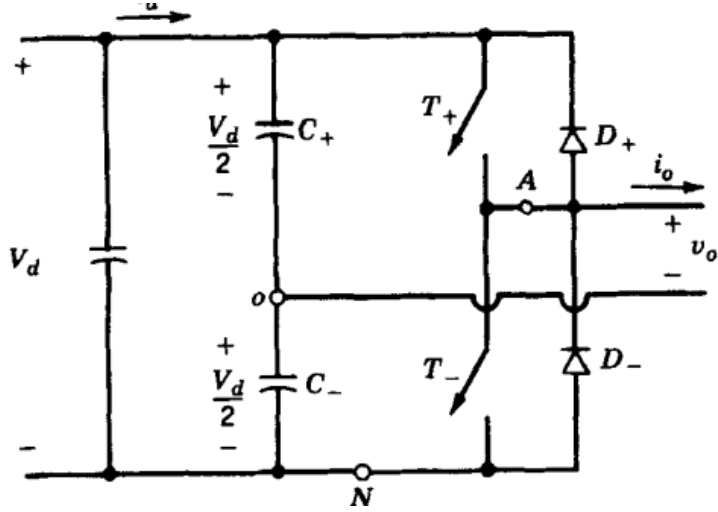


Figure 1-21. Single phase half bridge inverter

### 1.3.3 Choppers

DC to DC power conversion is mostly used in regulated power supplies applications like dc drive motors, the reason behind that is because rectifiers usually produce unregulated dc voltage from the grid line, and hence, the unregulated dc voltage should be applied to the DC to DC switch mode to get a controlled dc output at a desired voltage level. The most common DC to DC converters are the step down (buck) converter, the step up (boost) converter, and the step down/step up (buckboost) converter.

#### 1.3.3.1 Buck Converter

In buck converters, the controlled average output dc voltage is lower than the input dc voltage. The idea behind the step down converters can be demonstrated based on the buck converter example shown in Figure 1-22, when the switch is turned on, the diode becomes reverse biased and the energy is stored in the inductor, while when the switch is turned off, the diode becomes forward biased and the energy stored in the inductor goes to the load, the output voltage here can be controlled based on the switching time (duty cycle D) according to the formula:  $V_o = DV_d$ .

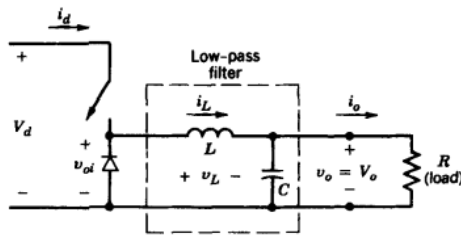


Figure 1-22. Step-down converter

The inductor and capacitor values in the step down converter determines the output voltage ripple (see Figure 1-23) where lower ripple voltages are always preferred.

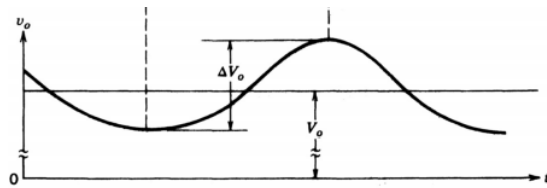


Figure 1-23. Output voltage ripple of a step-down converter

### 1.3.3.2 Boost converter

Boost converters produce higher regulated output voltage compared with the input voltage, Figure 1-24 shows a basic step-up converter, it has the same idea of step down converters, i.e when the switch is on the diode is reversed and the inductor stores the energy, and when the switch is off the diode is forward biased and the inductor transmits the stored energy, however the set up of the circuit gives an output voltage according to the formula:  $V_o = \frac{V_d}{1-D}$ , and since the duty cycle is always lower than 1 the output voltage is always higher than the input voltage.

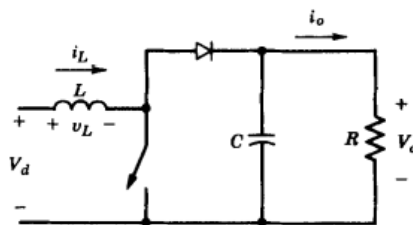


Figure 1-24. Step-up DC-DC converter

Figure 1-25 shows the output voltage of a typical step-up converter, the ripple voltage here is also controlled by the inductor and the capacitor values.

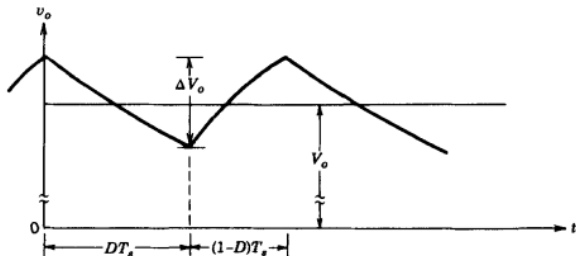


Figure 1-25. Step-up converter output voltage ripple

### 1.3.3.3 Buck-Boost Converter

Step-up/step-down converter can produce higher or lower voltage compared to the input based on the application needs, the main idea here is to connect both the buck converter and the boost converter in a cascade connection as shown in Figure 1-26.

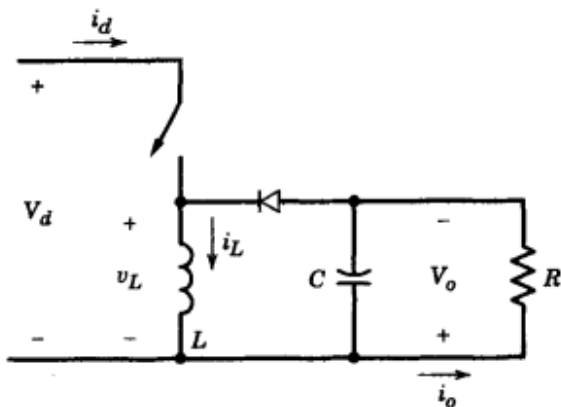


Figure 1-26. Buck-boost converter

The output voltage here is also controlled by the switch duty cycle according to the formula:  $V_o = \frac{DV_d}{1-D}$ , according to this formula; when D is lower than 0.5 the output voltage is lower than the input voltage and the converter is working in the buck mode, while when D is higher than 0.5 the converter works in the boost mode since the output voltage is higher than the input voltage.

### 1.3.4 AC to AC Converters

AC to AC converters are used to produce controlled magnitude and frequency AC signals. Usually, AC to AC converters are designed in an indirect way, i.e. a DC to AC converter followed by a DC to AC converter and a DC link in between both converters as shown in Figure 1-27.

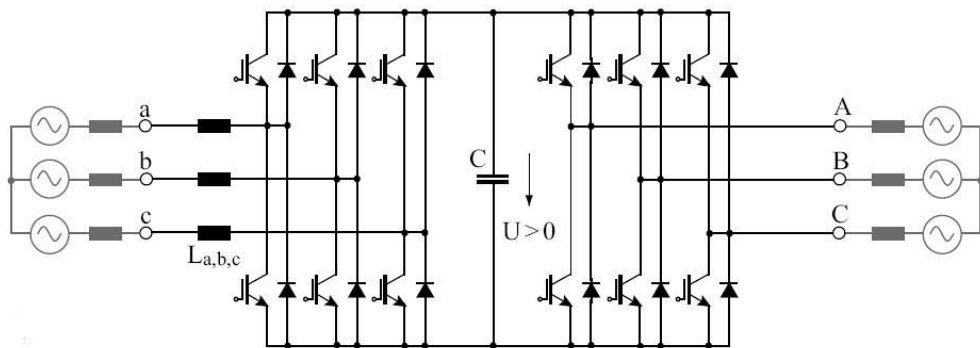


Figure 1-27. Topology of (regenerative) voltage-source inverter AC/DC-AC converter

In addition to the indirect way of converting AC to AC signals, there are several known direct AC to AC converters like cycloconverters, matrix converters, hybrid matrix converters, and AC voltage converters. However, the reliance of this research on AC to AC converters does not exist, and hence, the details of such converters will be skipped in this section.

## 1.4 Filters

Electrical filters are used to pass only certain desired band of frequencies and reject the other frequencies. In general, filters are classified into active filters, passive filters, and hybrid filters.

### 1.4.1 Active Filters

Active filters are designed using an active gain element .i.e operational amplifiers with passive components like resistors and capacitors while the inductors usually

are not used in this type of filters because they are lossy, bulky, heavy and expensive in the low frequency range (Crecraft, 2002). The type of the active filter i.e high pass filter or low pass filter can be determined by the components connection as shown in Figure 1-28, while the value of these components can determine the filter frequencies range.

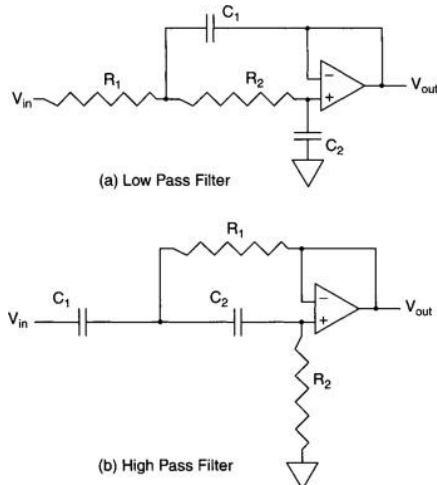


Figure 1-28. Active filters based on op-amps

#### 1.4.2 Passive Filters

Passive filters are designed using simple passive components like resistors, capacitors and inductors, and hence, it is cheaper than the active filters but has lower efficiency and quality output. Figure 1-29 shows a basic low pass filter and how it can remove the high frequency noises in the input signal.

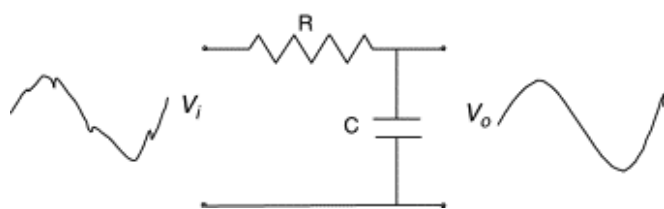


Figure 1-29. Passive low pass filter

### 1.4.3 Hybrid Filters

Hybrid filters are designed using a combination of active filters and/or passive filters in a series or parallel (or both) topologies. The idea behind hybrid filtering is to let the passive filters to remove the dominant harmonics like the 5th or the 7th harmonics and let the active filters to remove the higher harmonics which lead to reduce the overall size and cost of active filtering significantly (Masoum, 2015).

Figure 1-30 shows an example of different hybrid filters topologies.

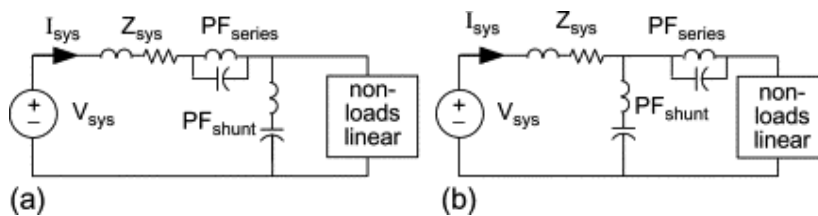


Figure 1-30. Single-phase hybrid filter (including two passive filters) as a combination of (a) passive-series and passive-shunt filters, (b) passive-shunt and passive-series filters.

## 1.5 Thermal Power Loss Modeling of Power Electronics Converters.

Thermal modeling aims to describe the transient thermal behaviors of power electronic devices to estimate the mean and varied temperature profiles during operations (Albarbar, 2018). The importance of the thermal modeling relies behind the fact that most of the power loss occurring in the power electronics converters is caused by the rapid changes in the drawn current and voltage that generate heat within devices, and hence, designing proper thermal networks to predict the thermal power loss behavior is essential in trying to reduce and optimize the devices actual thermal power losses. The most two well-known thermal networks for this purpose are the Cauer and Foster thermal models which are shown in Figure 1-31 and Figure 1-32 respectively.

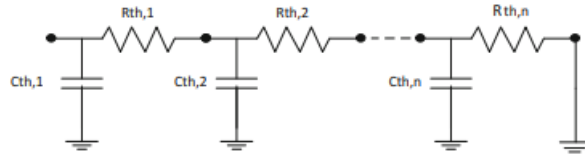


Figure 1-31. Equivalent thermal model of Cauer network

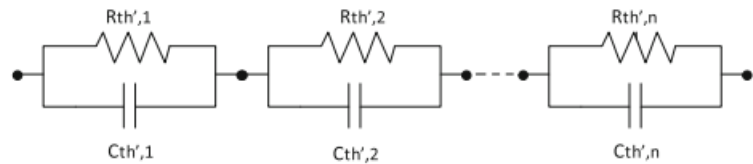


Figure 1-32. Equivalent thermal model of Foster network

The passive elements (capacitors and resistors) in the Cauer network represents the actual temperature distribution between the actual physical layers of the electronic devices such as the die, solder, substrate, etc., and the equivalent impedance can be found using the formula:

$$Z_{th}(s) = \frac{1}{sC_{th}, 1 + \frac{1}{R_{th}, 1 + \frac{1}{sC_{th}, 2 + \frac{1}{R_{th}, 2 + \frac{1}{sC_{th}, n + \frac{1}{R_{th}, n}}}}}}$$

While in the Foster model, each RC element does not represent actual thermal identity of any layer, the equivalent response has physical meaning for the junction layer, only, and hence, the Foster model is simpler compared to the Cauer model but the Cauer model is more precise. The thermal impedance of each RC' component of the Foster model can be found using:

$$Z_{th'}(s) = R_{th}' // (1/sC_{th'})$$

In order to use these thermal models properly, a power loss (which is equivalent to a voltage source) is subjected to the model and a heat source (equivalent to a

current source) is added, the resulted output voltage represent the transient thermal response of the power electronic device. Figure 1-33 and Figure 1-34 shows a demonstration of this connection topology for the Cauer and the Foster thermal network respectively.

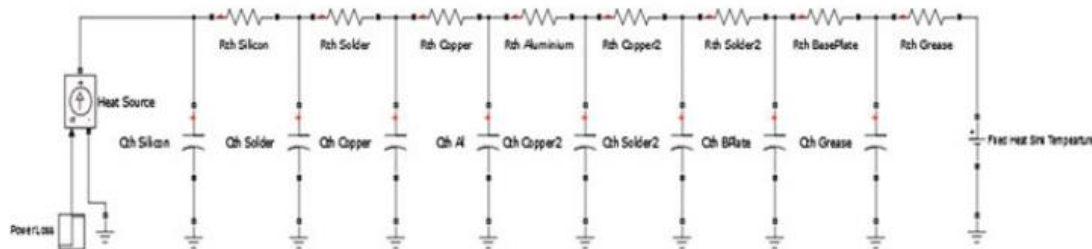


Figure 1-33. Equivalent thermal model of eighth-order system using Cauer network

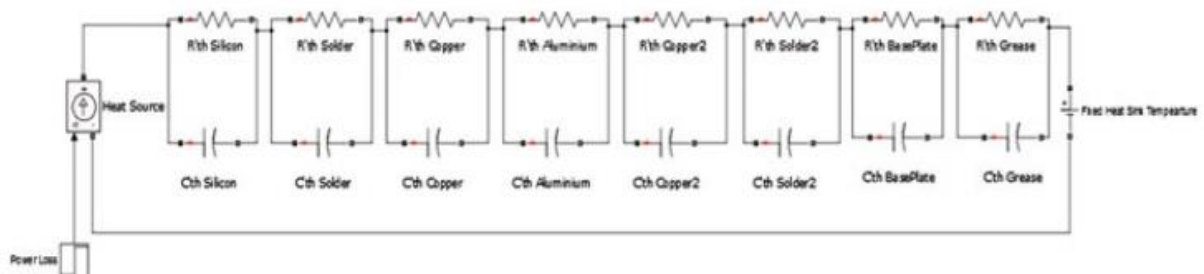


Figure 1-34. Equivalent thermal model Foster networks

## 1.6 Reliability Modeling and Lifetime Analysis

Lifetime analysis can be performed using the transient thermal response of the power electronics devices discussed in the previous section, the main goal here is to count the number of heating cycles ( $N_f$ ) that a device can achieve before failing, the thing that can be done using several known reliability models that can quantify the reliability performance such as:

**Coffin–Manson Model:**  $N_f = \alpha(\Delta T_j)^{-n}$ , where  $\alpha$  and  $n$  area constants and  $\Delta T_j$  is the extracted peak to peak junction temperature of the device.

**Coffin–Manson–Arrhenius Model:**  $N_f = A(\Delta T_j)^\alpha \cdot e^{\frac{E_a}{k_b T_m}}$ , which is an extended version of the basic Coffin–Manson model that takes the mean temperature ( $T_m$ ), the Boltzmann constant ( $K_B$ ), the activation energy  $E_a$ , and another constant  $A$  into account while performing the reliability analysis.

**Norris–Landzberg Model:**  $N_f = A \cdot f^{-n_2} (\Delta T_j)^{-n_1} \cdot e^{\left(\frac{E_a}{k_B T_m}\right)}$ , which takes the cycling frequency  $f$  of the junction temperature into account.

**Bayerer Model:**  $N_f = K \cdot (\Delta T_j)^{-\beta_1} \cdot e^{\frac{\beta_2}{T_m}} \cdot t_{on}^{\beta_3} \cdot I^{\beta_4} \cdot V^{\beta_5} \cdot D^{\beta_6}$ , which considers a number of parameters like the  $t_{on}$  is the heating time,  $I$  is the applied DC current,  $D$  the diameter of the bond wire, and  $V$  the blocking voltage.

After calculating the number of heating cycles ( $N_f$ ), the total life time consumption can be found using the Palmgren–Miner linear damage accumulation rule:

$$LC = \sum_{i=1}^j \frac{n_i}{N_i}$$

where  $n_i$  is the number of cycles,  $N_i$  is the measured lifetime in the  $i$ th profile and  $j$  is the total number of load profile. The rule states that failure happens when condition  $TLC = 1$  occurs

## 1.7 Neural Networks Models

Neural networks have been rapidly improving in the recent year due to its powerful role in the machine learning and artificial intelligence applications. The main function of neural networks is shown in Figure 1-35, this network converts complex dynamic models into black box models (hidden layers with trained weights) that learns the output of the dynamic model from training the model using several (pre-known) input and output dataset.

For instance, trained neural network models can predict the transient heat response of power electronic devices in a power system from a given wind and solar profiles

directly without looking into the system dynamics, and hence, it can save a lot of time and complexity and even give more accurate results.

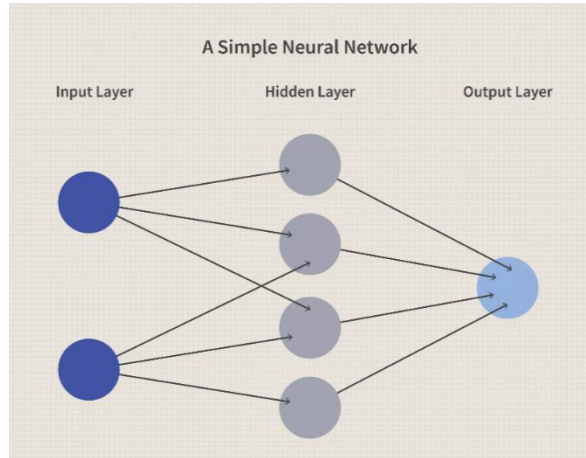


Figure 1-35. A simple neural network

In the literature, several algorithms were developed in order to train the neural models, like the backpropagation algorithm, recurrent neural networks, deep convolutional feedforward neural networks, Levenberg-Marquardt algorithm and many more algorithms. It is very difficult to know which training algorithm will be the fastest for a given problem. It depends on many factors, including the complexity of the problem, the number of data points in the training set, the number of weights and biases in the network, the error goal, and whether the network is being used for pattern recognition (discriminant analysis) or function approximation (regression). For simplicity, this work doesn't consider which algorithm is faster and more accurate as much as achieving the goal of having a reliable model that can predict the responses sufficiently, and hence, only Levenberg-Marquardt algorithm will be used since it gave acceptable and accurate results after testing it.

## 1.8 Problem Statement

The most expensive component in a power system is the power electronics components, however, these components face the issue of heating up so fast, and hence, their lifetime may get degraded if they kept working under extreme

conditions, the main factor that cause the heating is letting the power electronic devices working under high frequencies. Our system proposes an automated system to reduce the frequency using artificial intelligent systems, however, reducing the frequency affects the output energy quality, and hence, a trade-off between lifetime and energy quality is presented, this system is designed to optimize this trade-off by reducing the operating frequency when the junction temperatures are expected to go high, and hence, reducing the lifetime consumption of the power electronic devices. Also, and in order to compensate the reduction of the output quality when reducing the carrier frequency, bigger passive filters can be used depending on the fact that the energy quality can be enhanced if we used larger filters which is a cheaper option in comparison with the changing the power electronics components in a certain period.

## **1.9 Thesis Organization**

This thesis presents a proposed design using the artificial intelligence to enhance the reliability and lifetime of power electronics components. In chapter 1, the theoretical background of the system was discussed, this includes the electricity generation from solar and wind plants, power electronics converters concepts, the filters concepts, thermal analysis and modelling, reliability and lifetime analysis, and the neural networks. While in chapter 2, several related works in the literature were presented and discussed. In chapter 3, the proposed system models are presented component by component, and in chapter 4, the results and discussion were presented. Finally, chapter 5 concluded the work and suggested some future works.



## CHAPTER 2

### LITERATURE REVIEW

In this chapter, we will discuss several related literatures works, and the sections will be divided based on the sub-topics we used to build our work.

#### 2.1 Condition Monitoring of Power Electronics Circuits

One of the simplest works that used the artificial neural network to enhance the lifetime of power electronics devices was done by (Salman Mohagheghi, 2009), he used the concept shown in Figure 2-1, where he trained the neural networks to predict the dynamic response of the power electronics circuit, and after that, he compared the actual output with the output calculated by the neural network in order to find the error signal  $e(t)$ , if an error occurred, then something wrong happened in the system, and hence, the monitor should take action to fix it and try to prevent any possible fatal damage in the whole system.

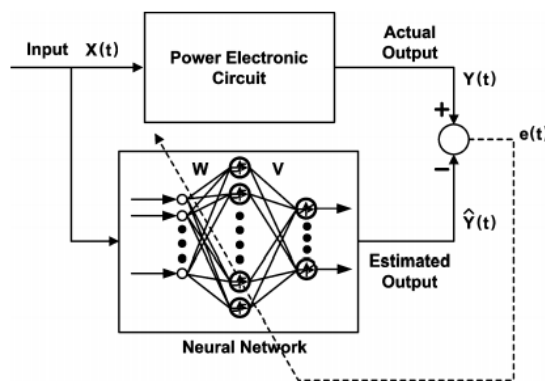


Figure 2-1. Schematic diagram of training the NN.

Figure 2-2 shows the error signal of this NN by comparing the actual output of a power electronics circuit with the estimated output, we can see here that the neural network managed to predict the actual output accurately.

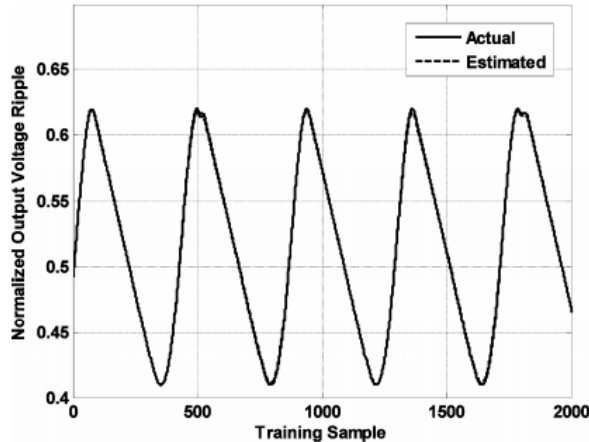


Figure 2-2. Actual and estimated values of the normalized output voltage ripple of a power electronics circuit under normal operating conditions (Mohagheghi, 2009).

## 2.2 Lifetime Analysis for Discrete IGBT Devices

Several works in the literature have been done to find a suitable reliability model that can be used in estimating the power electronics circuits (PECs) lifetime. (Albarbar and Batunlu, 2018) has proposed the flowchart shown in Figure 2-3 in order to estimate the lifetime of a single IGBT device, first we need to find a suitable thermal model (which have been discussed in section 1.5) of the IGBT and implement real time mission profiles to it in order to find the thermal cycles of the device, after that, we need to extract the power cycling from power loss models in order to find the number of cycles that a device can handle before failing in order to insert it in a reliability model and estimate the lifetime consumption. They performed this methodology on a real switching device while adjusting temperature swing ( $\Delta T$ ) as 90 and 40 °C with average temperatures ( $T_m$ ) of 80 and 60 °C and extracted the lifetime curves shown in Figure 2-3. Scheme of lifetime consumption study made by (Albarbar and Batunlu in 2018

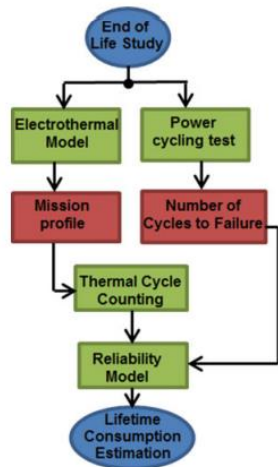


Figure 2-3. Scheme of lifetime consumption study made by (Albarbar and Batunlu in 2018).

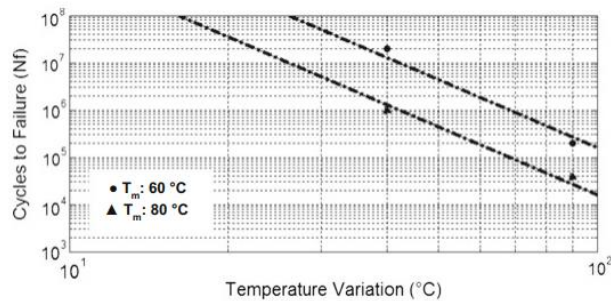


Figure 2-4. Lifetime curves for Albarbar and Batunlu study in 2018

A similar work has been done by (Wang, 2009) but with taking more details into account, their proposed reliability prediction procedure for power electronic systems is shown in the flowchart in Figure 2-5, we can see here that they took into the account the stress and strength of the IGBT component at the input stage and built physical models and inject it to several failure mechanisms to find their effects on the reliability, durability, and robustness of the device at the output stage. They managed to build the cycle to failure models for each of the IGBT device layers shown in Figure 2-6. separately, Their results for the baseplate solder joints, chip solder joints, and the wirebonds cycle to failure models under a testing condition using the Coffin-Mansion model and their proposed model given in equation 3 in their paper are shown in Figure 2-7.

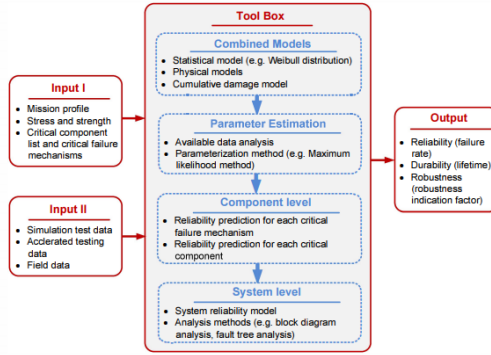


Figure 2-5. Proposed reliability prediction procedure for power electronic systems (Wang, 2009).

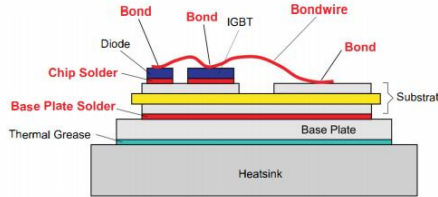


Figure 2-6. Structural details of an IGBT module (Wang, 2009).

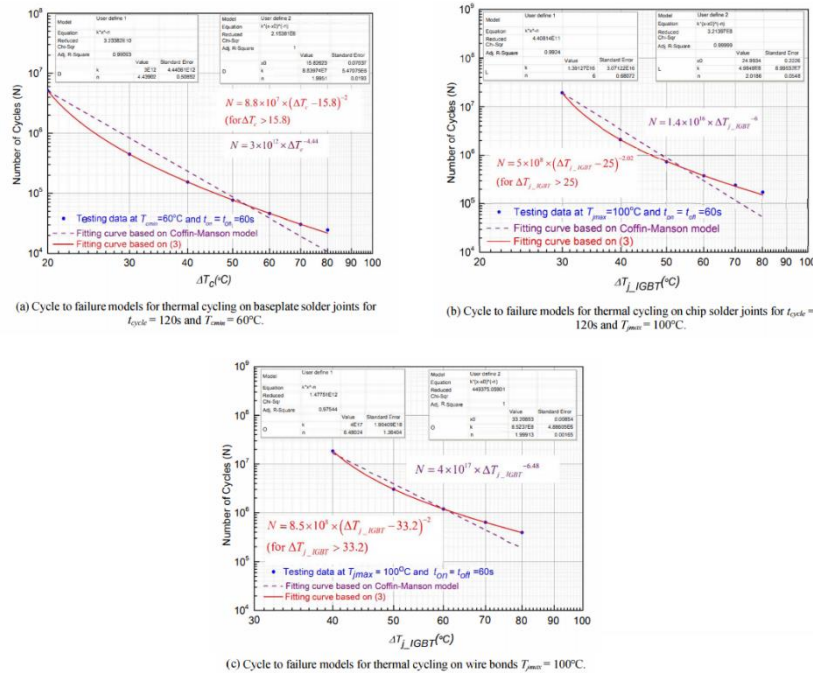


Figure 2-7. Cycle to failure models for different layers of the IGBT device (Wang, 2009).

A similar work has been presented by (Yang, 2008), their proposed design for reliability methodology shown in the flowchart in Figure 2-8, their extended the reliability performance to see the indirect effects of the thermal loading, voltage or current stress, and the stress margin.

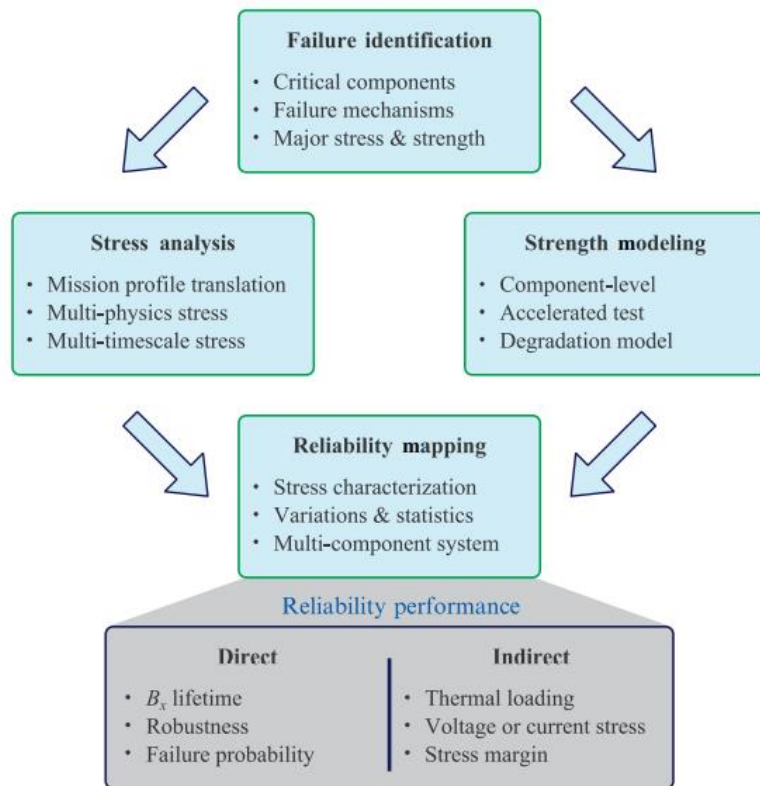


Figure 2-8. Reliability prediction process of the design for reliability (DfR) approach for power electronic systems, where  $\beta_x$  is the lifetime (Yang, 2008).

Among the methodologies for lifetime analysis discussed in this section, we will follow the first methodology for (Albarbar and Batunlu, 2018) to do our reliability analysis.

## 2.3 Using Neural Networks Algorithms in the Lifetime Analysis of Discrete IGBT Devices

Instead of going through the time-consuming traditional way of the reliability design, several works in the literature have suggested to use the neural networks to accelerate the lifetime analysis of power electronics devices.

For instance, (Pang, 2009) have suggested to use the improved fireworks algorithm which is explained in the flowchart shown in Figure 2-9. The flowchart of the improved fireworks algorithm, and optimize this algorithm using the Grey Neural Network (GNN) model which is used to set up grey differential equations through a small amount of discontinuous information. The basic idea of grey model is to use the original data to form the original sequence, which can weaken the randomness of the original data and reflect the continuous change process of internal things, the general topology of the multi-dimensional GNN model neural network is shown in Figure 2-10.

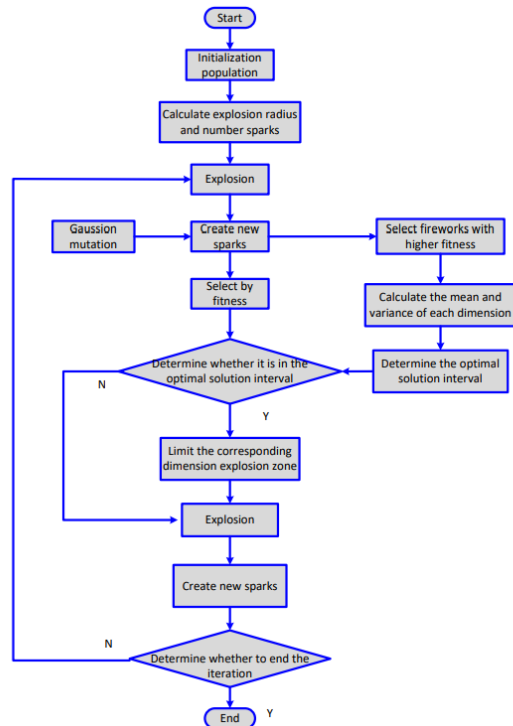


Figure 2-9. The flowchart of the improved fireworks algorithm (Pang, 2009).

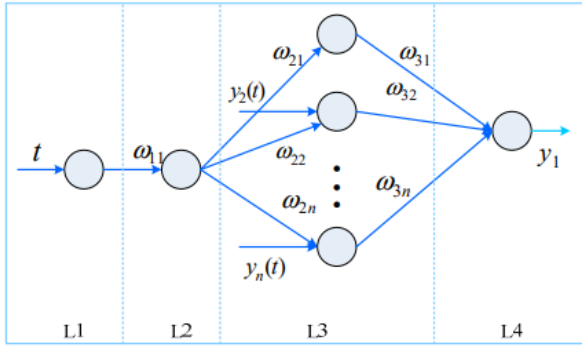


Figure 2-10. The general topology of the GNN model (Pang, 2009).

They tested this proposed lifetime analysis on the electrical relays and they managed to get the accurate pattern of the actual lifetime as shown in Figure 2-11.

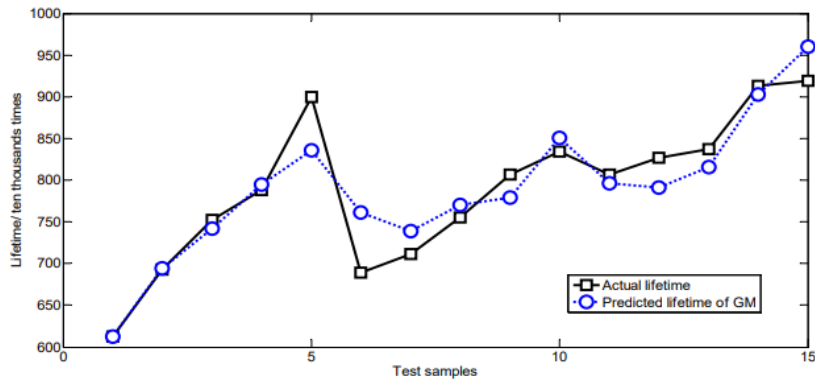


Figure 2-11. The comparison of prediction value using GM (1, 5) dimension with actual value of an electrical relay (Pang, 2009).

Another work that used the neural networks algorithm in the lifetime analysis was done by (Rosmaliati, 2018), they used the Nguyen widrow alogrithm (which is a modified version of the backbropogation neural netwrok that has a technique to initialize the weights in order to do faster networks training), they first transformed the input current into wavelet transformation, which provides an efficient tool for signal processing in time-frequency domain, they used 3 wavelet transforms in order to compare between them; Haar wavelet, Meyer wavelet, and Daubechies wavelet, after that they calculated the energy and power spectral density of this wavelet signals in the frequency domain, then they used normal backbropagation neural network which is shown in Figure 2-12, and finally they used the Nguyen

Widrow weights initializing to accelerate the training speed and accuracy, they tested this algorithm on practical electrical transformer data and the results are shown in Table 2.1. Forecast result of (Rosmaliati, 2018) for predicting the transformer lifetime using Nguyen Widrow neural networks.

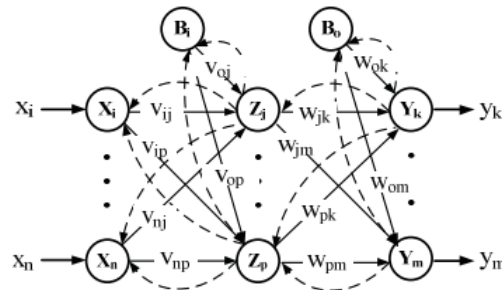


Figure 2-12. Backpropagation network architecture (Rosmaliati, 2018).

Table 2.1. Forecast result of (Rosmaliati, 2018) for predicting the transformer lifetime using Nguyen Widrow neural networks.

Dataset Proportion		MSE	
Training	Testing	Nguyen-Widrow NN	BPNN
Haar wavelet			
100%	100%	0.126	0.129
75%	25%	0.024	0.027
50%	50%	0.032	0.035
Meyer Wavelet			
100%	100%	0.090748	0.098951
75%	25%	0.023189	0.025874
50%	50%	0.031689	0.036791
Daubechies Wavelet			
100%	100%	0.090962	0.095484
75%	25%	0.031132	0.30354
50%	50%	0.032525	0.035864

## 2.4 Using the Artificial Intelligence in Automating and Enhancing the Reliability Designs of Discrete IGBTs

In addition to use the neural networks to accelerate the reliability and lifetime analysis, it can be used to automate the reliability design and enhance it. For instance, (Dragicevic, 2018) proposed the algorithm shown in Figure 2-13 in order to find the yearly lifetime consumption based on the inductor size design parameter of a typical power electronics converter. First they took the input parameters

(switching frequency, ambient temperature, dc link voltage, and input power to extract the IGBT junction temperature and trained a neural network model to do that automatically, after that, they took the junction temperature in addition to the yearly input mission profile of solar and ambient temperature and injected it to the rainflow counting algorithm to find the lifetime consumption, then they trained a second neural network model to automate the lifetime consumption calculation, and finally, they used both neural networks model to extract the inductor size design parameter from the input data directly without going to the system dynamics.

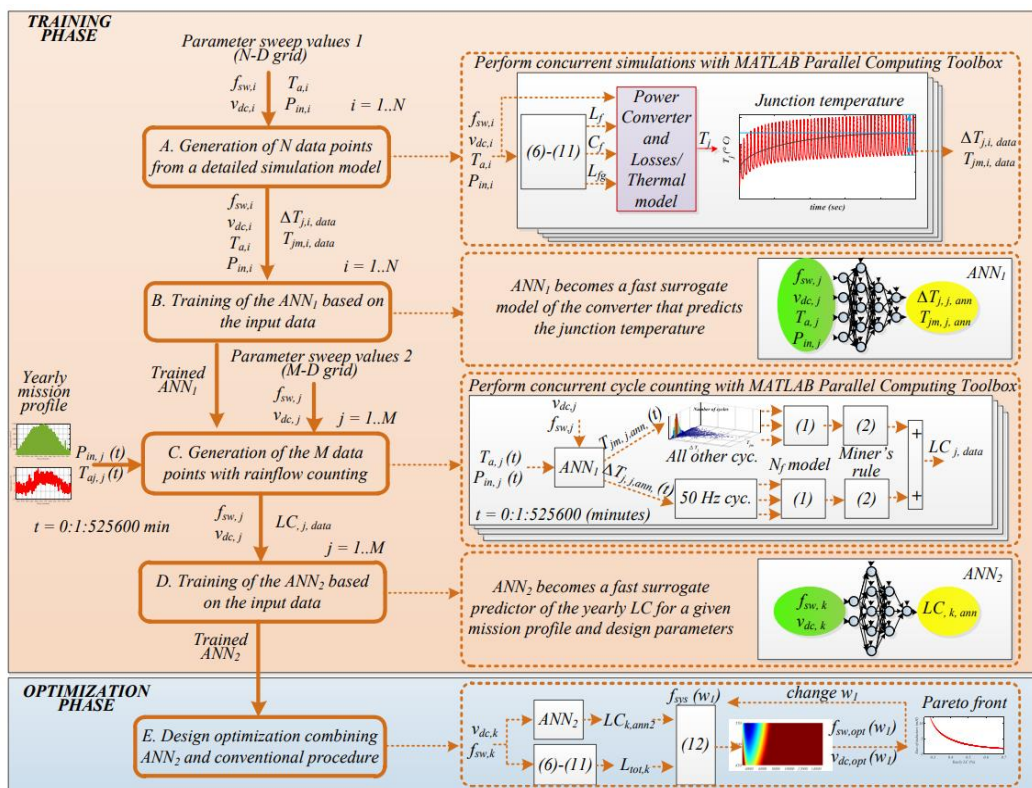


Figure 2-13. Flow diagram of the proposed artificial intelligence by (Dragicevic, 2018) based design optimization of the power electronic system.

The results of this proposed system show that when the inductor size increases, the lifetime consumption of the IGBTs decreases as shown in Figure 2-14.

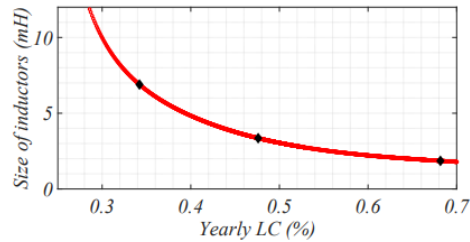


Figure 2-14. The relation between yearly lifetime consumption with the size of inductors according to the (Dragicevic, 2018) study.

Another work that used the artificial intelligence to automate the reliability design was done by (Sanwongwanich, 2017), in this work they evaluated the lifetime of PV inverters with taking into account the PV panel degradation rate, their flowchart work is shown in Figure 2-15., they first used the input mission profiles to find the junction temperature of PV inverters, then they used the rainflow algorithm to extract the mean temperature and the peak to peak temperature in order to calculate the lifetime consumption using lifetime models.

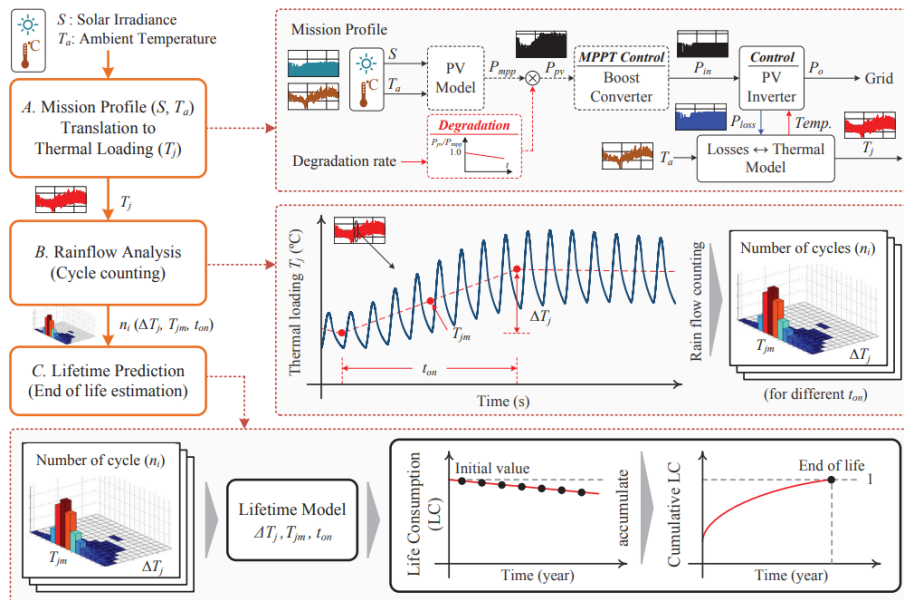


Figure 2-15. Flow diagram of the mission profile-based lifetime evaluation of PV inverters considering the PV panel degradation done by (Sanwongwanich, 2017)

## **2.5 Gap in the Literature**

In the literature, There is no work done to check the remaining lifetime for variable weather condition using hybrid wind and solar system. This work will utilize the available mission profiles from the solar system placed in METU NCC in addition to the upcoming wind system to fill this gap for hybrid energy systems.

Another gap in the literature that will be addressed in this work is the fact that there is no work used the neural networks to build a real-time control model that can enhance the PECs lifetime based on the working condition of the system, the NNs were just used to perform lifetime analysis or determine a fixed design parameter in the system, so we used neural networks to build a control model that automatically works to enhance the reliability of PECs based on the variable working conditions.



## CHAPTER 3

### METHODOLOGY

In this chapter, we will discuss our proposed methodology to automate the lifetime reliability enhancement part by part using MATLAB Simulink and MathWorks environments.

#### 3.1 Solar Panel Modelling

In order to simulate the power production from solar PV panel we used the equivalent circuit discussed in Figure 1-8. Equivalent circuit of a real solar cell to build two solar modules and connect them in parallel as shown in Figure 3-1 , the solar panels here takes the irradiance data as an input, and according to it, the system produces the PV power which will be injected to the power system. Figure 3-2 shows the PV characteristics of this model for 25 C and 45 C ambient temperatures, while Figure 3-3. Generated power by the solar model from 500 W/m<sup>2</sup> irradiance input shows the generated power from a 500 W/m<sup>2</sup> irradiance input.

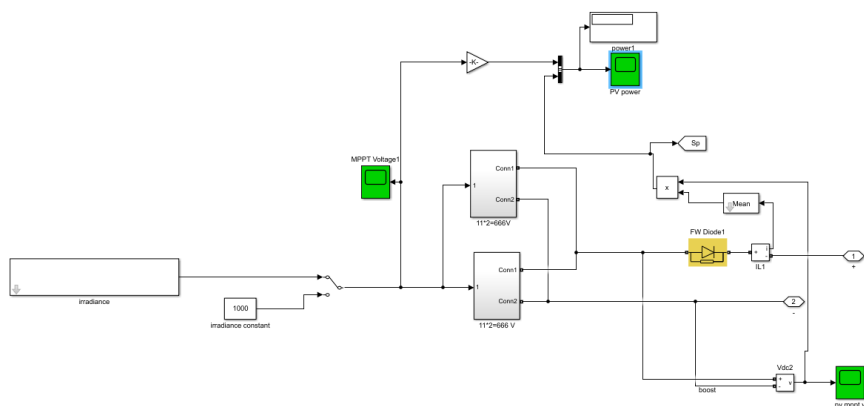


Figure 3-1. Structure of solar panel model.

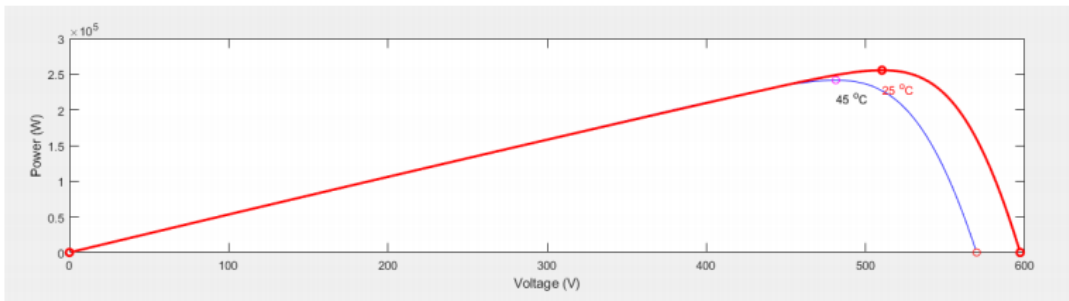


Figure 3-2. PV characteristics for the solar panel model under two different ambient temperatures.

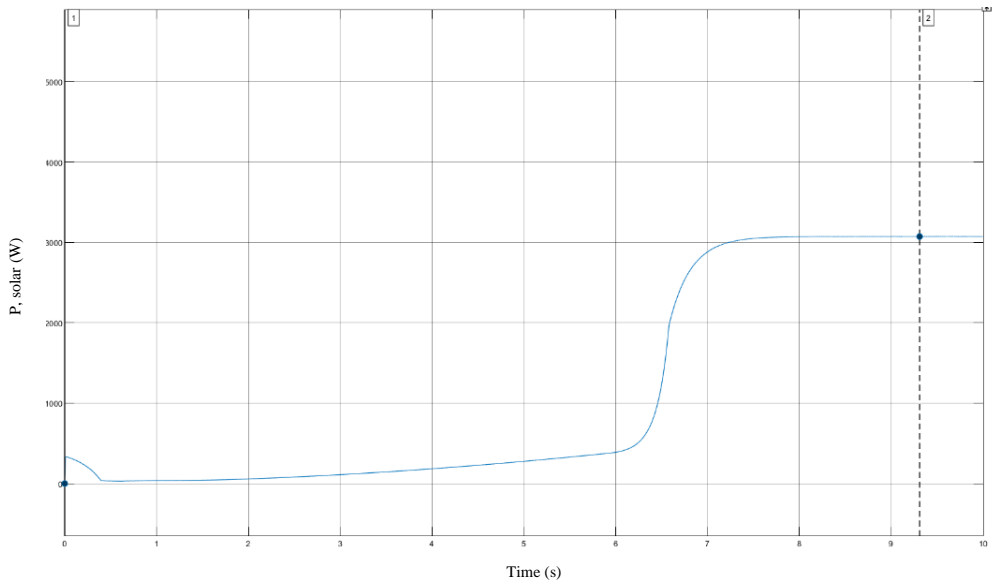


Figure 3-3. Generated power by the solar model from 500 W/m<sup>2</sup> irradiance input.

### 3.2 Wind Turbine Modelling

For the wind turbine modelling using Simulink, we followed the work done by (Dr. Siva, 2021) which uses the permanent magnet synchronous generator to produce the energy from the wind but with removing the 2 mass drive train he used because its control drags our system to produce no power, and after this wind turbine, we added a rectifier to convert our energy into DC and adapt it with the whole system, our wind turbine model is shown in Figure 3-4 and the wind turbine power characteristics is shown in Figure 3-5.

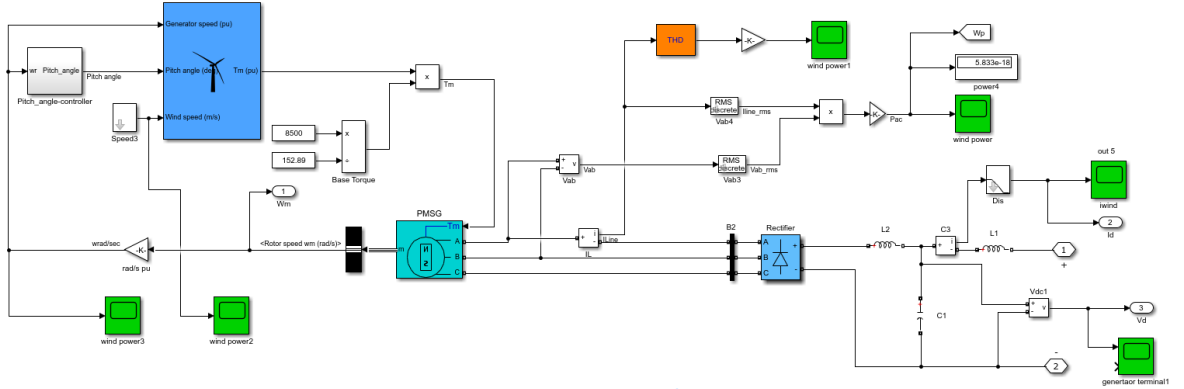


Figure 3-4. Structure of wind turbine model that uses PMSG

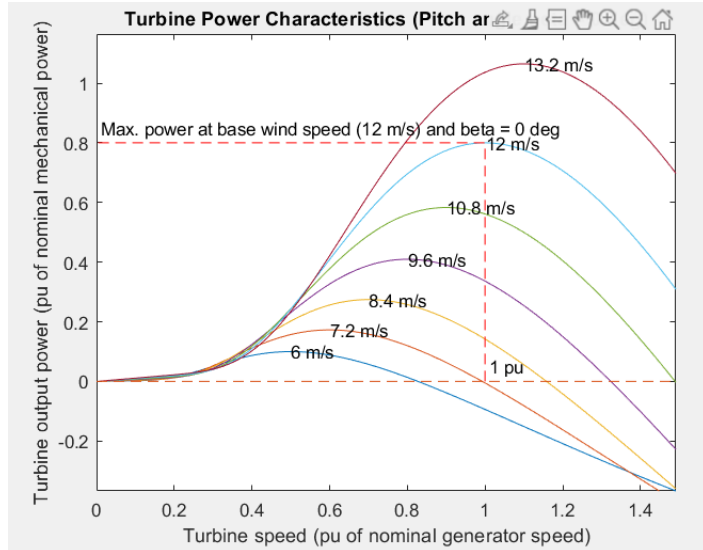


Figure 3-5. Turbine power characteristics

### 3.3 DC to DC Converter Modelling for Input Power Regulation

It is known that the generated energy from renewable resources is random, and hence, a DC-to-DC converter is needed to maintain the energy at a certain limit, in our work, we used an identical 100 Vdc DC/DC converter for both sources to do this job, this converter is shown in Figure 3-6., we used MATLAB built-in look up table for the PV data for both converters in the controlling stage of the IGBT of the converter (labeled as Ppv).

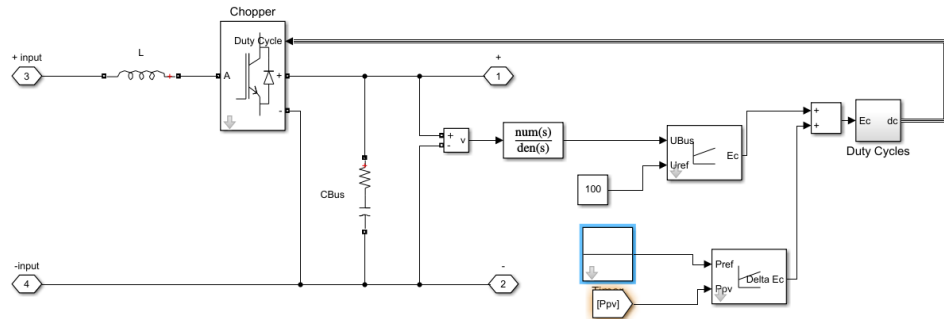


Figure 3-6. Structure of 100 Vdc DC-to-DC converter

### 3.4 Wind Maximum Power Point Tracking

Maximum power point tracking (MPPT) system is used to track the I-V characteristics to find the optimal point that produces the maximum possible power, we used a maximum power point tracker for the wind source in our work and controlled it based on the generated torque from the wind turbine, this tracker is shown in Figure 3-7.

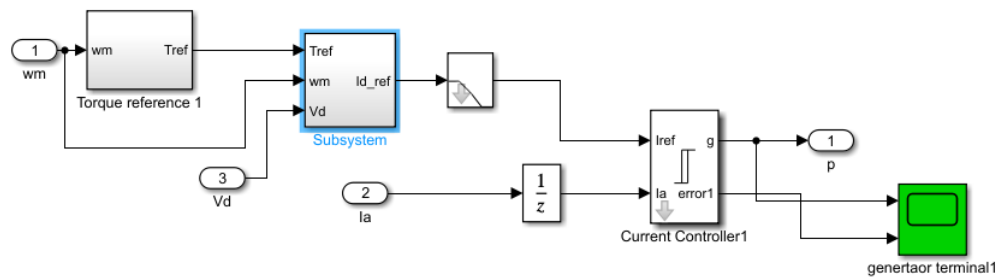


Figure 3-7. Structure of wind MPPT

### 3.5 2-Levels Power Inverter Modelling

Since our work is focused on discrete IGBT lifetime analysis, the built-in MATLAB inverters was not useful for us since it considers several IGBTs in one block, and hence, we needed to build the 2-levels from scratch by our own, Figure 3-8 shows the structure of 6 discrete IGBTs which form a 2-levels inverter and they are controlled by a PWM technique.

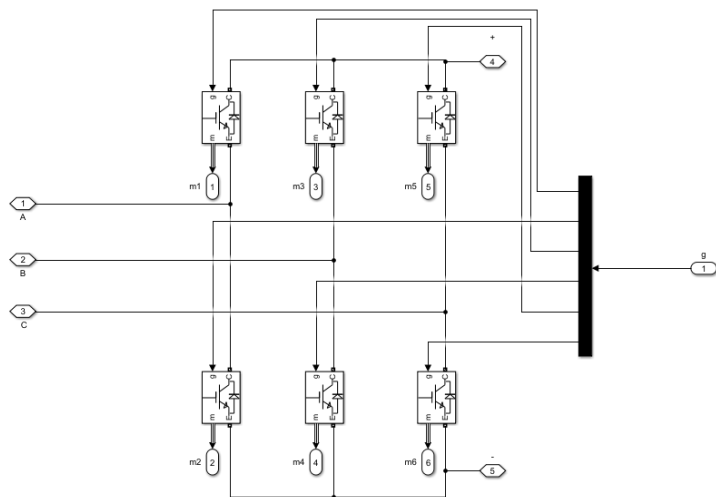


Figure 3-8. Structure of 2-levels 6 IGBTs inverter

### 3.6 Thermal Network of Discrete IGBT Modelling

In our work, we used the Foster thermal model discussed in section 1.5, this thermal network is shown in Figure 3-9. Foster thermal network of a discrete IGBT and the resistors and capacitors values are taken from (C. Batunlu,2015) study where they summarized these values for an IGBT layers in Table 2 in the reference. In addition to the thermal network, a power loss model is needed as an input for the thermal network, the structure of such power loss model is shown in Figure 3-10.

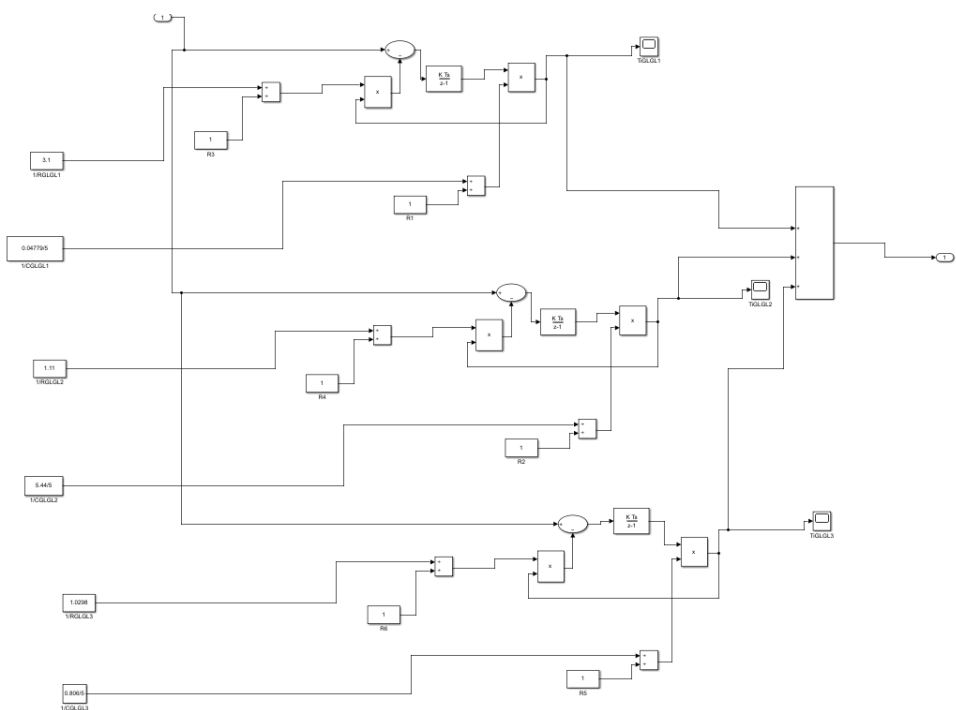


Figure 3-9. Foster thermal network of a discrete IGBT

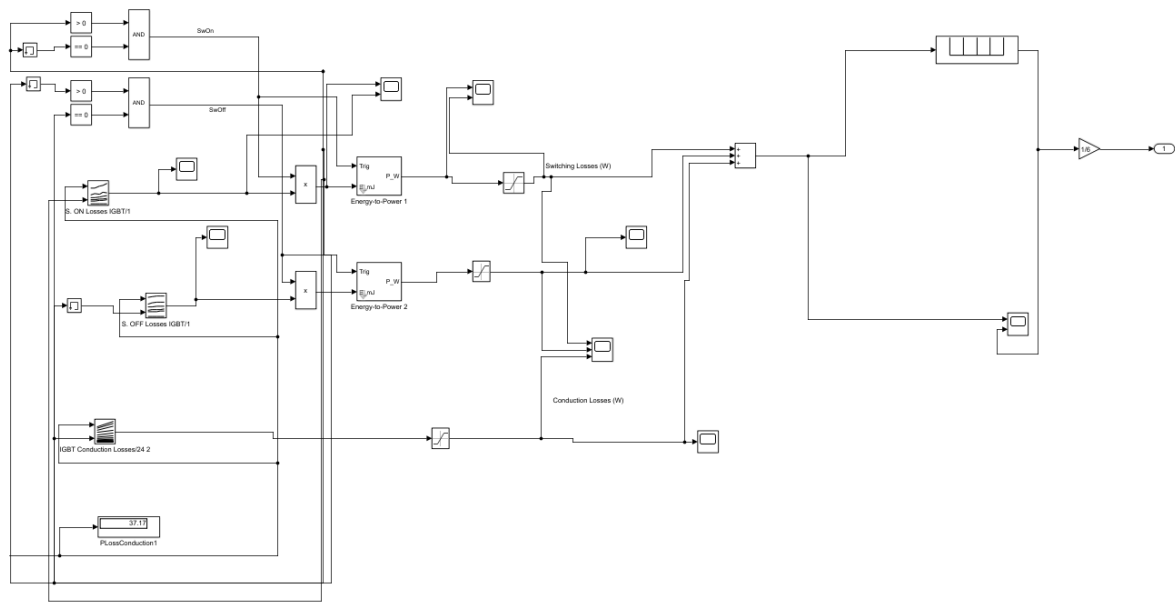


Figure 3-10. Power loss model for a discrete IGBT

### 3.7 Neural Network Modelling

In our work, we used two neural networks, the first one (ANN1) to predict the DC link voltage from the wind and solar mission profile data, and the second one (ANN2) to predict the mean temperature and the peak-to-peak temperature from the resulted DC link voltage from ANN1 in addition to the ambient temperature profile and the switching frequency of the inverter (triangle carrier signal frequency), we used the Levenberg-Marquardt neural network algorithm because it was the fastest and the most accurate among the built-in MATLAB training options by trial, also, we determined the number of hidden layers for each network by trial and error, we tested both networks for a loop of hidden layers goes from one to hundred and chose the number of layers that gives the lowest mean square error value compared to the actual value, the structure for ANN1 was found to be best fitted at 29 hidden layers as shown in Figure 3-11, while for ANN2, 30 hidden layers fitted the best and the structure is shown in Figure 3-12.

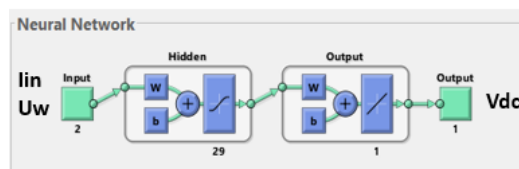


Figure 3-11. Structure of ANN1

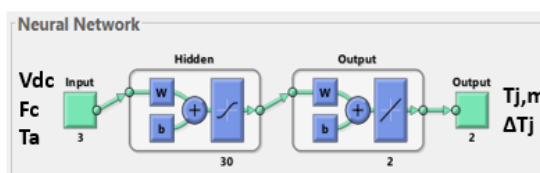


Figure 3-12. Structure of ANN2

After training both networks, we transferred them into Simulink environment in order to automate the inverter frequency adjustment, the model of the proposed frequency adjustment process is shown in Figure 3-13. Proposed neural network model that controls the carrier frequency for the inverter where we used two feedback systems with PID controllers. The first controller controls the actual junction temperature and prevents it to go above Tref which represents the

temperature that we don't want the IGBT to go over it, while the second controller controls the peak to peak junction temperature in one heating cycle and keep it below a pre-defined dTref value. A switch is connected after that to choose the lowest frequency resulted from both controllers.

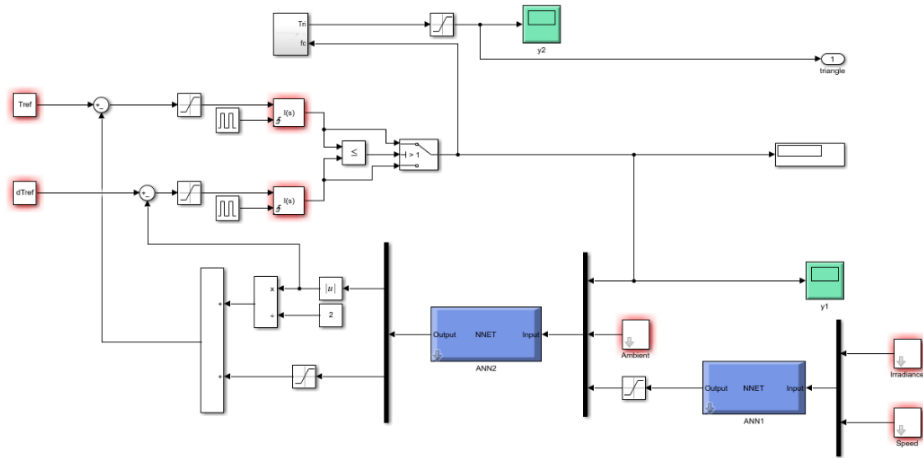


Figure 3-13. Proposed neural network model that controls the carrier frequency for the inverter to keep the temperature below pre-defined limit

### 3.8 Inverter Control Modelling

Figure 3-14. Structure of the inverter controller shows the inverter control modelling which uses the PWM technique to convert the DC signal to AC, this PWM model is shown in Figure 3-15. Structure of PWM generator model where we used the Neural network model discussed in the previous section which controls the IGBT temperature.

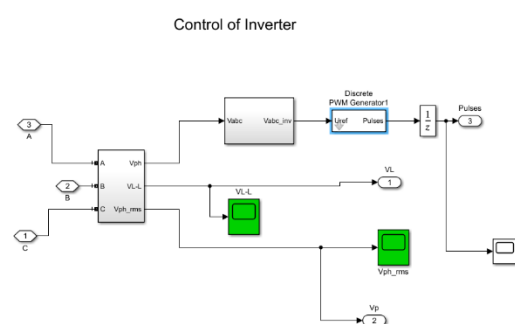


Figure 3-14. Structure of the inverter controller

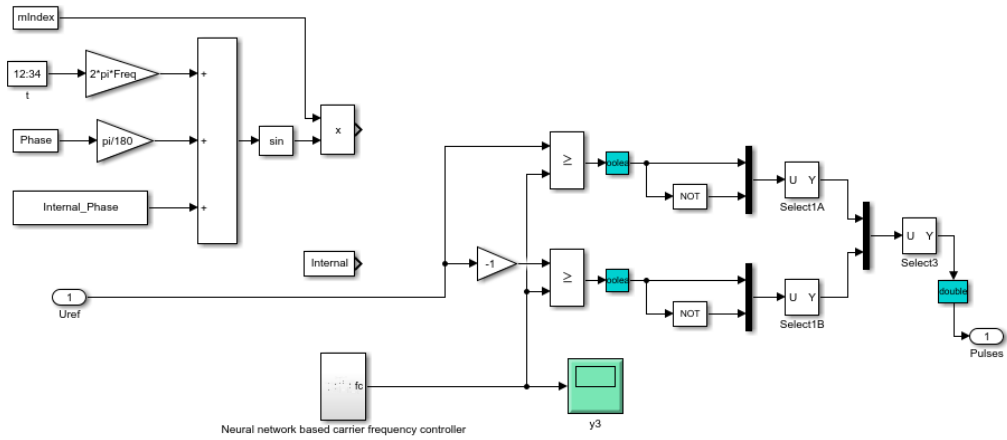


Figure 3-15. Structure of PWM generator model

### 3.9 Passive Filter Modelling

Figure 3-16 shows the basic low-pass filter that we used in our work in order to filter the harmonics in the resulted energy, the higher the filter components are, the clearer (less harmonics) the output signal was.

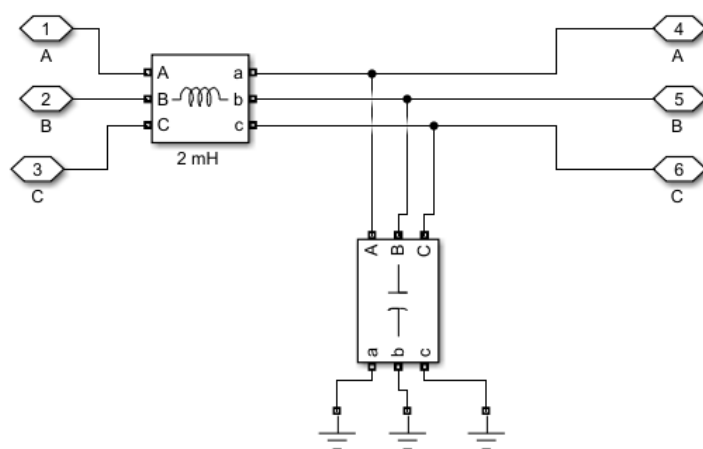


Figure 3-16. Structur of the low-pass passive filter modelling

### 3.10 Overall Design and Methodology

The overall design of the models discussed in this chapter is shown in Figure 3-17 while Figure 3-18. Proposed methodology to enhance the lifetime reliability of power electronics devices show the followed proposed methodology to enhance the lifetime reliability of power electronics devices. Firstly, the solar and wind power generators read the input mission profiles of the solar irradiance and the wind speed in order to generate the power according to them, after that, a DC/DC converter is connected at both generators to regulate the random generated profile, after that, the currents generated from both generators are summed up through a hybrid connection and transferred to the DC-link capacitors, which get charged and pass the energy to the inverter to convert it to AC signal to inject it to the grid, this inverter is controlled by the control of inverter model which uses the neural network models to control the IGBT junction temperature by changing the carrier frequency of the inverter, these neural networks are trained first by applying several mission profile data under several ambient temperatures and carrier frequencies, i.e. running several simulations in order to generate a dataset, and once the dataset is ready, the neural network can be found and placed in the system. The junction temperature is calculated using the power loss model and the Foster thermal network. And finally, the generated AC signal from the inverter is applied to the low-pass filter model to reduce the harmonics and generate a sinusoidal output voltage at the output.

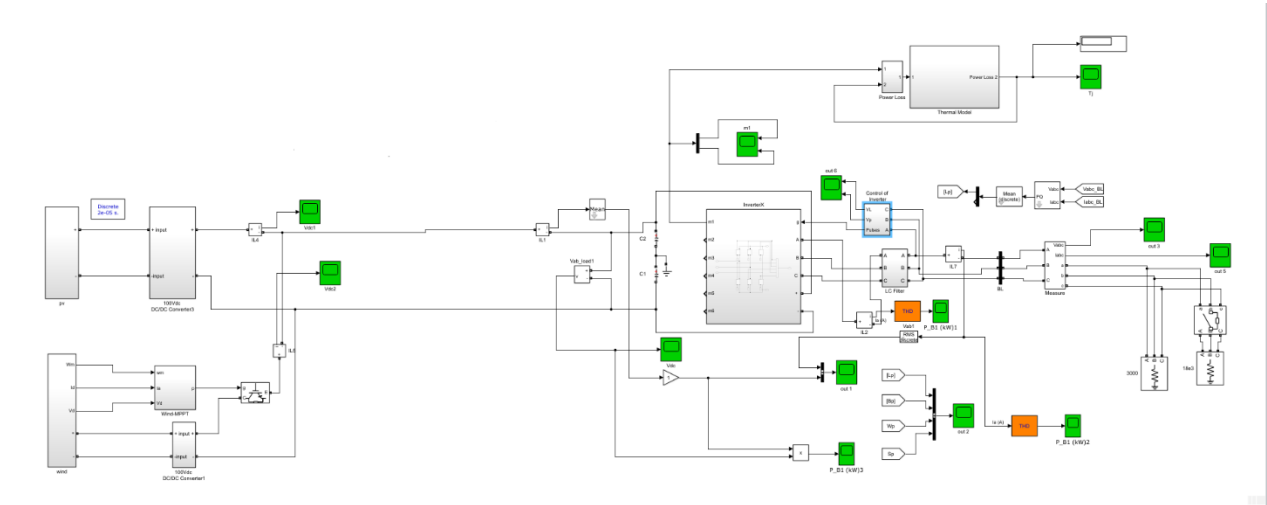


Figure 3-17. The overall design of the proposed system

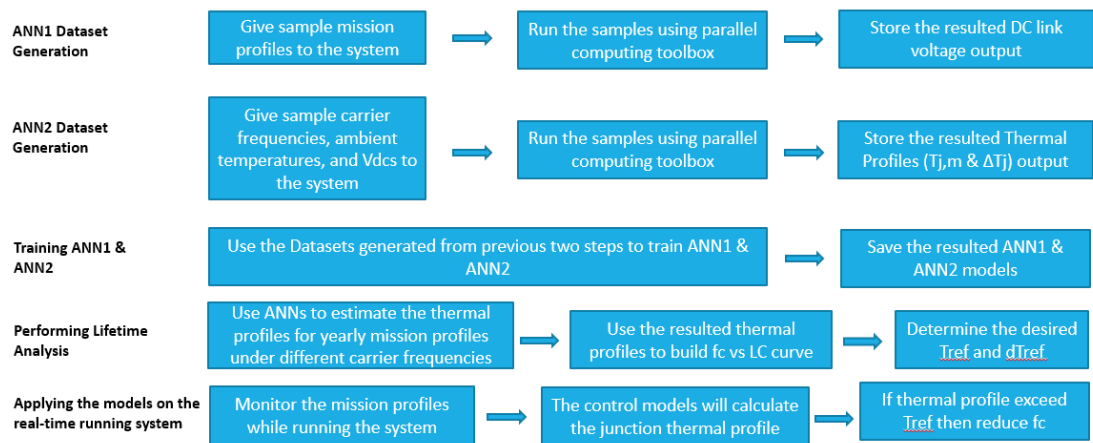


Figure 3-18. Proposed methodology to enhance the lifetime reliability of power electronics devices



## CHAPTER 4

### RESULTS AND DISCUSSION

In this chapter, we will show our models results and discuss them part by part.

#### 4.1 Power Generated from Solar Panels

The solar panels generate power according to the solar irradiance input Figure 4-1. 0 W Power generated from the solar panels at 0 W/m<sup>2</sup> irradiance., Figure 4-2, and Figure 4-3 show the generated power for  $0 \frac{W}{m^2}$ ,  $500 \frac{W}{m^2}$ , and  $1000 \frac{W}{m^2}$  solar irradiances, respectively, we can see here that the relation of the generated power is direct with the solar irradiance, also the maximum power generated from the maximum solar irradiance is 10 kW, this is because the load at the grid size was configured to be 10 kW and no more power can be generated under these circumstances, also, we can see that there are some delays before reaching the steady state power, this is due to the system dynamics.

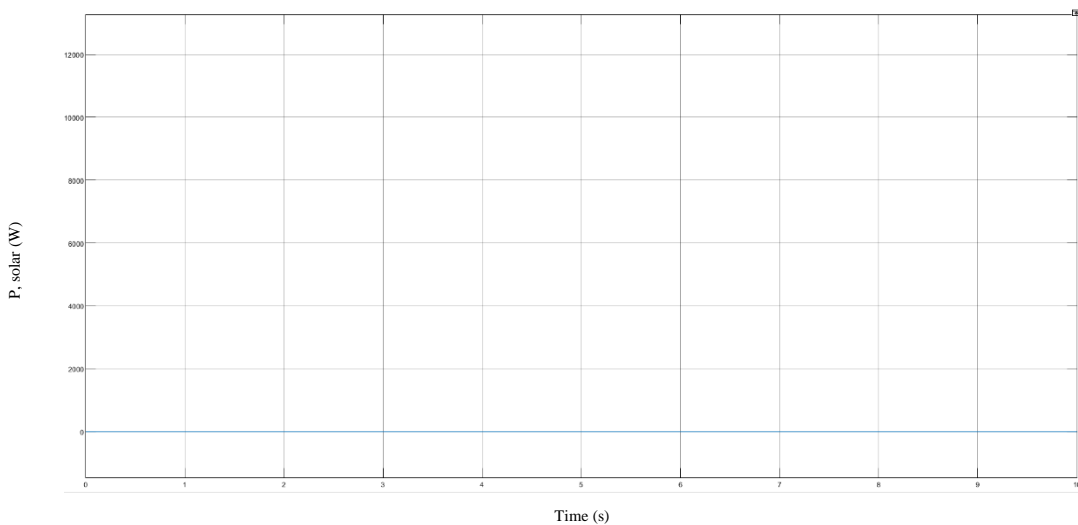


Figure 4-1. 0 W Power generated from the solar panels at 0 W/m<sup>2</sup> irradiance.

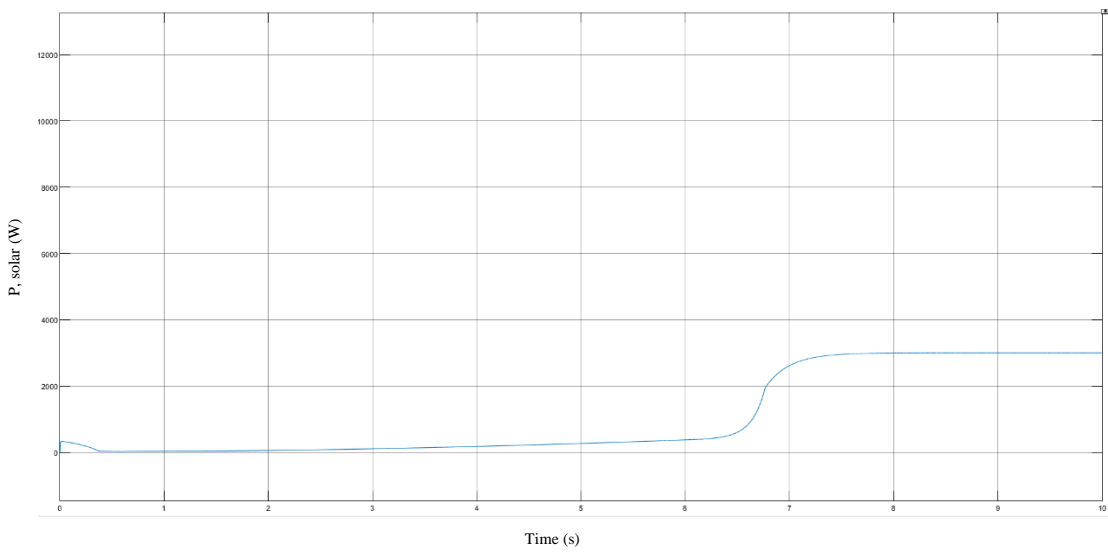


Figure 4-2. 3000 W Power generated from the solar panels at 500 W/m<sup>2</sup> irradiance.

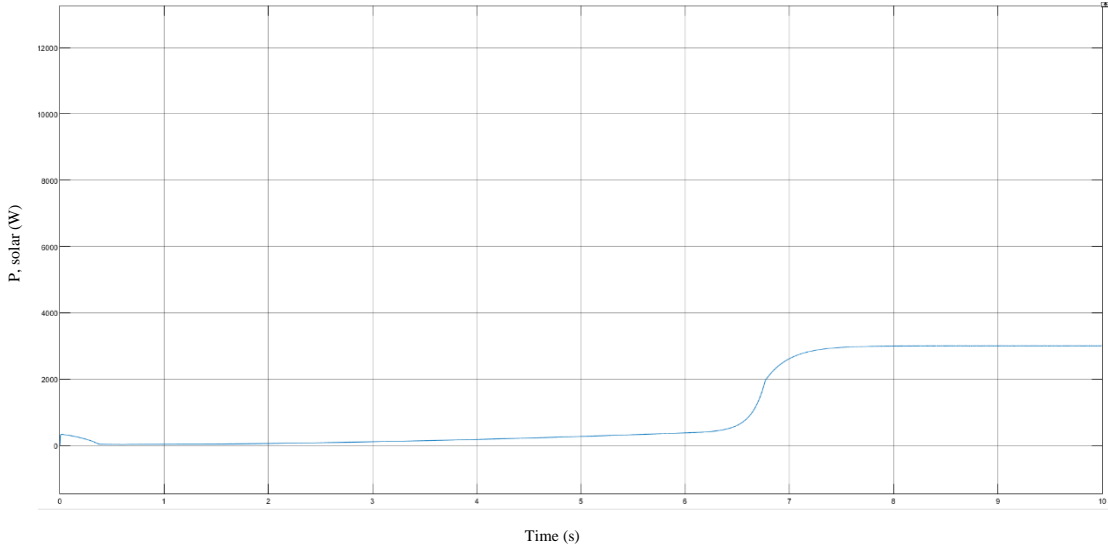


Figure 4-3. 10000 W Power generated from the solar panels at 1000 W/m<sup>2</sup> irradiance.

## 4.2 Power Generated from Wind Turbine Model

The generated power from the wind turbine is in direct relation with the wind speed at the turbine, Figure 4-4, Figure 4-5, and Figure 4-6 show the power generated under 0 m/s, 9 m/s, and 18 m/s, respectively, we chose the maximum speed to be 18 m/s because this is the highest recorded speed in our case study.

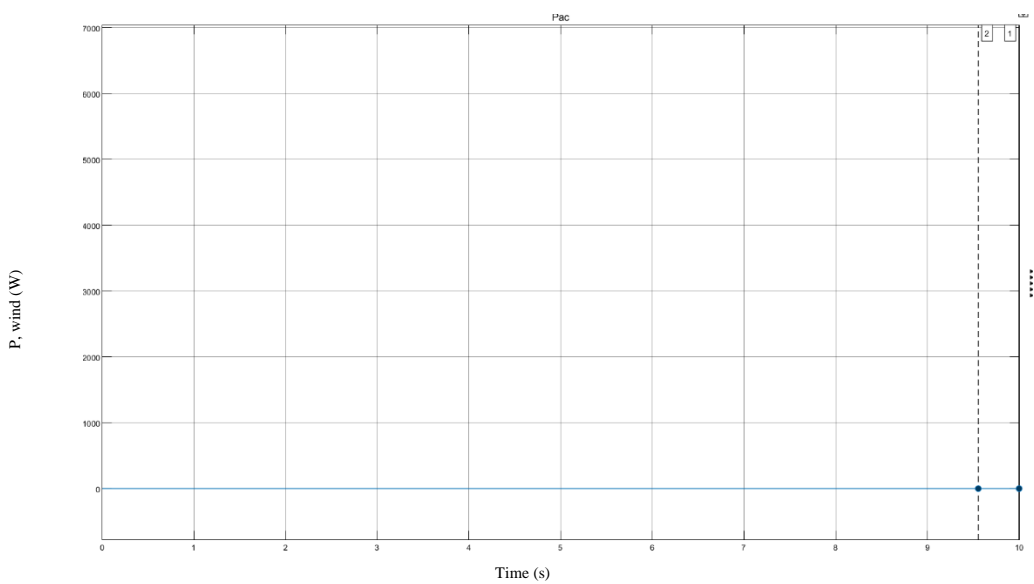


Figure 4-4. 0 W generated from the wind turbine under 0 m/s wind speed

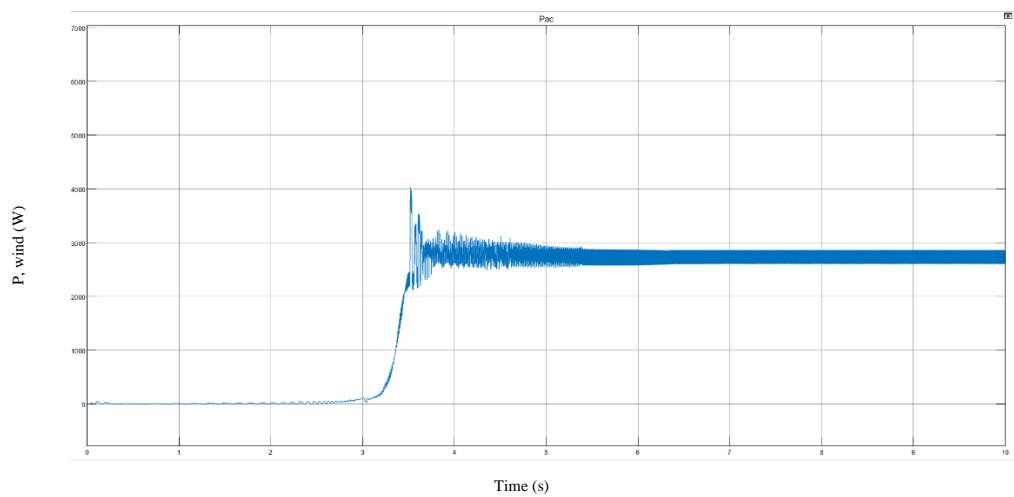


Figure 4-5. 2750 W generated from the wind turbine under 9 m/s wind speed

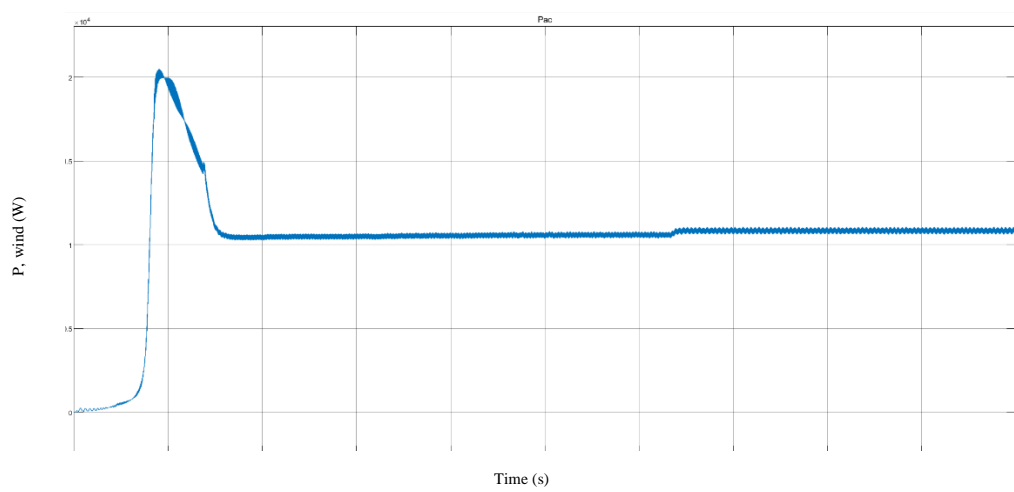


Figure 4-6. 10000 W generated from the wind turbine under 18 m/s wind speed

### 4.3 Generated Power from the Hybrid Combination of Solar and Wind Power Plants

The hybrid connection of both solar panel and wind turbine plants is designed to sum up the energy produced in both plants and pass it to the DC link capacitors, Figure 4-7 shows the case where the solar plant is on under a 1000 W/m<sup>2</sup> solar irradiance while the wind turbine is off under 0 m/s wind speed, while Figure 4-8 shows the opposite case where the wind turbine operates under 18 m/s wind speed and the solar plant is off (0 W/m<sup>2</sup> irradiance), when turning on both plants on a solar irradiance of 700 W/m<sup>2</sup> and wind speed of 5 m/s for example, the generated power from both plants is summed up and transferred to the DC link capacitors, this is the case shown in Figure 4-9.

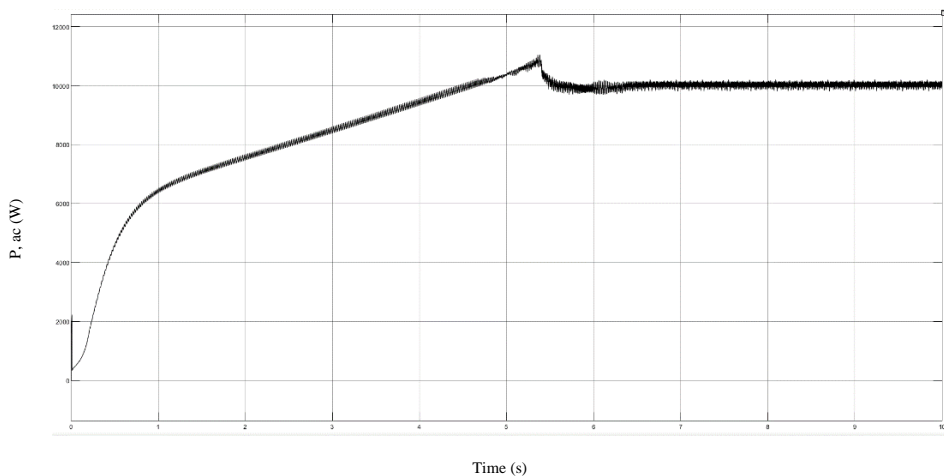


Figure 4-7. Generated power when the solar panel is on and the wind turbine is off

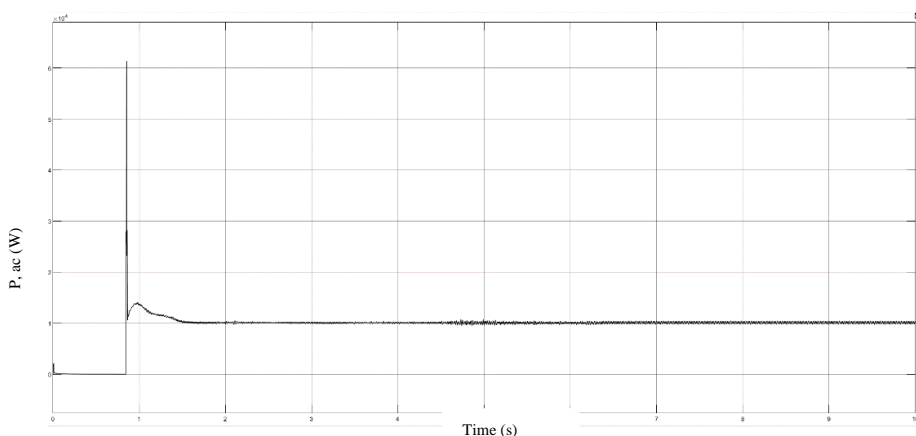


Figure 4-8. Generated power when the solar panel is off and the wind turbine is on

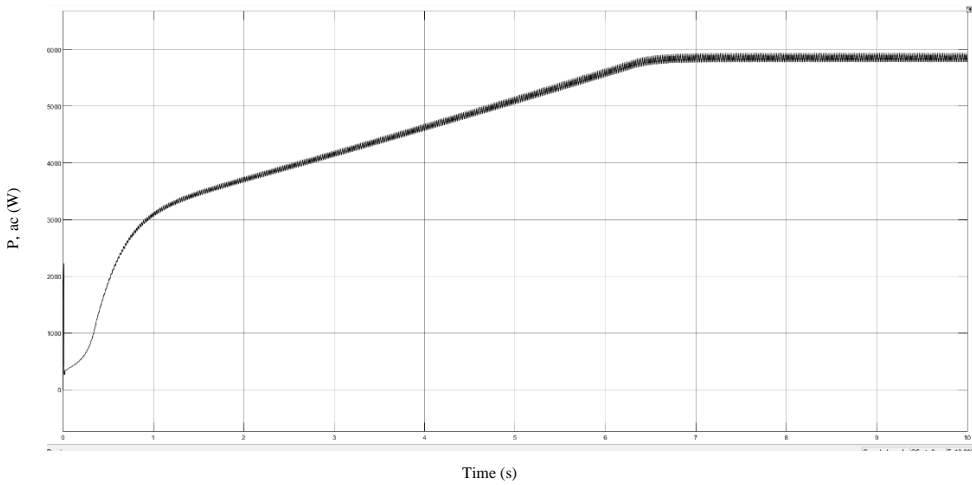


Figure 4-9. Generated power when both plants are on.

#### 4.4 DC-Link Voltage

After generating the power from the renewable plants, it goes and charge the DC-link voltage of the inverter through capacitors, this voltage is dependent on the current produced from the power plants (not directly related to the generated power), this is why the DC-link voltage is lower in the case where the solar plant is operating at the maximum solar irradiance while the wind turbine is turned off (shown in Figure 4-10. DC-link voltage when the solar panel is on and the wind turbine is off) and higher in the opposite case (shown in Figure 4-11). Figure 4-12 shows the arbitrary case discussed in the previous section when both plant are on under 700 W/m<sup>2</sup> solar irradiance and 5 m/s wind speed.

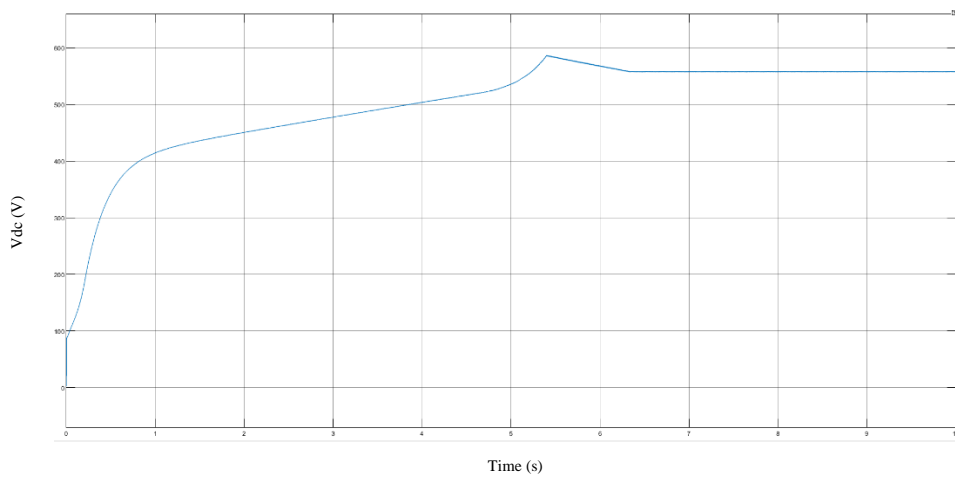


Figure 4-10. DC-link voltage when the solar panel is on and the wind turbine is off

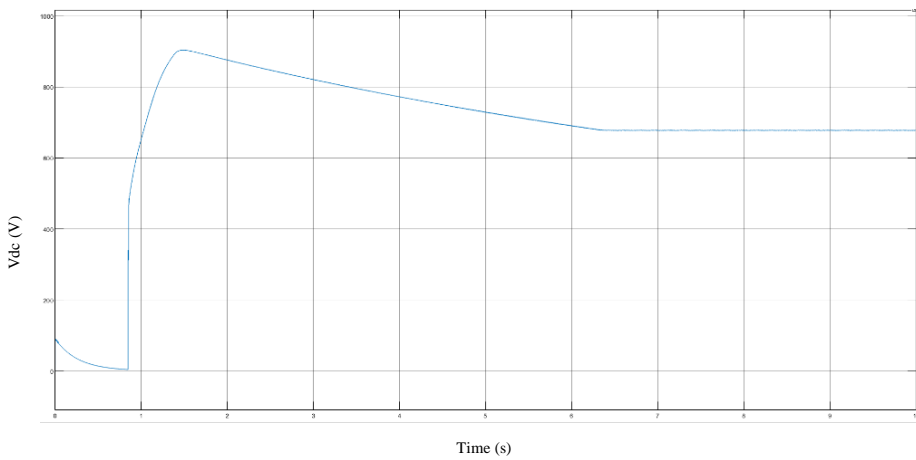


Figure 4-11. DC-link voltage when the solar panel is off and the wind turbine is on

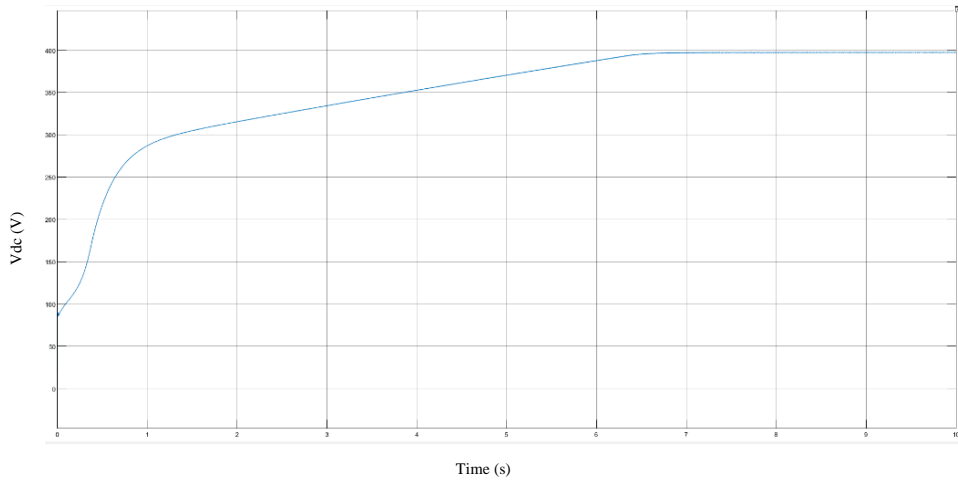


Figure 4-12. DC-link voltage when both plants are on but the solar panel has the dominant energy production.

#### 4.5 Junction Temperature Calculation using Thermal Modelling

The junction temperature in the discrete IGBT inside our power inverter is mainly dependent on the DC-link voltage discussed in the previous section, the ambient temperature, and the carrier frequency of the triangle wave which is used to control the inverter, and hence, we will discuss the effect of each one of these parameters on the junction temperature in this section.

#### 4.5.1 DC-Link Voltage Effect on the Junction Temperature

Figure 4-13 shows the junction temperature response for the conditions DC-link voltage ( $V_{dc}$ ) = 200 V, carrier frequency ( $f_c$ ) = 2000 Hz, and ambient temperature ( $T_a$ ) = 0 C, while Figure 4-14 shows the junction temperature response for the operating conditions  $V_{dc}$  = 508 V,  $f_c$  = 2000 Hz, and  $T_a$  = 0 C. We can see here, that when the  $V_{dc}$  is higher the mean junction temperature and the peak-to-peak junction temperature is higher, and hence, the relation between the junction temperature and the DC-link voltage is direct.

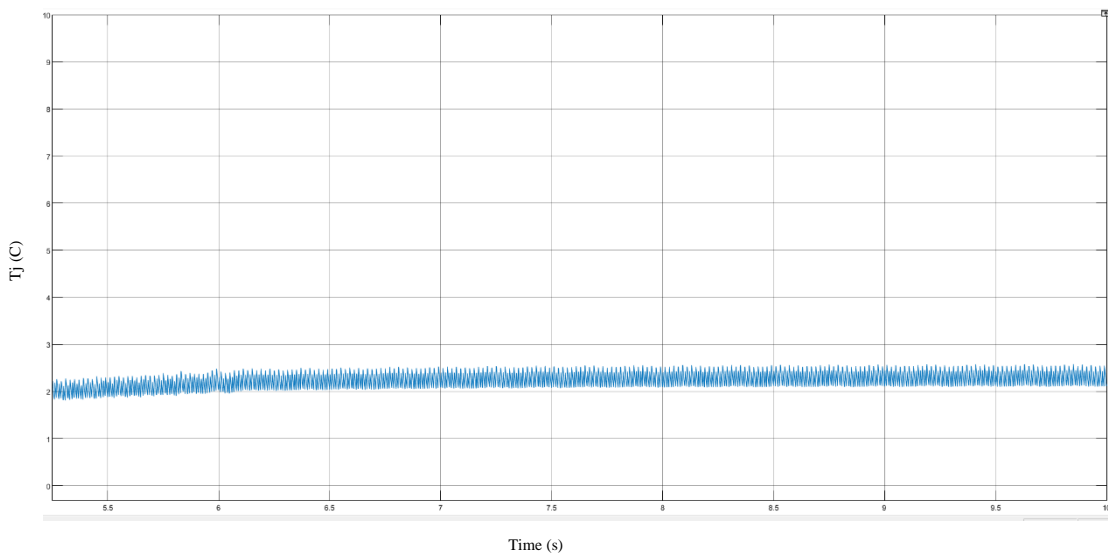


Figure 4-13. Junction temperature response for the 200 V  $V_{dc}$  case

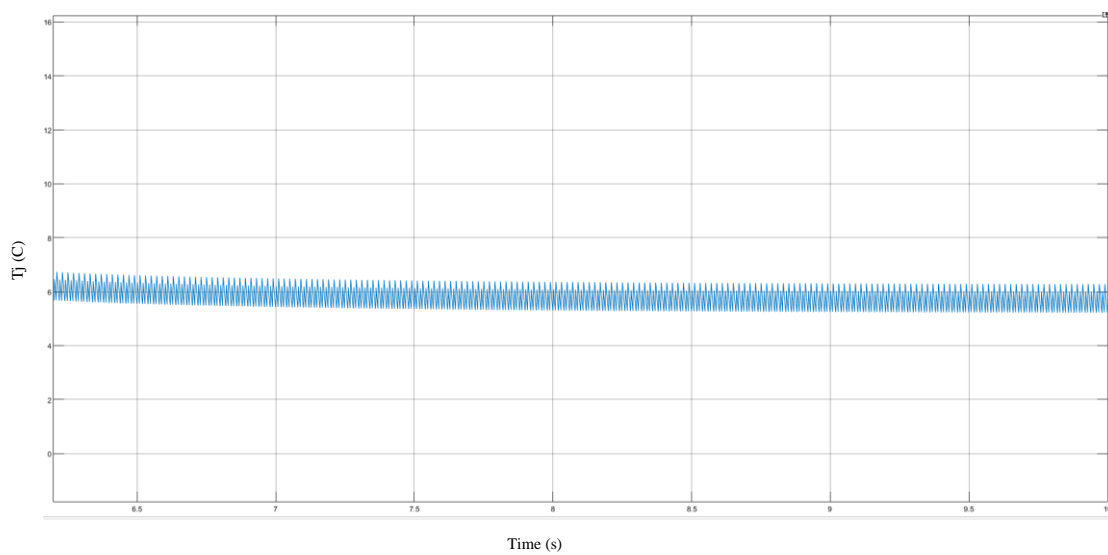


Figure 4-14. Junction temperature response for the 508 V  $V_{dc}$  case

#### 4.5.2 Carrier Frequency Effect on the Junction Temperature

Figure 4-13 Figure 4-15 shows the junction temperature response for the conditions  $V_{dc} = 508$  V,  $f_c = 2000$  Hz, and  $T_a = 0$  C, while Figure 4-16 shows the junction temperature response for the operating conditions  $V_{dc} = 508$  V,  $f_c = 10000$  Hz, and  $T_a = 0$  C. We can see here, that when the  $f_c$  is higher the mean junction temperature and the peak-to-peak junction temperature is higher, and hence, the relation between the junction temperature and the carrier frequency is also direct.

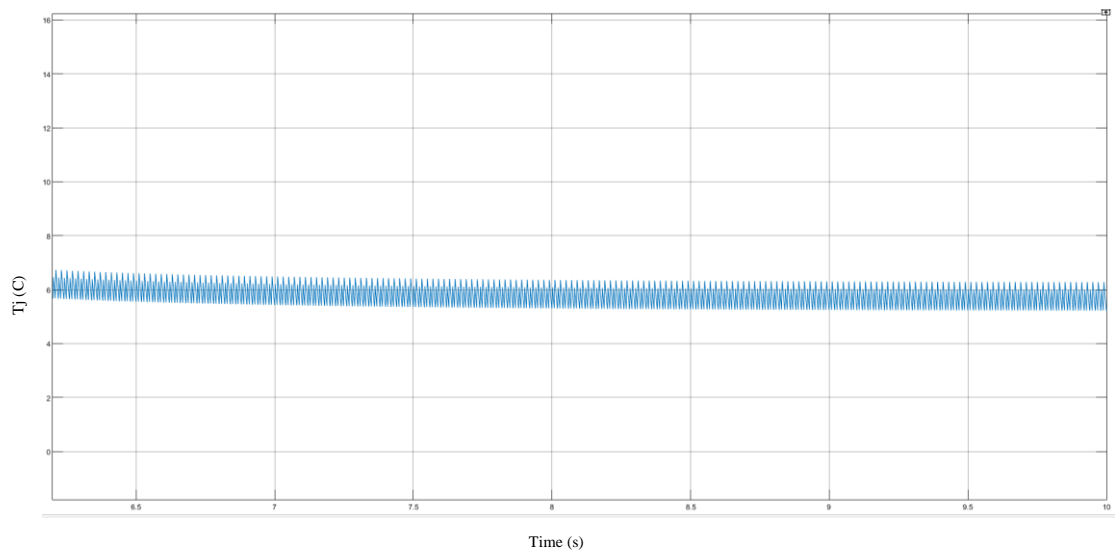


Figure 4-15. Junction temperature response for the 2000 Hz carrier frequency case

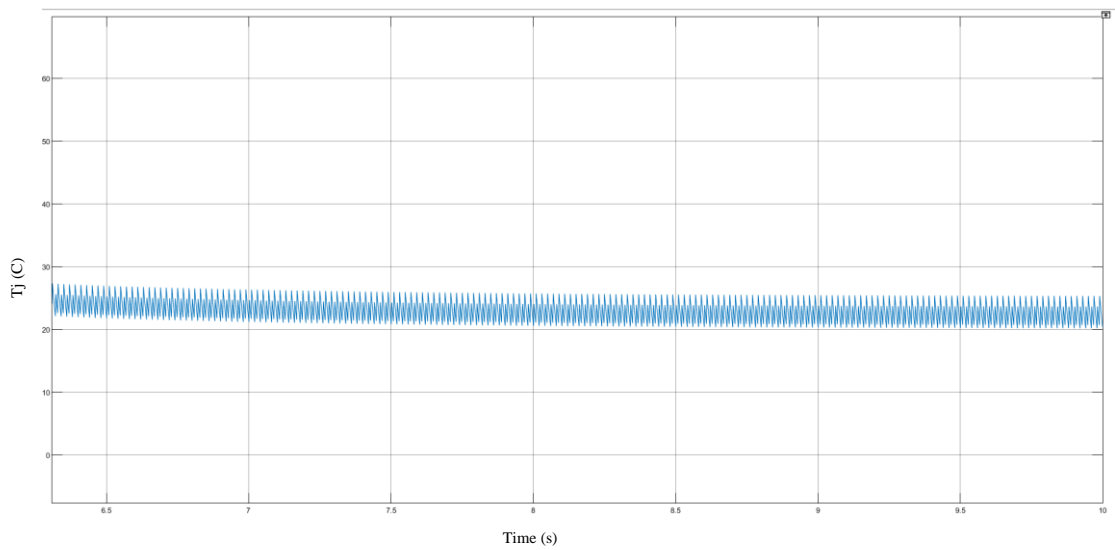


Figure 4-16. Junction temperature response for the 10000 Hz carrier frequency case

#### 4.5.3 Ambient Temperature Effect on the Junction Temperature

Figure 4-17 shows the junction temperature response for the conditions  $V_{dc} = 508$  V,  $f_c = 2000$  Hz, and  $T_a = 0$  C, while shows the junction temperature response for the operating conditions  $V_{dc} = 508$  V,  $f_c = 2000$  Hz, and  $T_a = 20$  C. We can see here, that when the ambient temperature is higher the mean junction temperature and the peak-to-peak junction temperature is higher, and hence, the relation between the junction temperature and the ambient temperature is also direct.

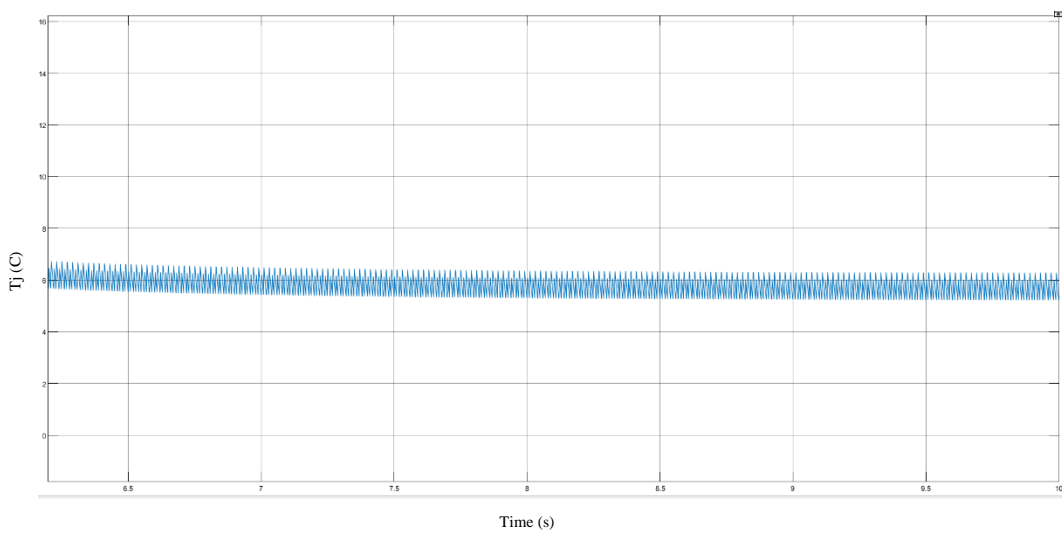


Figure 4-17. Junction temperature response for the 0 C ambient temperature case

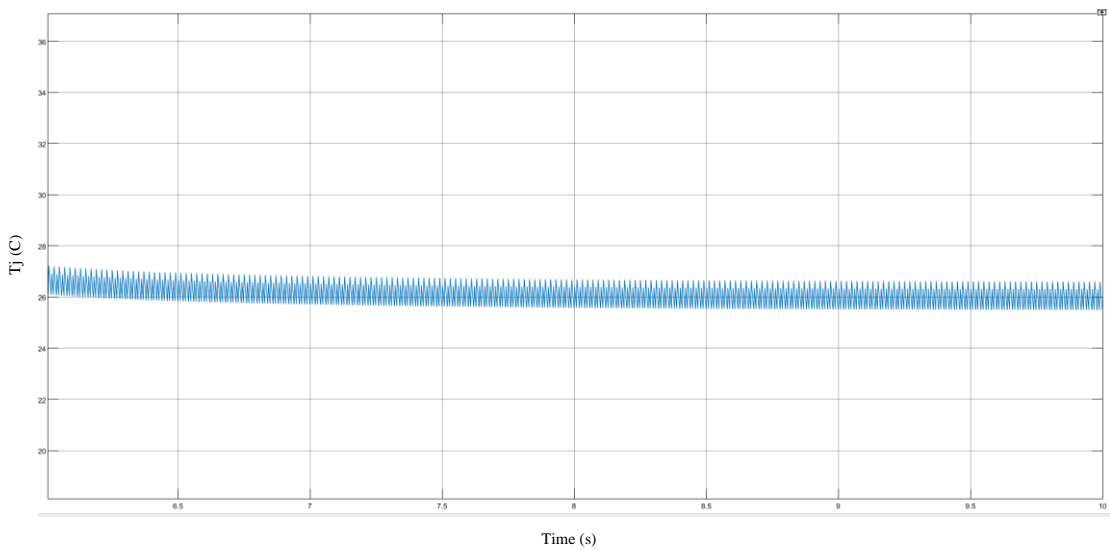


Figure 4-18. Junction temperature response for the 20 C ambient temperature case

## 4.6 Neural Networks Training Criteria

The neural network was built using Simulink simulation parallel tool dataset, for the first neural network (ANN1), we gave an input irradiance from 0 W/m<sup>2</sup> to 1000 W/m<sup>2</sup> with a 50 W/m<sup>2</sup> step, the thing that leads to 21 solar irradiance operating points, while for the wind speed, we gave an input of 0 m/s to 20 m/s with 1 m/s step, which leads to another 21 wind speed operating points, then we used the Simulink parallel tool to run several simulations of the system through the whole operating conditions, i.e. 441 times as shown in Figure 4-19. In each of these simulation points, we recorded the generated power for study purposes and the DC-Link voltage to be the target of ANN1 and the input of ANN2, and these data were tabulated and can be seen in Appendix A. The similar process has been followed to generate the dataset for ANN2, here we varied the DC-link voltage between 0 V and 700 V with a step of 50 V, we varied the ambient temperature between 0 C and 40 C, and we varied the carrier frequency between 2000 Hz and 20000 Hz, this resulted in  $15 \times 9 \times 10 = 1350$  dataset which were obtained again by the parallel tool in the MATLAB simulink as shown in Figure 4-20 and attached in Appendix B.

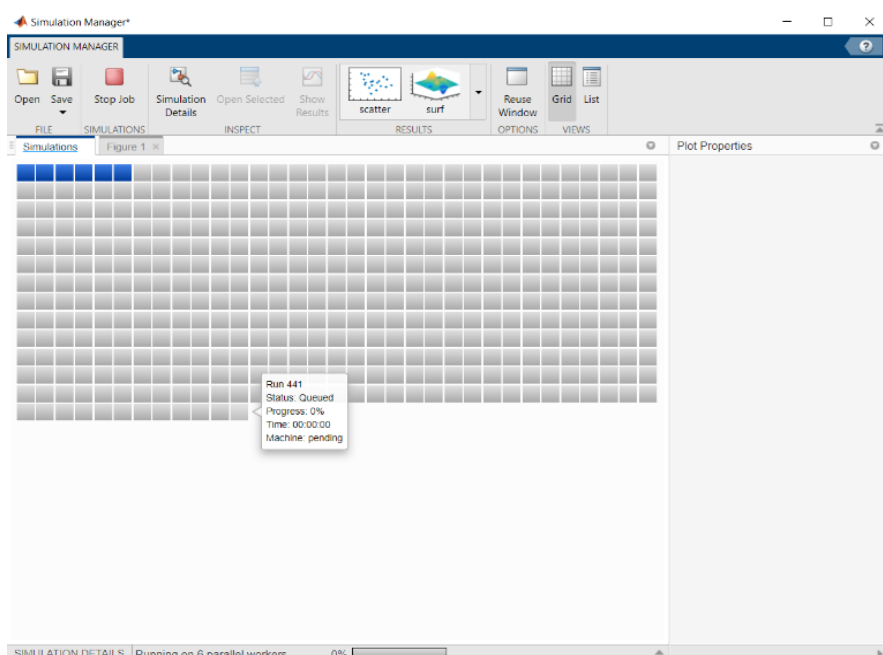


Figure 4-19. Generating the dataset for ANN1

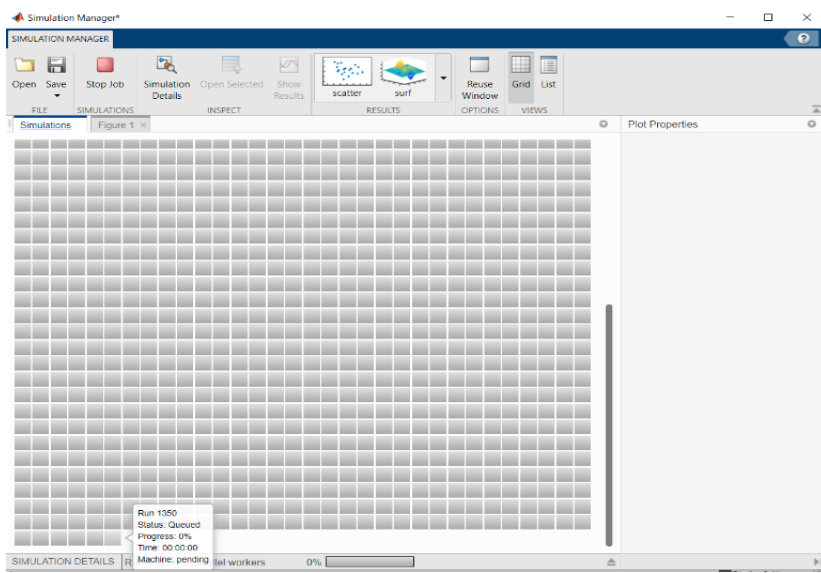


Figure 4-20. Generating the dataset for ANN2

After setting the datasets we used the built-in Levenberg-Marquardt training algorithm to train both neural networks, the number of hidden layers of ANN1 was chosen by trial and error to be 29 hidden layers as shown in the training stage in Figure 4-21 and the root mean square error (RMSE) for the training data was 6.67, while for ANN2 we used 30 hidden layers as shown in the training stage in Figure 4-22 and the mean square error (MSE) for the training data was 0.1476.

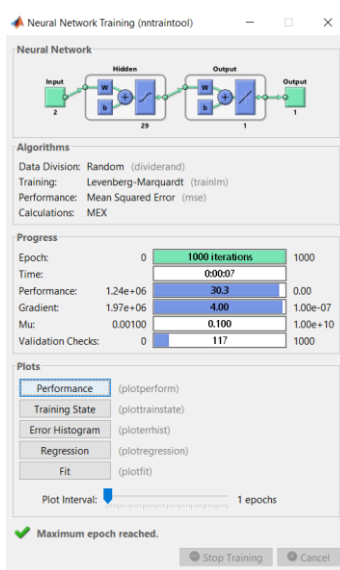


Figure 4-21. Training stage of ANN1

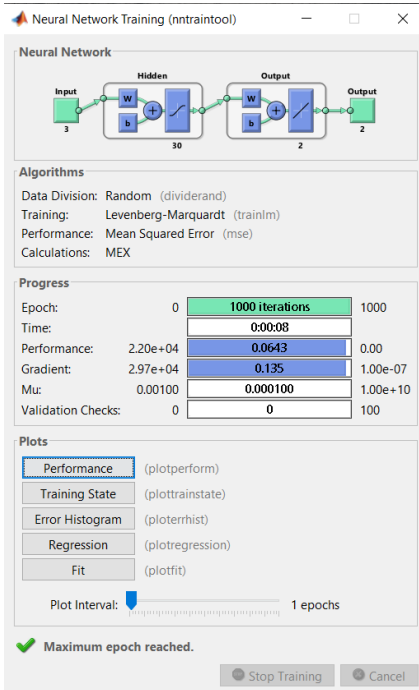


Figure 4-22. Training stage of ANN2

After that, we tested both neural networks validity using a real wind speed, solar irradiance, and ambient temperature mission profiles taken from the METU NCC campus by (Taylan, 2018), Table 4.1 shows 5 of the mission profiles operating conditions results under 2000 HZ carrier frequency and compare between the simulated temperature using MATLAB and the predicted temperature by the ANNs, we can see the ANNS almost predicted the results correctly, and hence, they are reliable to use directly without going through the system dynamics.

Table 4.1. Comparison between simulated and predicted results using some mission profiles operating points done by (Taylan,2018)

Operating condition	Iin (W/m2)	Uw (m/s)	Ta (C)	fc (Hz)	Simulated Vdc (V)	Predicted Vdc (V)	Simulated Tj,m (C)	Predicted Tj,m (C)	Simulated ΔT (C)	Predicted ΔT (C)
Number 1	497.00	3.16	17.40	2000.00	282	283.7	20.6	21.9687	0.597	0.7247
Number 2	798.89	6.09	13.20	2000.00	453.5	461.38	18.45	20.3	0.962	1.24
Number 3	272.98	9.75	15.10	2000.00	347.6	352.98	19.2	21	0.737	0.9722
Number 4	341.78	11.95	18.20	2000.00	443.2	448.25	23.4	25.25	0.95	1.24
Number 5	874.62	0.61	26.10	2000.00	496.6	517.92	32	36.83	1.1	2

## 4.7 Lifetime Analysis Results

After preparing the neural networks, we used the mission profiles done by (Tylan,2018) in METU NCC campus as a case study, this mission profile contained 8760 hours data in the year 2017 of the solar irradiance, wind speed, and ambient temperature as shown respectively in Figure 4-23, we applied a carrier frequency on these mission profiles and varied it between 2000 Hz to 15000 Hz and extracted the mean junction temperature  $T_m$  and the peak-to-peak junction temperature for each operating condition using the designed ANNs, after that, we used the Coffin–Manson–Arrhenius Model discussed in section 1.6 to calculate the lifetime, the constants in the model were used from the reference (Dragicevi, 2018) paper, and the relation between the yearly life time consumption (LC) with the frequency was plotted in Figure 4-244 we can see here that as the frequency goes higher, the lifetime consumption increases, and hence, to increase the lifetime, we need to operate under low frequencies.

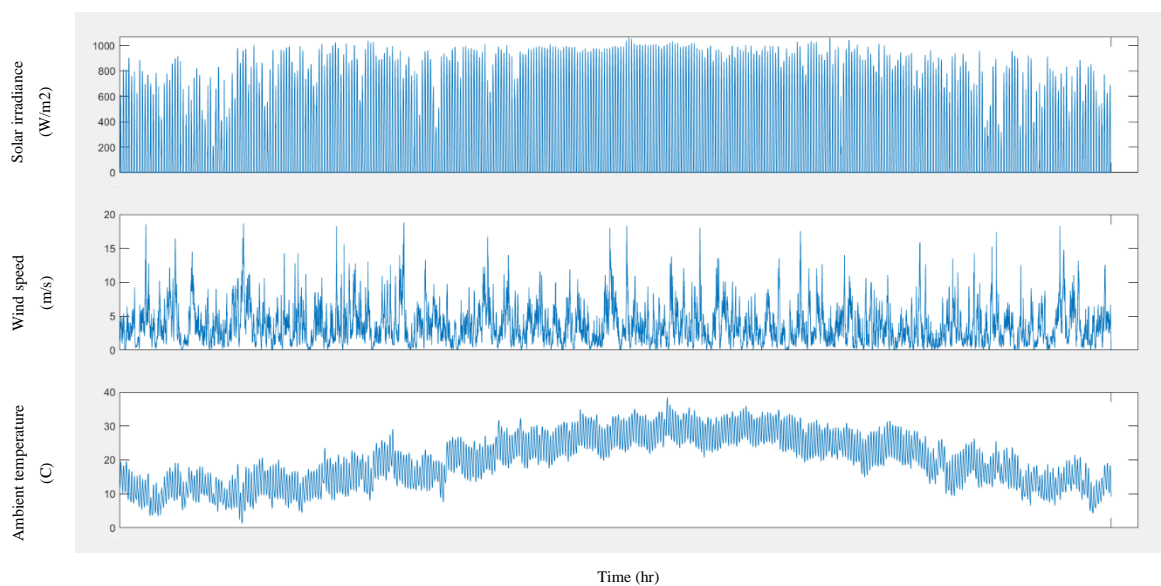


Figure 4-23. Yearly mission profiles of solar irradiance, wind speed, and ambient temperature from the REDAR search group at METU NCC

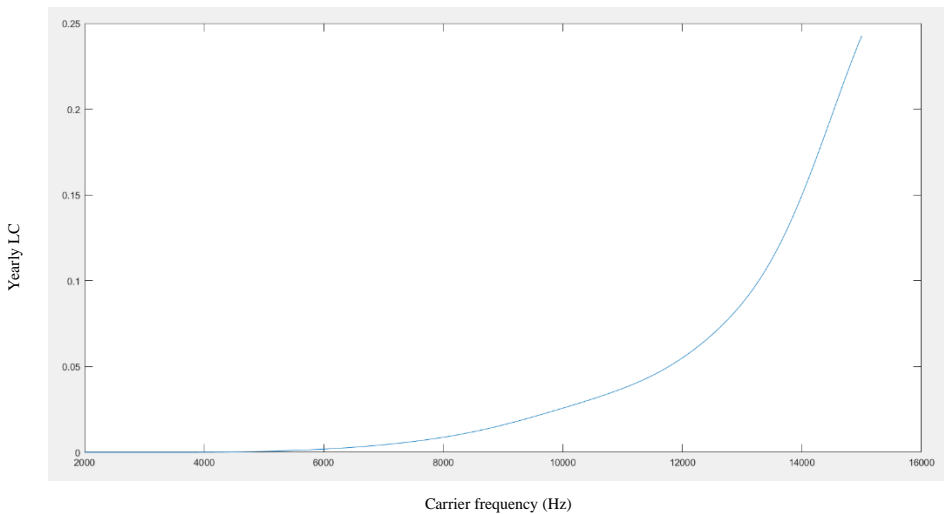


Figure 4-24. Relation between the frequency and the yearly lifetime consumption

#### 4.8 Carrier Frequency and Filtering Effects on the Output Signal Quality

Even though lower carrier frequencies increase the lifetime as discussed in the previous section, the output voltage quality increases with increasing the carrier frequency or the output LC filter components, for instance, Figure 4-25. 3 phase output voltage for 2000 Hz carrier frequency shows a 3-phase output voltage from an inverter that works under 2000 Hz carrier frequency and the output LC filter was built from a 36 mH inductor and a 8 uF capacitor, we can see here that the output voltage quality has a lot of noisy harmonics and hence, a solution is required.

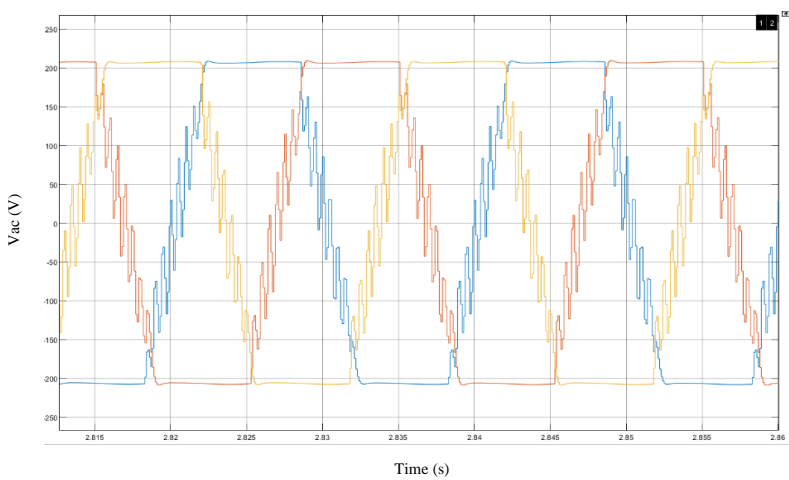


Figure 4-25. 3 phase output voltage for 2000 Hz carrier frequency, 36 mH and 8 uF LC filter components

The first solution can be done by using larger filter components, Figure 4-266 shows the 3-phase output voltage from an inverter working under the same carrier frequency (2000 Hz) but with increasing the capacitor value in the LC filter to 25 uF and keeping the inductor as 36 mH, we can see here that the output voltage quality has enhanced compared to the original case.

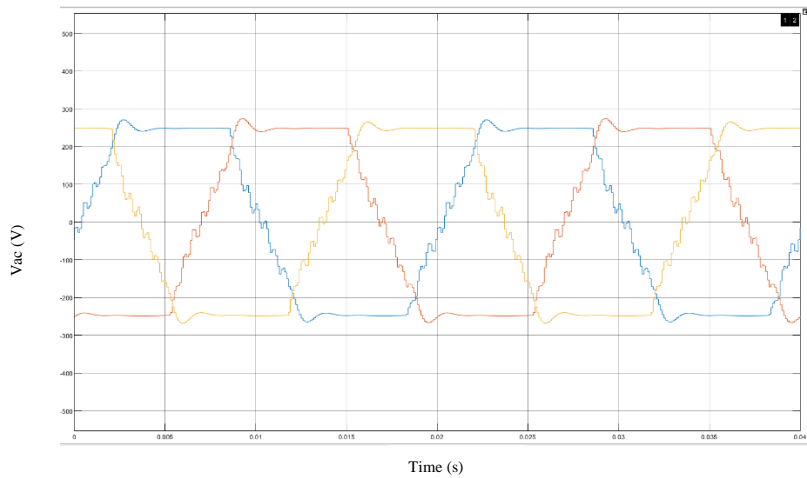


Figure 4-26. 3 phase output voltage for 2000 Hz carrier frequency, 36 mH and 25 uF LC filter components

Another better solution can be done by simply increasing the carrier frequency, this can be shown in Figure 4-277 where the carrier frequency was increased to 15000 Hz and the LC filter components were kept as 36 mH inductor and 8 uF capacitor, however, this solution is more expensive compared to the first solution because the yearly life time consumption is increased to almost 0.24 when working under 15000 Hz carrier frequency according to Figure 4-24. Relation between the frequency and the yearly lifetime consumption, which means that the inverter is expected to collapse after almost 4 years, while in the first solution, replacing the 7 uF capacitor with a 25 uF capacitor will cost much more less and will keep the expected yearly lifetime consumption significantly lower (the inverter can work more than 20 years).

Table 4.2. Financial summary of 2 solutions that can enhance the output voltage quality shows the financial summary of both solutions, where the prices were taken

from the official ABB and Vishay manufacturers pricelist, we can see here that the cost of operating the inverter under high frequencies can be 3 times more expensive than replacing the LC filter components with larger components, however, operating under high carrier frequency can give much better output voltage quality, and hence, a trade-off should be done between the inverter produced energy quality and the inverter's component lifetime.

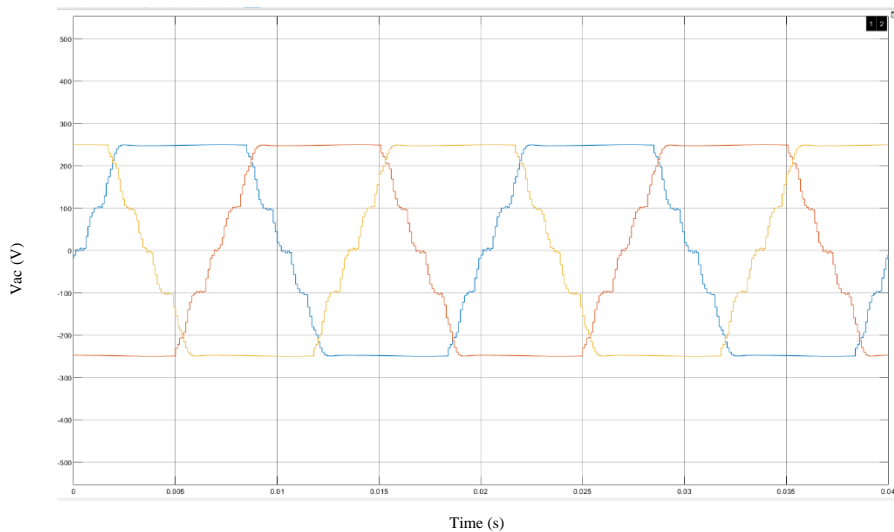


Figure 4-27. 3 phase output voltage for 15000 Hz carrier frequency, 36 mH and 8 uF LC filter components

Table 4.2. Financial summary of 2 solutions that can enhance the output voltage quality of an inverter

Case Scenario	Carrier Frequency	LC Filter Components	Inverter Cost & Lifetime	Capacitor Cost & Lifetime	O&M Cost in 12 Years	Notes
Base case	fc=2000 Hz	L= 36 mH, C= 7 uF	1600 USD (ABB), works for more than 10 years	5.66 USD (Vishay), works for almost 12 years	1605.66 USD	
Solution 1	fc=2000 Hz	L= 36 mH, C= 25 uF	1600 USD (ABB), works for more than 10 years	20.74 USD (Vishay), works for almost 7 years	1641.8 USD	This solution is cheap but the output voltage quality still needs enhancement
Solution 2	fc=15000 Hz	L= 36 mH, C= 7 uF	1600 USD (ABB), works for almost 4 years	5.66 USD (Vishay), works for almost 12 years	4805.66 USD	This solution is expensive but the output voltage quality is much better than solution 1

The state of art of our proposed model is to combine the advantages of both solutions at the same time by reducing the lifetime consumption of the inverter at high frequencies, this can be done using the fact that a large portion of the lifetime increment is happening at extreme high temperature points, and hence, if we

reduced the carrier frequency at these extreme (pre-defined threshold temperature or peak-to-peak heating cycle) points and return it to the high operating carrier frequencies when the normal temperature points return, the lifetime consumption when working at high carrier frequencies can be very close to the lifetime consumption when working under low carrier frequencies, and hence, the inverter will not need frequent replacement and the O&M cost will not increase by much. On the other hand, replacing the LC filter components with larger capacitors can still be useful to remove the harmonics in the few moments when the inverter reduces its carrier frequency at the extreme temperature points.

This model was justified on the base scenario discussed earlier in this chapter, we set the threshold temperature to be 70 C and peak-to-peak heating cycle to 10 C, which means that when the junction temperature goes above 70 C or its peak-to-peak heating cycle goes above 10 C, the controller drags the carrier frequency down and return it to the normal high frequency when it goes below the references points again, after that, we did the lifetime analysis and we found that the lifetime consumption went from 0.24 without our model to 0.047 when using the proposed model, and hence the inverter can almost work for 20 years under high carrier frequencies without any need to replace it.

## **CHAPTER 5**

### **CONCLUSION AND FUTURE WORK**

#### **5.1 Conclusion**

In this work, we proposed an automated system which works using the artificial intelligence to enhance the lifetime reliability of power electronics devices, the main idea behind the system is to reduce the frequency when the junction temperature of a discrete IGBT goes above a pre-defined threshold or peak-to-peak heating cycle, this will help the inverter to keep operating under high carrier frequencies and provide optimal quality output without going to the risk of increasing the lifetime consumption by much due to the high frequencies. Also, the LC filter capacitors can be increased to compensate the ripples that may occur when the carrier frequency is reduced at the rare high junction temperature operating points.

#### **5.2 Future Work**

In this work, we used a 2-level battery-less power electronics inverters, the proposed system can be extended in the future to deal with 3-level inverters and with power system that uses storage unit to store the excessive energy and see the effects of adding such system on the power electronics components in addition to the storage units. Preliminary studies already showed that the voltage waveforms will be much smoother with the integration of the batteries into the system. The voltage waveforms can be depicted in Figure 5.1. In the proposed work, the lifetime calculation algorithms designed in neural networks, and it was tested in this thesis initially in a battery less in purpose to validate the performance of the method in a harsh environment.

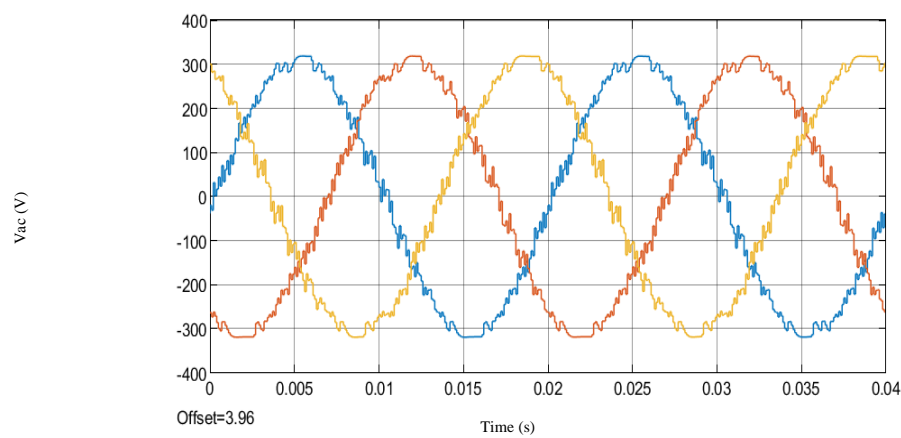


Figure 5-1. 3 phase output voltage within a battery integrated system for 15000 Hz carrier frequency, 36 mH and 8 uF LC filter component



## **REFERENCES**

- Alan S. Morris, Reza Langari, 2012, Measurement and Instrumentation, Theory and Application, Butterworth-Heinemann.
- Alhussein Albarbar, Canras Batunlu, 2018, Thermal Analysis of Power Electronic Devices Used in Renewable Energy Systems, Springer International Publishing.
- C.Batunlu and A.Albarbar, 2015, A Technique for Mitigating Thermal Stress and Extending Life Cycle of Power Electronic Converters Used for Wind Turbines, Electronics 2015, 4, 947-968; doi:10.3390/electronics4040947
- D.I. Crecraft, S. Gergely, 2002, Analog Electronics: Circuits, Systems and Signal Processing, Butterworth-Heinemann.
- Dr. Siva Malla, (2021). PMSG based Wind Power Generation System (<https://www.mathworks.com/matlabcentral/fileexchange/36116-pmsg-based-wind-power-generation-system>), MATLAB Central File Exchange. Retrieved August 8, 2021.
- Gilbert M. Masters, July 28, 2004, Renewable and Efficient Electric Power Systems, John Wiley & Sons. DOI:10.1002/0471668826.
- Howard Austerlitz, 2003, Data Acquisition Techniques Using PCs (Second Edition), Academic Press.
- H. Wang, K. Ma, and F. Blaabjerg, 2012, "Design for reliability of power electronic systems," in Proc. IECON 2012, pp. 33-44.
- Mohammad A.S. Masoum, Ewald F. Fuchs, 2015, Power Quality in Power Systems and Electrical Machines (Second Edition), Academic Press.

- N. Sønnichsen, Jun 22, 2021, Global electricity consumption 1980-2018, <https://www.statista.com/statistics/280704/world-power-consumption>.
- M. Shahbazi, A. Khorsandi, 2017, Power Electronic Converters in Microgrid Applications, Microgrid, Sciencedirect.
- Ned Mohan, Tore M Undeland, William P Robbins, 2003, Power electronics: converters, applications, and design, John wiley & sons.
- Nikolaus Kriegeskorte, Tal Golan, 2019, Neural network models and deep learning, CellPress.
- Rosmaliati, Novie Elok Setiawati, Mauridhi Hery Purnomo, and Ardyono Priyadi, 2018, Nguyen-Widrow Neural Network for Distribution Transformer Lifetime Predictio, International Conference on Computer Engineering, Network and Intelligent Multimedia (CENIM)
- Sadati S.M.S., Jahani E., Taylan O., Baker D.K. (2018), “Sizing of PV-Wind-Battery Hybrid System for a Mediterranean Island Community Based on Estimated and Measured Meteorological Data”, Journal of Solar Energy Engineering, 140, p. 011006, doi:10.1115/1.4038466.
- Salman Mohagheghi, Ronald G. Harley, Thomas G. Habetler, and Deepak Divan, 2009, Condition Monitoring of Power Electronic Circuits Using Artificial Neural Networks, IEEE TRANSACTIONS ON POWER ELECTRONICS, VOL. 24, NO. 10.
- Sangwongwanich, A., Yang, Y., Sera, D., & Blaabjerg, F. (2017). Lifetime Evaluation of Grid-Connected PV Inverters Considering Panel Degradation Rates and Installation Sites. IEEE Transactions on Power Electronics, PP(99), 1-10
- Slimen A., Tlijani H., Dhaoui M., Younes R.B. , 2019, Control of Wind Turbine Based on PMSG Using Pitch Angle Control. In: Derbel N., Zhu Q. (eds) Modeling, Identification and Control Methods in Renewable Energy Systems. Green Energy and Technology. Springer, Singapore.  
[https://doi.org/10.1007/978-981-13-1945-7\\_7](https://doi.org/10.1007/978-981-13-1945-7_7).

Tomislav Dragicevi, Patrick Wheeler, and Frede Blaabjerg, 2018, Artificial Intelligence Aided Automated Design for Reliability of Power Electronic Systems, IEEE Transactions on Power Electronics, DOI: 10.1109/TPEL.2018.2883947

Vaughn Nelson, 2009, Wind Energy: Renewable Energy and the Environment, CRC Press, Taylor & Francis Group.

Ulutaş, Alper & DURU, Tarık, 2019, Variable-Speed Direct-Drive Permanent Magnet Synchronous Generator Wind Turbine Modeling and Simulation. Kocaeli Journal of Science and Engineering. 2. 21-27. 10.34088/kojose.515467.

U.S. Department of Energy, 2021, Hybrid Wind & Solar Electric Systems  
<https://www.energy.gov/energysaver/hybrid-wind-and-solar-electric-systems>.

Xuelian Pang, Zhuo Li , Ming-Lang Tseng, Kaihua Liu, Kimhua Tan and Hengyi Li, 2020, Electric Vehicle Relay Lifetime Prediction Model Using the Improving Fireworks Algorithm–Grey Neural Network Model, Applied Sciences, MDPI.

Yang, Y., Wang, H., Sangwongwanich, A., & Blaabjerg, F. (2018). Design for Reliability of Power Electronic Systems. In M. H. Rashid (Ed.), Power Electronics Handbook (4 ed., pp. 1423–1440). Elsevier.  
<https://doi.org/10.1016/B978-0-12-811407-0.00051-9>.

## APPENDICES

### A. Generated Dataset for ANN1

Irradiance (W/m2)	Wind speed (m/s)	Generated ac power (W)	DC link voltage (V)
0	0	1.10069008031251e-05	0.0175096484203272
0	1	0.000543220266100190	0.123360278802853
0	2	0.00871656095405573	0.494245342089428
0	3	4.61907326323674e-06	0.0113040659445360
0	4	1.25381739361884e-05	0.0186207953499209
0	5	2.90890752659268e-05	0.0283612811115847
0	6	404.674131151822	119.539364730849
0	7	1383.82076987922	170.769363657442
0	8	1651.29361530287	216.447569854824
0	9	2519.99308565689	264.734692039843
0	10	3390.50858489574	307.048874854223
0	11	4381.75061347356	349.086319957199
0	12	5488.50362058594	390.698660600549
0	13	6642.76482297183	429.865492614222
0	14	8013.07958726058	472.111505577802
0	15	9513.37915490739	514.356982319829
0	16	10003.1404166259	584.656267138021
0	17	10207.8527551915	660.592959133964
0	18	10174.2180086720	678.493602586861
0	19	10127.2313054630	679.753635002585
0	20	10231.2092277243	680.826328045918
50	0	4.38069994500178	11.0458918887327
50	1	4.36823356185805	11.0301243976690
50	2	4.74524866257614	11.5065089302255
50	3	4.37616882917599	11.0372160548459
50	4	4.38130830083325	11.0465301537672
50	5	4.38868121127242	11.0553605784060
50	6	530.117049538238	134.440323601593
50	7	1354.57076524997	180.096981247282
50	8	1836.97384524546	226.017865547454
50	9	2554.87720632611	266.551584606313
50	10	3390.50854225899	307.046760883700
50	11	4381.49972813331	349.090612902053
50	12	5489.65517354725	390.703000496565
50	13	6643.19544714088	429.866954749515
50	14	8012.34970786173	472.100003427703

50	15	9512.68903545241	514.358957423054
50	16	10000.6071119057	584.626028590635
50	17	10169.4359488086	660.617585464157
50	18	10161.2793150909	678.540279683594
50	19	10168.2229142174	679.734810219507
50	20	10197.8722653002	680.835228479188
100	0	17.5268623578883	22.0943440062770
100	1	17.5031499916971	22.0783656998243
100	2	17.5102524504389	22.0808431066112
100	3	17.5148876904664	22.0829520469312
100	4	17.5278913546728	22.0947480358900
100	5	807.205852514796	126.336497457234
100	6	783.214527106524	164.504740766407
100	7	1503.09312954691	204.470892642287
100	8	2105.76766043353	242.001461641732
100	9	2828.29081394688	280.466253833698
100	10	3669.55553003837	319.437023767003
100	11	4628.14059144986	358.771722088541
100	12	5708.95320412731	398.446667778037
100	13	6816.0832299516	435.397356471217
100	14	8152.49220296171	476.138576794049
100	15	9611.67943684837	517.061878279156
100	16	10027.9323111552	584.629118224838
100	17	10183.4003787005	660.589237615774
100	18	10152.7235545304	678.466814346531
100	19	10147.1668941258	679.699569430496
100	20	10175.4505186705	680.865175273577
150	0	39.4386145303235	33.1428494337754
150	1	39.4022930104531	33.1274765131147
150	2	39.4050726261370	33.1284227882897
150	3	39.4110070419851	33.1292789409379
150	4	39.4431055680643	33.1437215543774
150	5	879.077510375925	156.311471935963
150	6	1262.76890541275	187.374611412572
150	7	1757.77701249118	221.113263920219
150	8	2372.50109998085	256.868776935980
150	9	3105.76093474310	293.846384353065
150	10	3960.07760076225	331.793138592104
150	11	4925.49415725239	370.082960446399
150	12	6024.21513960378	409.316322609734
150	13	7173.94281157665	446.670758883936
150	14	8462.74060170150	485.185877626979
150	15	9939.81348345028	525.807814559462
150	16	10029.4223188489	584.618961063772

150	17	10162.0993654207	660.642366127172
150	18	10157.3169743635	678.472132578838
150	19	10152.0356332991	679.695259526614
150	20	10152.8685218119	680.833410404427
200	0	70.1152824537461	44.1911558190019
200	1	70.0666249141013	44.1756324969969
200	2	70.0738845380391	44.1752960516258
200	3	70.0797952764707	44.1753267786975
200	4	279.751905272670	93.7342031493034
200	5	1098.97900878048	174.796425869343
200	6	1501.32935599443	204.320581686830
200	7	2013.93102640611	236.661718425977
200	8	2643.60179594577	271.131527537410
200	9	3388.41919002521	306.935724190370
200	10	4256.69522787242	344.054909076894
200	11	5228.95894420739	381.340537272502
200	12	6348.95749610514	420.184370111758
200	13	7535.16812527302	457.725010208128
200	14	8780.98302425555	494.204830028330
200	15	10023.0629941141	540.449684608155
200	16	9999.42620690240	584.613077787429
200	17	10208.6310837496	660.593970453077
200	18	10161.0276543999	678.463300865928
200	19	10126.0488835569	679.695385118121
200	20	10154.6260455338	680.843780777509
250	0	109.558492338079	55.2397927541358
250	1	109.505022962656	55.2235094851638
250	2	109.497866710415	55.2234875312465
250	3	109.519372996707	55.2256520545843
250	4	1005.66317003901	167.223615279280
250	5	1325.34171230081	192.039654317165
250	6	1747.44701011794	220.465534088842
250	7	2277.47593123076	251.667426832716
250	8	2922.04369044052	285.080779335667
250	9	3677.66418865394	319.819826269505
250	10	4565.42854885984	356.284130380299
250	11	5541.71065450135	392.554766645526
250	12	6681.91265328559	431.058689380515
250	13	7897.38209396954	468.636724117522
250	14	9107.45131977298	503.227227974840
250	15	10032.8507184980	558.305478767956
250	16	10005.6734104292	584.646823572914
250	17	10146.9434322701	660.608641367724
250	18	10123.2698676674	678.461732350132

250	19	10182.9615808357	679.719399076706
250	20	10104.7767565919	680.858355312771
300	0	157.766700050479	66.2882702218915
300	1	157.682169540479	66.2700169899452
300	2	157.673534554658	66.2674872377394
300	3	157.704558359028	66.2740088057396
300	4	1252.23589301360	186.645380692562
300	5	1571.50880470526	209.088352098068
300	6	2007.96983219099	236.305247844357
300	7	2552.46521429642	266.431182317208
300	8	3211.57980459133	298.879390703582
300	9	3977.71604013071	332.607149221712
300	10	4883.64148534331	368.550607718774
300	11	5862.28462586204	403.746861565990
300	12	7024.57515290452	441.953321812582
300	13	8269.27104055579	479.517003734204
300	14	9477.15349846853	513.383839835137
300	15	10009.9293433954	559.219226861676
300	16	10027.0319919664	584.641346264908
300	17	10213.8179173231	660.578466419612
300	18	10125.6906081673	678.553781645758
300	19	10127.3063078869	679.757106504928
300	20	10201.1989876967	680.821369316241
350	0	214.741086896944	77.3368691826905
350	1	214.678526502855	77.3177281947658
350	2	214.685208346925	77.3099657425477
350	3	1444.68335327220	199.961264113730
350	4	1541.73691360414	207.063946230377
350	5	1839.40261116541	226.178367338872
350	6	2285.14389224785	252.088863600326
350	7	2842.29060409565	281.149949411398
350	8	3514.23145024620	312.636949766975
350	9	4288.91966135175	345.374427930065
350	10	5214.94428552257	380.853050457590
350	11	6191.36772724267	414.939411237526
350	12	7375.72214409880	452.873319852817
350	13	8647.83308620683	490.419594771068
350	14	9928.8444201475	525.484870493705
350	15	10007.9507381136	559.221434564361
350	16	9997.95356147537	584.658032377697
350	17	10118.2461704792	660.626992396210
350	18	10127.1401300231	678.541713559558
350	19	10095.2725071424	679.737480432791
350	20	10103.4123517531	680.882889031369

400	0	280.482326785429	88.3856508149311
400	1	280.513909866495	88.3626457019404
400	2	280.339070629783	88.3615447933557
400	3	1973.35226804327	234.393983829279
400	4	1974.13507397066	234.448118808185
400	5	2151.36007845196	244.601531805781
400	6	2582.30105875017	267.991132800811
400	7	3149.00260885180	295.936483111273
400	8	3831.98477013903	326.434164404599
400	9	4612.36559383247	358.146386380540
400	10	5558.94307416708	393.218377849092
400	11	6529.05156142403	426.144755657332
400	12	7735.28297475043	463.797010032756
400	13	9037.98517539822	501.306890978719
400	14	10028.5979611976	552.971092396149
400	15	10007.8884171830	559.220510117079
400	16	9971.76101203747	584.646224951407
400	17	10166.2971622884	660.636553243474
400	18	10157.9973838015	678.489849715348
400	19	10176.1201863785	679.688565905298
400	20	10075.8352313564	680.884403535697
450	0	354.901534654719	99.4221041635129
450	1	354.800915955195	99.4055043907164
450	2	354.975499734557	99.4045653138611
450	3	2498.33802232357	263.739291349943
450	4	2498.56520375302	263.772062958332
450	5	2520.62446876669	264.837727478682
450	6	2900.29890092741	284.024061067126
450	7	3474.48404919349	310.860649866809
450	8	4164.21433118410	340.299244167088
450	9	4947.40180879991	370.960735617711
450	10	5915.67525830751	405.637437443719
450	11	6907.45679845264	438.292534539628
450	12	8106.20840116003	474.780350093867
450	13	9433.70874062265	512.207339660367
450	14	10048.0191259323	559.117774157719
450	15	10012.8310323402	559.226831318638
450	16	10053.4160953812	584.570603686818
450	17	10183.1286205013	660.592819104188
450	18	10170.8090543268	678.555956058338
450	19	10097.9950901847	679.773176852992
450	20	10202.0257773418	680.832150327140
500	0	3084.74595682017	293.115125807677
500	1	3083.96752648803	293.073018753389

500	2	3084.33315058366	293.065636302560
500	3	3084.31815960360	293.056525682495
500	4	3084.59540726589	293.088326449179
500	5	3085.35697159124	293.079654392462
500	6	3285.94613771077	302.321473972225
500	7	3818.38171790053	325.858019455089
500	8	4510.86657999571	354.224409327392
500	9	5311.36521250379	384.334366836128
500	10	6286.08322787199	418.117931356742
500	11	7322.89133110866	451.289205181037
500	12	8487.53629186817	485.743062457902
500	13	9839.45098471130	523.137886167970
500	14	10047.1735565939	559.106359434779
500	15	10010.2699994812	559.217173864672
500	16	10028.2178054994	584.585034197606
500	17	10132.8073061232	660.634629974469
500	18	10172.0763146535	678.540493876939
500	19	10125.0487340498	679.723354661865
500	20	10102.3947552773	680.866478153116
550	0	3732.67543247561	322.432386494996
550	1	3731.59560871897	322.370657583727
550	2	3731.95154188988	322.375578145989
550	3	3732.07806374289	322.358296718479
550	4	3732.83623936772	322.394491650659
550	5	3732.08880022540	322.363758257443
550	6	3748.33250738306	322.966362207632
550	7	4182.31645862267	341.038341119349
550	8	4873.54063863344	368.171588142636
550	9	5710.39281176477	398.538610820050
550	10	6668.86299954869	430.645650640075
550	11	7743.86332867606	464.068607293128
550	12	8872.14550992246	496.743699529398
550	13	10041.8094458069	543.474275558135
550	14	10029.3603841814	559.104777771329
550	15	10007.7567907241	559.216248438102
550	16	9996.07094796506	584.625341373956
550	17	10212.4022865562	660.605312289269
550	18	10174.9366088834	678.555758991263
550	19	10146.5670493972	679.704756413356
550	20	10153.0471798315	680.865418107823
600	0	4442.61856199236	351.761306441501
600	1	4442.38572677939	351.750460055702
600	2	4441.78601094334	351.682648263898
600	3	4440.95111990690	351.653861467399

600	4	4441.81383203180	351.690500144854
600	5	4441.44141521877	351.651807806108
600	6	4442.25581986530	351.685400557818
600	7	4648.77711288002	359.536450249730
600	8	5253.30803681515	382.231565740907
600	9	6121.82602868349	412.613010655444
600	10	7059.62822460497	443.099276112912
600	11	8174.20554418024	476.787076134328
600	12	9263.11697201959	507.560777035143
600	13	9999.22848808833	558.986111206520
600	14	10007.7970597006	559.103072363305
600	15	10008.5216284446	559.224191886362
600	16	9972.73253715506	584.655892287302
600	17	10098.4262070810	660.626567607120
600	18	10175.8707190088	678.523136327890
600	19	10124.3810847978	679.735350246740
600	20	10179.9675599328	680.862062781623
650	0	5213.98058843331	381.077456363601
650	1	5213.88371463078	381.073061667135
650	2	5212.37424220543	380.993717781024
650	3	5212.37437912259	380.961370923611
650	4	5213.01240415086	380.986084760396
650	5	5212.82297711469	380.970097246703
650	6	5213.78195821713	380.985005673207
650	7	5231.71552705779	381.568712737304
650	8	5690.76662334688	397.835011971165
650	9	6537.94629274980	426.457736636910
650	10	7460.17364388645	455.539404111737
650	11	8613.34247029735	489.445161201132
650	12	9662.40679399370	518.416202142848
650	13	9999.75097389084	558.983570171254
650	14	10008.2030453254	559.106418498909
650	15	10012.1532022673	559.219791382439
650	16	10032.4068089306	584.606588606188
650	17	10179.7486374113	660.614346240581
650	18	10156.4410287097	678.468173709634
650	19	10124.5175964344	679.757463406507
650	20	10201.6178276693	680.831266263617
700	0	6047.05697673614	410.393603707649
700	1	6047.02848085897	410.392140501273
700	2	6045.60311876688	410.304915012977
700	3	6044.39758979907	410.268966981234
700	4	6046.18303567399	410.291733041334
700	5	6047.08922960752	410.292604784450

700	6	6046.39559024142	410.299725864884
700	7	6048.34238554783	410.407439266054
700	8	6238.90180147072	416.498266967891
700	9	6960.70118682479	440.011074338402
700	10	7876.67951613846	468.052301197020
700	11	9057.11054362566	501.933552236671
700	12	10050.8312205740	548.442370180994
700	13	10021.0476873877	558.991717662787
700	14	10028.2150742040	559.113513840430
700	15	10009.0880898584	559.224789811886
700	16	10030.0956999183	584.644520309502
700	17	10166.4029142606	660.595316439929
700	18	10171.5159769482	678.500618631967
700	19	10146.6296728831	679.703086903364
700	20	10099.2944076503	680.839626996122
750	0	6941.84776171838	439.709750625421
750	1	6941.86202660629	439.709913550049
750	2	6940.07457313168	439.611799188423
750	3	6939.99331305240	439.571670605458
750	4	6940.05069020449	439.594673358775
750	5	6941.60743997863	439.630361249939
750	6	6941.30666952983	439.612532353494
750	7	6942.42986209641	439.646262156563
750	8	6967.20154245427	440.347770433538
750	9	7481.41690421326	456.157686932970
750	10	8313.18413398881	480.837507292278
750	11	9501.63694756242	514.083742951047
750	12	10023.4285447614	558.893874393005
750	13	10025.0172668169	558.987673484875
750	14	10008.6379134514	559.105910924744
750	15	10010.2100657712	559.220161817678
750	16	9998.82521305659	584.643225779365
750	17	10099.9178818030	660.627579919814
750	18	10157.2438695295	678.476346768461
750	19	10151.3570562278	679.701610566065
750	20	10093.9209879679	680.858361472000
800	0	7898.35295486294	469.025895389417
800	1	7898.39726959910	469.027054181088
800	2	7897.37290728714	468.925156740316
800	3	7895.15232973855	468.859059301919
800	4	7895.98017104661	468.905825704795
800	5	7898.62861289451	468.952495531934
800	6	7896.78615721333	468.903401286572
800	7	7898.34891119336	468.961354351499

800	8	7899.31650969169	468.944067157770
800	9	8078.06736010792	473.965210192448
800	10	8871.46481685932	496.726011193144
800	11	9959.28129579331	526.276696914680
800	12	10019.6054038028	558.895821634135
800	13	10021.6358554887	558.992195077783
800	14	10005.8059187516	559.111621636774
800	15	9971.05449340605	559.217847275963
800	16	10025.6405822583	584.595294074235
800	17	10163.0421221541	660.597416288174
800	18	10165.1062954573	678.463684785143
800	19	10209.8679820228	679.706834201370
800	20	10208.2053289733	680.819505075197
850	0	8916.57251453231	498.342039210218
850	1	8916.63257792721	498.343625208657
850	2	8914.16562136031	498.220450620750
850	3	8913.32430539117	498.178752639832
850	4	8914.67888182220	498.219957668002
850	5	8916.06309959570	498.275605215308
850	6	8915.67304817855	498.256478112345
850	7	8916.08715261897	498.268338807413
850	8	8917.11624685870	498.266008950763
850	9	8947.93392151514	499.004464833274
850	10	9434.50923753067	512.247826690582
850	11	10026.6583511888	558.801138268523
850	12	10017.8147295140	558.892108348490
850	13	10021.1281545613	558.986241336207
850	14	10013.9448144316	559.114852664385
850	15	10008.4463019521	559.231840373822
850	16	9973.18448105541	584.632595196349
850	17	10098.3049054324	660.642106456127
850	18	10161.5771963770	678.527905931791
850	19	10183.8604931458	679.714186600554
850	20	10207.0315300689	680.851317223037
900	0	9996.50645453535	527.658181914660
900	1	9996.57447610757	527.659919518650
900	2	9994.59339747638	527.522924309282
900	3	9992.98060107708	527.490392035080
900	4	9993.89004022956	527.537720160971
900	5	9994.88081152406	527.586717887336
900	6	9996.25629107335	527.591396024971
900	7	9996.91522559316	527.578421297754
900	8	9996.13552918998	527.572763827307
900	9	9996.45757347867	527.558228118544

900	10	9982.44956034132	558.700782072277
900	11	10003.3199424524	558.802840648168
900	12	10061.3991236894	558.900907488764
900	13	10001.9684359417	558.992970489431
900	14	10030.6376259309	559.117795019192
900	15	10008.8965062562	559.220561515986
900	16	10026.0434350666	584.613925965218
900	17	10163.8620098530	660.628786556466
900	18	10160.6682296139	678.461870138652
900	19	10151.0411961210	679.758691812799
900	20	10177.7125548047	680.842511876112
950	0	10015.6717709309	558.697636139432
950	1	9997.76000982619	558.698180691867
950	2	10000.4394753569	558.700223358322
950	3	10038.0587012806	558.695963799930
950	4	10040.2022114393	558.696508231868
950	5	9998.01629643391	558.695503434512
950	6	10037.1688623096	558.696965778159
950	7	10040.3941637534	558.696767559777
950	8	9996.90728988161	558.698539221452
950	9	9980.78318920097	558.700639228514
950	10	10000.3271909790	558.692692560169
950	11	10041.7515053127	558.805839605811
950	12	10019.7816319704	558.894389433545
950	13	9997.80578024716	558.988231736045
950	14	10028.6611388691	559.115992392943
950	15	10010.3147305415	559.225446051224
950	16	10028.5159629491	584.637023398640
950	17	10163.7137970865	660.628640895771
950	18	10167.1195851323	678.562898307523
950	19	10175.6473007805	679.733112496297
950	20	10242.1776436664	680.790278944691
1000	0	9997.79201283533	558.698723079163
1000	1	9977.04090264452	558.700473113255
1000	2	10037.1855943887	558.696430899085
1000	3	10000.2692141249	558.698885484392
1000	4	9999.84410074673	558.699552441235
1000	5	9996.65447209230	558.698986675256
1000	6	9999.83315350819	558.696508210742
1000	7	10016.8955970584	558.698788290592
1000	8	10017.6417641350	558.698090866907
1000	9	10017.0075517891	558.696388777920
1000	10	9982.67408345372	558.692011637559
1000	11	10025.304603569	558.805357866783

1000	12	10059.4892353081	558.899029324478
1000	13	10041.3035500705	558.994068995529
1000	14	10030.6433331169	559.124185831616
1000	15	10007.9616361626	559.225553135783
1000	16	10002.6770537640	584.634418329995
1000	17	10094.7142904400	660.614830273508
1000	18	10163.1957434837	678.468858250127
1000	19	10123.4331580247	679.728628741139
1000	20	10162.2655484003	680.835684005174

## B. Generated Dataset for ANN2

Carrier frequency (Hz)	Ambient temperature (C)	DC link voltage (V)	$\Delta T$ (C)	$T_{j,m}$ (C)
2000	0	1.14E-02	3.44E-05	0.000215
4000	0	0.011505402	5.51E-05	0.000327
6000	0	0.011595464	7.87E-05	0.000437
8000	0	1.16E-02	9.76E-05	0.000538
10000	0	1.15E-02	0.000133384	0.00062
12000	0	1.15E-02	0.000107977	0.00057
14000	0	0.011507811	0.000125574	0.000697
16000	0	0.011456441	0.000111786	0.000636
18000	0	0.011451671	0.000141131	0.000748
20000	0	0.011444482	0.000163042	0.000772
2000	5	0.011441393	3.48E-05	5.000218
4000	5	0.011505402	5.58E-05	5.000332
6000	5	0.011595464	7.98E-05	5.000443
8000	5	0.011589809	9.88E-05	5.000545
10000	5	0.011456827	0.00013512	5.000628
12000	5	0.011470235	0.000109381	5.000578
14000	5	0.011507811	0.000127207	5.000706
16000	5	0.011456441	0.000113239	5.000644
18000	5	0.011451671	0.000142966	5.000758
20000	5	0.011444482	0.000165164	5.000782
2000	10	0.011441393	3.53E-05	10.00022
4000	10	0.011505402	5.65E-05	10.00034
6000	10	0.011595464	8.08E-05	10.00045
8000	10	0.011589809	0.000100116	10.00055
10000	10	0.011456827	0.000136857	10.00064
12000	10	0.011470235	0.000110785	10.00058
14000	10	0.011507811	0.000128839	10.00072
16000	10	0.011456441	0.000114692	10.00065
18000	10	0.011451671	0.000144801	10.00077
20000	10	0.011444482	0.000167286	10.00079
2000	15	0.011441393	3.57E-05	15.00022
4000	15	0.011505402	5.72E-05	15.00034
6000	15	0.011595464	8.18E-05	15.00045
8000	15	0.011589809	0.000101385	15.00056
10000	15	0.011456827	0.000138593	15.00064
12000	15	0.011470235	0.000112189	15.00059
14000	15	0.011507811	0.000130472	15.00072

16000	15	0.011456441	0.000116146	15.00066
18000	15	0.011451671	0.000146636	15.00078
20000	15	0.01144482	0.000169407	15.0008
2000	20	0.011441393	3.62E-05	20.00023
4000	20	0.011505402	5.79E-05	20.00034
6000	20	0.011595464	8.28E-05	20.00046
8000	20	0.011589809	0.000102654	20.00057
10000	20	0.011456827	0.000140329	20.00065
12000	20	0.011470235	0.000113592	20.0006
14000	20	0.011507811	0.000132105	20.00073
16000	20	0.011456441	0.000117599	20.00067
18000	20	0.011451671	0.000148471	20.00079
20000	20	0.01144482	0.000171529	20.00081
2000	25	0.011441393	3.66E-05	25.00023
4000	25	0.011505402	5.87E-05	25.00035
6000	25	0.011595464	8.38E-05	25.00047
8000	25	0.011589809	0.000103923	25.00057
10000	25	0.011456827	0.000142065	25.00066
12000	25	0.011470235	0.000114996	25.00061
14000	25	0.011507811	0.000133737	25.00074
16000	25	0.011456441	0.000119052	25.00068
18000	25	0.011451671	0.000150306	25.0008
20000	25	0.01144482	0.000173651	25.00082
2000	30	0.011441393	3.71E-05	30.00023
4000	30	0.011505402	5.94E-05	30.00035
6000	30	0.011595464	8.49E-05	30.00047
8000	30	0.011589809	0.000105192	30.00058
10000	30	0.011456827	0.000143802	30.00067
12000	30	0.011470235	0.0001164	30.00061
14000	30	0.011507811	0.00013537	30.00075
16000	30	0.011456441	0.000120505	30.00069
18000	30	0.011451671	0.00015214	30.00081
20000	30	0.01144482	0.000175772	30.00083
2000	35	0.011441393	3.75E-05	35.00023
4000	35	0.011505402	6.01E-05	35.00036
6000	35	0.011595464	8.59E-05	35.00048
8000	35	0.011589809	0.000106461	35.00059
10000	35	0.011456827	0.000145538	35.00068
12000	35	0.011470235	0.000117804	35.00062
14000	35	0.011507811	0.000137003	35.00076
16000	35	0.011456441	0.000121959	35.00069
18000	35	0.011451671	0.000153975	35.00082

20000	35	0.01144482	0.000177894	35.00084
2000	40	0.011441393	3.80E-05	40.00024
4000	40	0.011505402	6.08E-05	40.00036
6000	40	0.011595464	8.69E-05	40.00048
8000	40	0.011589809	0.000107729	40.00059
10000	40	0.011456827	0.000147274	40.00068
12000	40	0.011470235	0.000119207	40.00063
14000	40	0.011507811	0.000138635	40.00077
16000	40	0.011456441	0.000123412	40.0007
18000	40	0.011451671	0.00015581	40.00083
20000	40	0.01144482	0.000180016	40.00085
2000	0	54.86902734	0.163328827	0.861058
4000	0	55.12646852	0.261929239	1.307944
6000	0	55.43325412	0.36471692	1.741963
8000	0	55.38350464	0.451655451	2.147165
10000	0	54.98901914	0.595991587	2.472869
12000	0	55.05536262	0.503374902	2.283791
14000	0	55.21772924	0.584312929	2.792249
16000	0	55.03504331	0.532344104	2.555655
18000	0	55.04001711	0.624243587	2.990045
20000	0	55.0355911	0.729561982	3.090723
2000	5	54.86902734	0.165456261	5.872276
4000	5	55.12646852	0.265336778	6.324961
6000	5	55.43325412	0.369460493	6.76462
8000	5	55.38350464	0.457529011	7.175091
10000	5	54.98901914	0.603750194	7.505022
12000	5	55.05536262	0.509918998	7.313481
14000	5	55.21772924	0.591910033	7.828553
16000	5	55.03504331	0.539264824	7.58888
18000	5	55.04001711	0.632359962	8.028921
20000	5	55.0355911	0.739056498	8.130904
2000	10	54.86902734	0.167583694	10.88349
4000	10	55.12646852	0.268744317	11.34198
6000	10	55.43325412	0.374204066	11.78728
8000	10	55.38350464	0.463402571	12.20302
10000	10	54.98901914	0.611508801	12.53717
12000	10	55.05536262	0.516463095	12.34317
14000	10	55.21772924	0.599507136	12.86486
16000	10	55.03504331	0.546185544	12.6221
18000	10	55.04001711	0.640476337	13.0678
20000	10	55.0355911	0.748551014	13.17108
2000	15	54.86902734	0.169711128	15.89471

4000	15	55.12646852	0.272151856	16.359
6000	15	55.43325412	0.378947639	16.80993
8000	15	55.38350464	0.46927613	17.23094
10000	15	54.98901914	0.619267408	17.56933
12000	15	55.05536262	0.523007191	17.37286
14000	15	55.21772924	0.607104239	17.90116
16000	15	55.03504331	0.553106264	17.65533
18000	15	55.04001711	0.648592712	18.10667
20000	15	55.0355911	0.75804553	18.21127
2000	20	54.86902734	0.171838561	20.90593
4000	20	55.12646852	0.275559396	21.37601
6000	20	55.43325412	0.383691212	21.83259
8000	20	55.38350464	0.47514969	22.25887
10000	20	54.98901914	0.627026015	22.60148
12000	20	55.05536262	0.529551288	22.40255
14000	20	55.21772924	0.614701342	22.93747
16000	20	55.03504331	0.560026984	22.68855
18000	20	55.04001711	0.656709087	23.14555
20000	20	55.0355911	0.767540046	23.25145
2000	25	54.86902734	0.173965995	25.91715
4000	25	55.12646852	0.278966935	26.39303
6000	25	55.43325412	0.388434785	26.85525
8000	25	55.38350464	0.48102325	27.28679
10000	25	54.98901914	0.634784622	27.63363
12000	25	55.05536262	0.536095384	27.43224
14000	25	55.21772924	0.622298445	27.97377
16000	25	55.03504331	0.566947704	27.72178
18000	25	55.04001711	0.664825463	28.18442
20000	25	55.0355911	0.777034562	28.29163
2000	30	54.86902734	0.176093428	30.92836
4000	30	55.12646852	0.282374474	31.41005
6000	30	55.43325412	0.393178358	31.87791
8000	30	55.38350464	0.48689681	32.31472
10000	30	54.98901914	0.642543228	32.66579
12000	30	55.05536262	0.542639481	32.46194
14000	30	55.21772924	0.629895548	33.01008
16000	30	55.03504331	0.573868423	32.755
18000	30	55.04001711	0.672941838	33.2233
20000	30	55.0355911	0.786529078	33.33181
2000	35	54.86902734	0.178220862	35.93958
4000	35	55.12646852	0.285782013	36.42707
6000	35	55.43325412	0.397921931	36.90056

8000	35	55.38350464	0.49277037	37.34264
10000	35	54.98901914	0.650301835	37.69794
12000	35	55.05536262	0.549183577	37.49163
14000	35	55.21772924	0.637492651	38.04638
16000	35	55.03504331	0.580789143	37.78823
18000	35	55.04001711	0.681058213	38.26218
20000	35	55.0355911	0.796023594	38.37199
2000	40	54.86902734	0.180348295	40.9508
4000	40	55.12646852	0.289189552	41.44409
6000	40	55.43325412	0.402665504	41.92322
8000	40	55.38350464	0.49864393	42.37057
10000	40	54.98901914	0.658060442	42.73009
12000	40	55.05536262	0.555727674	42.52132
14000	40	55.21772924	0.645089754	43.08269
16000	40	55.03504331	0.587709863	42.82145
18000	40	55.04001711	0.689174588	43.30105
20000	40	55.0355911	0.80551811	43.41217
2000	0	98.81232052	0.29479049	1.553995
4000	0	262.9186082	1.273809358	6.006092
6000	0	264.6900599	1.791333136	8.248456
8000	0	264.4684516	2.231004266	10.18052
10000	0	99.00986112	1.078364763	4.475361
12000	0	99.1280498	0.910548321	4.132079
14000	0	263.6524866	2.915382958	13.19421
16000	0	99.08976489	0.963298415	4.62573
18000	0	99.09795357	1.131083459	5.416858
20000	0	99.08940834	1.321983702	5.600853
2000	5	98.81232052	0.298630269	6.57424
4000	5	262.9186082	1.290367707	11.08419
6000	5	264.6900599	1.814617182	13.35568
8000	5	264.4684516	2.260003433	15.31287
10000	5	99.00986112	1.092402809	9.533551
12000	5	99.1280498	0.922385843	9.185798
14000	5	263.6524866	2.953274135	18.36571
16000	5	99.08976489	0.975821737	9.685867
18000	5	99.09795357	1.145789727	10.48729
20000	5	99.08940834	1.339187873	10.67367
2000	10	98.81232052	0.302470048	11.59449
4000	10	262.9186082	1.306926056	16.16228
6000	10	264.6900599	1.837901229	18.46291
8000	10	264.4684516	2.2890026	20.44522
10000	10	99.00986112	1.106440856	14.59174

12000	10	99.1280498	0.934223364	14.23952
14000	10	263.6524866	2.991165312	23.5372
16000	10	99.08976489	0.98834506	14.746
18000	10	99.09795357	1.160495994	15.55771
20000	10	99.08940834	1.356392044	15.74648
2000	15	98.81232052	0.306309826	16.61473
4000	15	262.9186082	1.323484405	21.24037
6000	15	264.6900599	1.861185275	23.57013
8000	15	264.4684516	2.318001767	25.57756
10000	15	99.00986112	1.120478902	19.64993
12000	15	99.1280498	0.946060885	19.29324
14000	15	263.6524866	3.029056489	28.70869
16000	15	99.08976489	1.000868383	19.80614
18000	15	99.09795357	1.175202261	20.62814
20000	15	99.08940834	1.373596215	20.81929
2000	20	98.81232052	0.310149605	21.63498
4000	20	262.9186082	1.340042754	26.31847
6000	20	264.6900599	1.884469322	28.67736
8000	20	264.4684516	2.347000934	30.70991
10000	20	99.00986112	1.134516948	24.70812
12000	20	99.1280498	0.957898407	24.34696
14000	20	263.6524866	3.066947666	33.88019
16000	20	99.08976489	1.013391705	24.86628
18000	20	99.09795357	1.189908528	25.69857
20000	20	99.08940834	1.390800385	25.89211
2000	25	98.81232052	0.313989384	26.65522
4000	25	262.9186082	1.356601103	31.39656
6000	25	264.6900599	1.907753368	33.78458
8000	25	264.4684516	2.376000101	35.84226
10000	25	99.00986112	1.148554994	29.76631
12000	25	99.1280498	0.969735928	29.40068
14000	25	263.6524866	3.104838843	39.05168
16000	25	99.08976489	1.025915028	29.92641
18000	25	99.09795357	1.204614796	30.769
20000	25	99.08940834	1.408004556	30.96492
2000	30	98.81232052	0.317829163	31.67547
4000	30	262.9186082	1.373159452	36.47465
6000	30	264.6900599	1.931037415	38.89181
8000	30	264.4684516	2.404999268	40.97461
10000	30	99.00986112	1.162593041	34.8245
12000	30	99.1280498	0.98157345	34.4544
14000	30	263.6524866	3.14273002	44.22317

16000	30	99.08976489	1.038438351	34.98655
18000	30	99.09795357	1.219321063	35.83943
20000	30	99.08940834	1.425208727	36.03773
2000	35	98.81232052	0.321668941	36.69571
4000	35	262.9186082	1.389717801	41.55275
6000	35	264.6900599	1.954321461	43.99903
8000	35	264.4684516	2.433998435	46.10695
10000	35	99.00986112	1.176631087	39.88269
12000	35	99.1280498	0.993410971	39.50812
14000	35	263.6524866	3.18044923	49.39421
16000	35	99.08976489	1.050961673	40.04669
18000	35	99.09795357	1.23402733	40.90986
20000	35	99.08940834	1.442412898	41.11055
2000	40	98.81232052	0.32550872	41.71596
4000	40	262.9186082	1.40627615	46.63084
6000	40	264.6900599	1.977591167	49.10624
8000	40	264.4684516	2.461873588	51.23475
10000	40	99.00986112	1.190669133	44.94088
12000	40	99.1280498	1.005248492	44.56184
14000	40	263.6524866	3.214859614	54.55161
16000	40	99.08976489	1.063484996	45.10682
18000	40	99.09795357	1.248733597	45.98029
20000	40	99.08940834	1.459617069	46.18336
2000	0	96.23762664	0.391972599	1.704094
4000	0	95.3540613	0.60675351	2.590798
6000	0	147.9287096	0.989687733	3.569573
8000	0	144.6667647	1.352189719	4.512603
10000	0	96.05071601	1.755582087	5.16831
12000	0	147.1704745	1.49538931	4.835422
14000	0	111.5926331	1.797950281	5.905029
16000	0	104.1831598	1.608149459	5.434019
18000	0	133.9979979	2.001472371	6.194237
20000	0	116.9471264	2.24894552	6.473628
2000	5	96.23762664	0.397077547	6.726295
4000	5	95.3540613	0.614646563	7.624508
6000	5	147.9287096	1.002560186	8.615999
8000	5	144.6667647	1.369774847	9.571291
10000	5	96.05071601	1.7784346	10.23551
12000	5	147.1704745	1.514830479	9.898286
14000	5	111.5926331	1.821326943	10.98181
16000	5	104.1831598	1.629056772	10.50466
18000	5	133.9979979	2.027501915	11.27478

20000	5	116.9471264	2.278216879	11.55779
2000	10	96.23762664	0.402182495	11.7485
4000	10	95.3540613	0.622539615	12.65822
6000	10	147.9287096	1.015432638	13.66243
8000	10	144.6667647	1.387359974	14.62998
10000	10	96.05071601	1.801287113	15.30271
12000	10	147.1704745	1.534271648	14.96115
14000	10	111.5926331	1.844703605	16.05858
16000	10	104.1831598	1.649964085	15.57531
18000	10	133.9979979	2.05353146	16.35531
20000	10	116.9471264	2.307488237	16.64195
2000	15	96.23762664	0.407287443	16.7707
4000	15	95.3540613	0.630432668	17.69193
6000	15	147.9287096	1.02830509	18.70885
8000	15	144.6667647	1.404945102	19.68867
10000	15	96.05071601	1.824139626	20.36991
12000	15	147.1704745	1.553712817	20.02401
14000	15	111.5926331	1.868080267	21.13536
16000	15	104.1831598	1.670871398	20.64595
18000	15	133.9979979	2.079561005	21.43585
20000	15	116.9471264	2.336759595	21.72611
2000	20	96.23762664	0.412392391	21.7929
4000	20	95.3540613	0.63832572	22.72564
6000	20	147.9287096	1.041177542	23.75528
8000	20	144.6667647	1.422530229	24.74736
10000	20	96.05071601	1.846992138	25.43711
12000	20	147.1704745	1.573153985	25.08688
14000	20	111.5926331	1.891456929	26.21214
16000	20	104.1831598	1.691778711	25.7166
18000	20	133.9979979	2.105590549	26.51639
20000	20	116.9471264	2.366030954	26.81027
2000	25	96.23762664	0.417497338	26.8151
4000	25	95.3540613	0.646218773	27.75935
6000	25	147.9287096	1.054049994	28.8017
8000	25	144.6667647	1.440115357	29.80604
10000	25	96.05071601	1.869844651	30.50431
12000	25	147.1704745	1.592595154	30.14974
14000	25	111.5926331	1.914833591	31.28891
16000	25	104.1831598	1.712686025	30.78724
18000	25	133.9979979	2.131620094	31.59693
20000	25	116.9471264	2.395302312	31.89443
2000	30	96.23762664	0.422602286	31.8373

4000	30	95.3540613	0.654111825	32.79306
6000	30	147.9287096	1.066922446	33.84813
8000	30	144.6667647	1.457700484	34.86473
10000	30	96.05071601	1.892697164	35.57152
12000	30	147.1704745	1.612036323	35.2126
14000	30	111.5926331	1.938210253	36.36569
16000	30	104.1831598	1.733593338	35.85789
18000	30	133.9979979	2.157649639	36.67747
20000	30	116.9471264	2.42457367	36.97859
2000	35	96.23762664	0.427707234	36.8595
4000	35	95.3540613	0.662004878	37.82677
6000	35	147.9287096	1.079794899	38.89456
8000	35	144.6667647	1.475285612	39.92342
10000	35	96.05071601	1.915549676	40.63872
12000	35	147.1704745	1.631477492	40.27547
14000	35	111.5926331	1.961586915	41.44247
16000	35	104.1831598	1.754500651	40.92853
18000	35	133.9979979	2.183679183	41.75801
20000	35	116.9471264	2.453845029	42.06275
2000	40	96.23762664	0.432812182	41.8817
4000	40	95.3540613	0.669897931	42.86048
6000	40	147.9287096	1.092667351	43.94098
8000	40	144.6667647	1.492870739	44.98211
10000	40	96.05071601	1.938402189	45.70592
12000	40	147.1704745	1.650918661	45.33833
14000	40	111.5926331	1.984963577	46.51924
16000	40	104.1831598	1.775407964	45.99918
18000	40	133.9979979	2.209708728	46.83854
20000	40	116.9471264	2.483116387	47.14691
2000	0	203.2432045	0.608623972	3.197481
4000	0	203.7349567	0.976019239	4.859627
6000	0	204.3122621	1.362912198	6.476126
8000	0	204.2181276	1.693786513	8.008555
10000	0	203.4750744	2.25288518	9.268973
12000	0	203.5949181	1.892846423	8.550327
14000	0	203.9100927	2.20514225	10.47314
16000	0	203.5698229	2.005359448	9.585163
18000	0	203.5777125	2.364160725	11.24455
20000	0	203.5685116	2.76630794	11.63097
2000	5	203.2432045	0.616551513	8.239137
4000	5	203.7349567	0.988716671	9.922856
6000	5	204.3122621	1.380638456	11.56036

8000	5	204.2181276	1.715813385	13.11271
10000	5	203.4750744	2.282212441	14.38949
12000	5	203.5949181	1.91745422	13.66149
14000	5	203.9100927	2.233812995	15.60931
16000	5	203.5698229	2.031430021	14.70977
18000	5	203.5777125	2.394899335	16.39075
20000	5	203.5685116	2.802307718	16.78218
2000	10	203.2432045	0.624479055	13.28079
4000	10	203.7349567	1.001414102	14.98609
6000	10	204.3122621	1.398364713	16.64459
8000	10	204.2181276	1.737840258	18.21687
10000	10	203.4750744	2.311539701	19.51001
12000	10	203.5949181	1.942062017	18.77265
14000	10	203.9100927	2.262483739	20.74548
16000	10	203.5698229	2.057500594	19.83439
18000	10	203.5777125	2.425637945	21.53694
20000	10	203.5685116	2.838307495	21.93339
2000	15	203.2432045	0.632406596	18.32245
4000	15	203.7349567	1.014111533	20.04931
6000	15	204.3122621	1.416090971	21.72882
8000	15	204.2181276	1.75986713	23.32103
10000	15	203.4750744	2.340866962	24.63052
12000	15	203.5949181	1.966669814	23.88381
14000	15	203.9100927	2.291154483	25.88166
16000	15	203.5698229	2.083571167	24.959
18000	15	203.5777125	2.456376556	26.68314
20000	15	203.5685116	2.874307273	27.08459
2000	20	203.2432045	0.640334138	23.36411
4000	20	203.7349567	1.026808965	25.11254
6000	20	204.3122621	1.433817229	26.81306
8000	20	204.2181276	1.781894003	28.42518
10000	20	203.4750744	2.370194223	29.75104
12000	20	203.5949181	1.991277611	28.99497
14000	20	203.9100927	2.319825227	31.01783
16000	20	203.5698229	2.10964174	30.08361
18000	20	203.5777125	2.487115166	31.82934
20000	20	203.5685116	2.910307051	32.2358
2000	25	203.2432045	0.648261679	28.40576
4000	25	203.7349567	1.039506396	30.17577
6000	25	204.3122621	1.451543487	31.89729
8000	25	204.2181276	1.803920875	33.52934
10000	25	203.4750744	2.399521483	34.87156

12000	25	203.5949181	2.015885408	34.10613
14000	25	203.9100927	2.348495972	36.154
16000	25	203.5698229	2.135712313	35.20822
18000	25	203.5777125	2.517853777	36.97554
20000	25	203.5685116	2.946306829	37.38701
2000	30	203.2432045	0.656189221	33.44742
4000	30	203.7349567	1.052203828	35.239
6000	30	204.3122621	1.469269745	36.98152
8000	30	204.2181276	1.825947747	38.6335
10000	30	203.4750744	2.428848744	39.99207
12000	30	203.5949181	2.040493205	39.21729
14000	30	203.9100927	2.377166716	41.29017
16000	30	203.5698229	2.161782886	40.33283
18000	30	203.5777125	2.548592387	42.12174
20000	30	203.5685116	2.982306607	42.53821
2000	35	203.2432045	0.664116762	38.48908
4000	35	203.7349567	1.064901259	40.30223
6000	35	204.3122621	1.486996003	42.06575
8000	35	204.2181276	1.84797462	43.73766
10000	35	203.4750744	2.458176004	45.11259
12000	35	203.5949181	2.065101002	44.32845
14000	35	203.9100927	2.40583746	46.42634
16000	35	203.5698229	2.187853459	45.45744
18000	35	203.5777125	2.579330998	47.26794
20000	35	203.5685116	3.018306385	47.68942
2000	40	203.2432045	0.672044303	43.53073
4000	40	203.7349567	1.07759869	45.36546
6000	40	204.3122621	1.50472226	47.14999
8000	40	204.2181276	1.870001492	48.84181
10000	40	203.4750744	2.487002131	50.23184
12000	40	203.5949181	2.089678067	49.43947
14000	40	203.9100927	2.433619301	51.55857
16000	40	203.5698229	2.213662319	50.58084
18000	40	203.5777125	2.608663732	52.40796
20000	40	203.5685116	3.052174702	52.83343
2000	0	250.8881669	0.754258762	3.967726
4000	0	251.4649348	1.211088143	6.033845
6000	0	252.154318	1.687529508	8.048503
8000	0	252.0304772	2.09905045	9.961382
10000	0	251.1526993	2.785535678	11.54154
12000	0	251.2983545	2.349368487	10.63811
14000	0	251.6687279	2.737140559	13.04626

16000	0	251.2559144	2.487655214	11.93217
18000	0	251.2654675	2.937093461	14.01726
20000	0	251.2520379	3.428972584	14.50127
2000	5	250.8881669	0.764076597	9.019383
4000	5	251.4649348	1.226836597	11.11232
6000	5	252.154318	1.709470298	13.15315
8000	5	252.0304772	2.126340302	15.0909
10000	5	251.1526993	2.821798205	16.69156
12000	5	251.2983545	2.379903872	15.77638
14000	5	251.6687279	2.772720906	18.21586
16000	5	251.2559144	2.519989073	17.08727
18000	5	251.2654675	2.975274366	19.19948
20000	5	251.2520379	3.473597401	19.68975
2000	10	250.8881669	0.773894433	14.07104
4000	10	251.4649348	1.242585051	16.19079
6000	10	252.154318	1.731411087	18.2578
8000	10	252.0304772	2.153630155	20.22043
10000	10	251.1526993	2.858060732	21.84159
12000	10	251.2983545	2.410439256	20.91464
14000	10	251.6687279	2.808301254	23.38545
16000	10	251.2559144	2.552322933	22.24236
18000	10	251.2654675	3.013455271	24.38169
20000	10	251.2520379	3.518222218	24.87824
2000	15	250.8881669	0.783712269	19.1227
4000	15	251.4649348	1.258333505	21.26927
6000	15	252.154318	1.753351877	23.36245
8000	15	252.0304772	2.180920007	25.34995
10000	15	251.1526993	2.894323259	26.99162
12000	15	251.2983545	2.44097464	26.05291
14000	15	251.6687279	2.843881602	28.55504
16000	15	251.2559144	2.584656793	27.39745
18000	15	251.2654675	3.051636175	29.56391
20000	15	251.2520379	3.562847036	30.06672
2000	20	250.8881669	0.793530104	24.17436
4000	20	251.4649348	1.274081959	26.34774
6000	20	252.154318	1.775292667	28.4671
8000	20	252.0304772	2.20820986	30.47947
10000	20	251.1526993	2.930585786	32.14164
12000	20	251.2983545	2.471510025	31.19118
14000	20	251.6687279	2.87946195	33.72463
16000	20	251.2559144	2.616990653	32.55254
18000	20	251.2654675	3.08981708	34.74613

20000	20	251.2520379	3.607471853	35.2552
2000	25	250.8881669	0.80334794	29.22601
4000	25	251.4649348	1.289830413	31.42622
6000	25	252.154318	1.797233456	33.57175
8000	25	252.0304772	2.235499712	35.60899
10000	25	251.1526993	2.966848313	37.29167
12000	25	251.2983545	2.502045409	36.32945
14000	25	251.6687279	2.915042298	38.89423
16000	25	251.2559144	2.649324513	37.70763
18000	25	251.2654675	3.127997985	39.92834
20000	25	251.2520379	3.65209667	40.44368
2000	30	250.8881669	0.813165776	34.27767
4000	30	251.4649348	1.305578867	36.50469
6000	30	252.154318	1.819174246	38.6764
8000	30	252.0304772	2.262789565	40.73851
10000	30	251.1526993	3.00311084	42.4417
12000	30	251.2983545	2.532580794	41.46772
14000	30	251.6687279	2.950622646	44.06382
16000	30	251.2559144	2.681658373	42.86272
18000	30	251.2654675	3.16617889	45.11056
20000	30	251.2520379	3.696721487	45.63217
2000	35	250.8881669	0.822983611	39.32933
4000	35	251.4649348	1.321327321	41.58316
6000	35	252.154318	1.841115036	43.78105
8000	35	252.0304772	2.290079418	45.86803
10000	35	251.1526993	3.039373367	47.59172
12000	35	251.2983545	2.563116178	46.60599
14000	35	251.6687279	2.986127051	49.23308
16000	35	251.2559144	2.713992233	48.01781
18000	35	251.2654675	3.204016063	50.29132
20000	35	251.2520379	3.74043497	50.81811
2000	40	250.8881669	0.832801447	44.38099
4000	40	251.4649348	1.337075775	46.66164
6000	40	252.154318	1.863055825	48.8857
8000	40	252.0304772	2.316600003	50.99369
10000	40	251.1526993	3.07282529	52.73219
12000	40	251.2983545	2.592573293	51.73945
14000	40	251.6687279	3.018683905	54.38841
16000	40	251.2559144	2.744430527	53.16386
18000	40	251.2654675	3.238582924	55.45674
20000	40	251.2520379	3.780466119	55.98926
2000	0	300.7830038	0.907730742	4.78269

4000	0	301.6956633	1.45769981	7.281538
6000	0	302.677875	2.035292142	9.720492
8000	0	302.4992593	2.534266904	12.04298
10000	0	301.2070129	3.358744896	13.95283
12000	0	301.4085015	2.832196065	12.85714
14000	0	301.9743327	3.307424281	15.79017
16000	0	301.3196438	3.005105139	14.42893
18000	0	301.3334738	3.536309468	16.964
20000	0	301.3136184	4.139584334	17.55415
2000	5	300.7830038	0.919521367	9.844833
4000	5	301.6956633	1.476630263	12.37612
6000	5	302.677875	2.061729023	14.84677
8000	5	302.4992593	2.567189717	17.19945
10000	5	301.2070129	3.402474261	19.13407
12000	5	301.4085015	2.868979093	18.02413
14000	5	301.9743327	3.350393097	20.99531
16000	5	301.3196438	3.044138486	19.61635
18000	5	301.3334738	3.582255289	22.1844
20000	5	301.3136184	4.193461655	22.78218
2000	10	300.7830038	0.931311992	14.90698
4000	10	301.6956633	1.495560715	17.47071
6000	10	302.677875	2.088165903	19.97304
8000	10	302.4992593	2.600112531	22.35592
10000	10	301.2070129	3.446203626	24.3153
12000	10	301.4085015	2.905762122	23.19111
14000	10	301.9743327	3.393361912	26.20046
16000	10	301.3196438	3.083171832	24.80377
18000	10	301.3334738	3.628201111	27.40481
20000	10	301.3136184	4.247338977	28.01021
2000	15	300.7830038	0.943102617	19.96912
4000	15	301.6956633	1.514491167	22.56529
6000	15	302.677875	2.114602784	25.09931
8000	15	302.4992593	2.633035344	27.51239
10000	15	301.2070129	3.489932991	29.49654
12000	15	301.4085015	2.94254515	28.3581
14000	15	301.9743327	3.436330727	31.4056
16000	15	301.3196438	3.122205178	29.99119
18000	15	301.3334738	3.674146932	32.62521
20000	15	301.3136184	4.301216298	33.23823
2000	20	300.7830038	0.954893242	25.03126
4000	20	301.6956633	1.53342162	27.65988
6000	20	302.677875	2.141039665	30.22559

8000	20	302.4992593	2.665958157	32.66886
10000	20	301.2070129	3.533662356	34.67778
12000	20	301.4085015	2.979328178	33.52509
14000	20	301.9743327	3.479299542	36.61074
16000	20	301.3196438	3.161238525	35.1786
18000	20	301.3334738	3.720092754	37.84562
20000	20	301.3136184	4.355093619	38.46626
2000	25	300.7830038	0.966683867	30.09341
4000	25	301.6956633	1.552352072	32.75446
6000	25	302.677875	2.167476546	35.35186
8000	25	302.4992593	2.69888097	37.82533
10000	25	301.2070129	3.577391721	39.85901
12000	25	301.4085015	3.016111206	38.69207
14000	25	301.9743327	3.522268357	41.81589
16000	25	301.3196438	3.200271871	40.36602
18000	25	301.3334738	3.766038575	43.06602
20000	25	301.3136184	4.40897094	43.69429
2000	30	300.7830038	0.978474492	35.15555
4000	30	301.6956633	1.571282525	37.84905
6000	30	302.677875	2.193913426	40.47814
8000	30	302.4992593	2.731803784	42.9818
10000	30	301.2070129	3.621121086	45.04025
12000	30	301.4085015	3.052894234	43.85906
14000	30	301.9743327	3.565237172	47.02103
16000	30	301.3196438	3.239305218	45.55344
18000	30	301.3334738	3.811977051	48.2864
20000	30	301.3136184	4.46267687	48.92185
2000	35	300.7830038	0.990265117	40.21769
4000	35	301.6956633	1.590212977	42.94363
6000	35	302.677875	2.220350307	45.60441
8000	35	302.4992593	2.764726597	48.13827
10000	35	301.2070129	3.663891234	50.21887
12000	35	301.4085015	3.089635542	49.02582
14000	35	301.9743327	3.606358152	52.21765
16000	35	301.3196438	3.277823693	50.73838
18000	35	301.3334738	3.854992246	53.4932
20000	35	301.3136184	4.512196709	54.13435
2000	40	300.7830038	1.002055742	45.27983
4000	40	301.6956633	1.60914343	48.03822
6000	40	302.677875	2.246028307	50.72734
8000	40	302.4992593	2.794617036	53.27965
10000	40	301.2070129	3.702206216	55.37956

12000	40	301.4085015	3.123245365	54.1783
14000	40	301.9743327	3.644844414	57.40116
16000	40	301.3196438	3.31298381	55.90721
18000	40	301.3334738	3.896299504	58.69158
20000	40	301.3136184	4.560303977	59.34032
2000	0	352.7962446	1.068543809	5.641427
4000	0	353.502715	1.715808023	8.57953
6000	0	354.3475222	2.393959136	11.45629
8000	0	354.2043251	2.984509181	14.20943
10000	0	353.1011516	3.959182849	16.49966
12000	0	353.2906855	3.339710855	15.1905
14000	0	353.7457997	3.896997995	18.66769
16000	0	353.2327516	3.547006417	17.05932
18000	0	353.245963	4.180579503	20.08548
20000	0	353.2226253	4.888474493	20.79024
2000	5	352.7962446	1.082399757	10.71461
4000	5	353.502715	1.73806661	13.69086
6000	5	354.3475222	2.425030003	16.605
8000	5	354.2043251	3.023256677	19.39393
10000	5	353.1011516	4.010731747	21.71386
12000	5	353.2906855	3.383059402	20.38768
14000	5	353.7457997	3.947602121	23.9101
16000	5	353.2327516	3.59305392	22.28078
18000	5	353.245963	4.234872474	25.34632
20000	5	353.2226253	4.952101207	26.06019
2000	10	352.7962446	1.096255705	15.78779
4000	10	353.502715	1.760325197	18.8022
6000	10	354.3475222	2.45610087	21.75371
8000	10	354.2043251	3.062004174	24.57843
10000	10	353.1011516	4.062280645	26.92805
12000	10	353.2906855	3.426407948	25.58485
14000	10	353.7457997	3.998206248	29.15252
16000	10	353.2327516	3.639101422	27.50224
18000	10	353.245963	4.289165444	30.60717
20000	10	353.2226253	5.01572792	31.33013
2000	15	352.7962446	1.110111653	20.86097
4000	15	353.502715	1.782583784	23.91353
6000	15	354.3475222	2.487171737	26.90242
8000	15	354.2043251	3.10075167	29.76294
10000	15	353.1011516	4.113829543	32.14225
12000	15	353.2906855	3.469756494	30.78203
14000	15	353.7457997	4.048810375	34.39493

16000	15	353.2327516	3.685148925	32.72371
18000	15	353.245963	4.343458414	35.86801
20000	15	353.2226253	5.079354633	36.60007
2000	20	352.7962446	1.123967601	25.93416
4000	20	353.502715	1.804842371	29.02486
6000	20	354.3475222	2.518242604	32.05113
8000	20	354.2043251	3.139499166	34.94744
10000	20	353.1011516	4.165378441	37.35644
12000	20	353.2906855	3.51310504	35.9792
14000	20	353.7457997	4.099414502	39.63734
16000	20	353.2327516	3.731196427	37.94517
18000	20	353.245963	4.397751384	41.12886
20000	20	353.2226253	5.142981347	41.87001
2000	25	352.7962446	1.137823549	31.00734
4000	25	353.502715	1.827100958	34.1362
6000	25	354.3475222	2.54931347	37.19984
8000	25	354.2043251	3.178246663	40.13195
10000	25	353.1011516	4.216927339	42.57063
12000	25	353.2906855	3.556453586	41.17638
14000	25	353.7457997	4.150018628	44.87975
16000	25	353.2327516	3.77724393	43.16664
18000	25	353.245963	4.452044354	46.3897
20000	25	353.2226253	5.20660806	47.13995
2000	30	352.7962446	1.151679497	36.08052
4000	30	353.502715	1.849359545	39.24753
6000	30	354.3475222	2.580384337	42.34855
8000	30	354.2043251	3.216994159	45.31645
10000	30	353.1011516	4.268476237	47.78483
12000	30	353.2906855	3.599802133	46.37355
14000	30	353.7457997	4.200080656	50.11964
16000	30	353.2327516	3.823282304	48.38804
18000	30	353.245963	4.504829409	51.64351
20000	30	353.2226253	5.267171811	52.39974
2000	35	352.7962446	1.165535444	41.1537
4000	35	353.502715	1.871618132	44.35887
6000	35	354.3475222	2.611455204	47.49726
8000	35	354.2043251	3.254957684	50.49669
10000	35	353.1011516	4.31562816	52.98411
12000	35	353.2906855	3.641862705	51.56472
14000	35	353.7457997	4.245910641	55.33912
16000	35	353.2327516	3.86633847	53.59502
18000	35	353.245963	4.553663287	56.87837

20000	35	353.2226253	5.32397	57.64345
2000	40	352.7962446	1.179391392	46.22689
4000	40	353.502715	1.893799543	49.46979
6000	40	354.3475222	2.63962059	52.63268
8000	40	354.2043251	3.288350756	55.65471
10000	40	353.1011516	4.360348243	58.17129
12000	40	353.2906855	3.680289451	56.73935
14000	40	353.7457997	4.291202667	60.55578
16000	40	353.2327516	3.907612291	58.79345
18000	40	353.245963	4.602443857	62.11295
20000	40	353.2226253	5.38074044	62.88708
2000	0	402.2813786	1.221616276	6.450496
4000	0	402.9393046	1.962342454	9.817817
6000	0	403.7182453	2.739088669	13.11674
8000	0	403.6063706	3.420759053	16.28458
10000	0	402.5734617	4.542263538	18.93338
12000	0	402.7594918	3.835490835	17.42161
14000	0	403.1813382	4.474032968	21.42862
16000	0	402.7136562	4.068138067	19.57587
18000	0	402.7246008	4.804132049	23.07474
20000	0	402.6937159	5.613383831	23.8843
2000	5	402.2813786	1.237437192	11.53407
4000	5	402.9393046	1.987778209	14.94512
6000	5	403.7182453	2.774617697	18.2869
8000	5	403.6063706	3.465148901	21.49593
10000	5	402.5734617	4.601402775	24.17906
12000	5	402.7594918	3.885252244	22.64764
14000	5	403.1813382	4.532109347	26.70679
16000	5	402.7136562	4.120929917	24.8299
18000	5	402.7246008	4.866501731	28.3743
20000	5	402.6937159	5.686444377	29.19431
2000	10	402.2813786	1.253258107	16.61765
4000	10	402.9393046	2.013213965	20.07242
6000	10	403.7182453	2.810146725	23.45707
8000	10	403.6063706	3.509538749	26.70728
10000	10	402.5734617	4.660542011	29.42473
12000	10	402.7594918	3.935013652	27.87367
14000	10	403.1813382	4.590185726	31.98495
16000	10	402.7136562	4.173721767	30.08394
18000	10	402.7246008	4.928871413	33.67387
20000	10	402.6937159	5.759504922	34.50431
2000	15	402.2813786	1.269079023	21.70123

4000	15	402.9393046	2.03864972	25.19973
6000	15	403.7182453	2.845675753	28.62724
8000	15	403.6063706	3.553928597	31.91863
10000	15	402.5734617	4.719681248	34.67041
12000	15	402.7594918	3.984775061	33.09971
14000	15	403.1813382	4.648262105	37.26312
16000	15	402.7136562	4.226513617	35.33797
18000	15	402.7246008	4.991241095	38.97343
20000	15	402.6937159	5.832565468	39.81431
2000	20	402.2813786	1.284899939	26.7848
4000	20	402.9393046	2.064085475	30.32703
6000	20	403.7182453	2.881204781	33.7974
8000	20	403.6063706	3.598318444	37.12997
10000	20	402.5734617	4.778820484	39.91609
12000	20	402.7594918	4.03453647	38.32574
14000	20	403.1813382	4.706338484	42.54128
16000	20	402.7136562	4.279305467	40.592
18000	20	402.7246008	5.053610778	44.27299
20000	20	402.6937159	5.905626014	45.12432
2000	25	402.2813786	1.300720855	31.86838
4000	25	402.9393046	2.08952123	35.45433
6000	25	403.7182453	2.916733809	38.96757
8000	25	403.6063706	3.642708292	42.34132
10000	25	402.5734617	4.837959721	45.16176
12000	25	402.7594918	4.084297878	43.55178
14000	25	403.1813382	4.764403866	47.8194
16000	25	402.7136562	4.332097317	45.84604
18000	25	402.7246008	5.115548988	49.57056
20000	25	402.6937159	5.97724462	50.43022
2000	30	402.2813786	1.316541771	36.95196
4000	30	402.9393046	2.114956985	40.58164
6000	30	403.7182453	2.952262837	44.13774
8000	30	403.6063706	3.68709814	47.55267
10000	30	402.5734617	4.895289713	50.40233
12000	30	402.7594918	4.133966787	48.77732
14000	30	403.1813382	4.819048296	53.08129
16000	30	402.7136562	4.383897058	51.09518
18000	30	402.7246008	5.172848208	54.84608
20000	30	402.6937159	6.043344789	55.71392
2000	35	402.2813786	1.332362687	42.03554
4000	35	402.9393046	2.14039274	45.70894
6000	35	403.7182453	2.987573423	49.30693

8000	35	403.6063706	3.728100032	52.74672
10000	35	402.5734617	4.94716577	55.62032
12000	35	402.7594918	4.179722697	53.98502
14000	35	403.1813382	4.870990755	58.32972
16000	35	402.7136562	4.431415063	56.32374
18000	35	402.7246008	5.228844037	60.11528
20000	35	402.6937159	6.108485164	60.99349
2000	40	402.2813786	1.348183603	47.11911
4000	40	402.9393046	2.164828066	50.83134
6000	40	403.7182453	3.01774513	54.45225
8000	40	403.6063706	3.765999185	57.92603
10000	40	402.5734617	4.99843523	60.83483
12000	40	402.7594918	4.223793154	59.18502
14000	40	403.1813382	4.922933205	63.57815
16000	40	402.7136562	4.478703484	61.5512
18000	40	402.7246008	5.284840186	65.38448
20000	40	402.6937159	6.173625222	66.27305
2000	0	451.3035272	1.375233943	7.261886
4000	0	452.0271968	2.210271829	11.05755
6000	0	452.8837096	3.087458215	14.78156
8000	0	452.7653704	3.855784857	18.37022
10000	0	451.6319025	5.126083412	21.37823
12000	0	451.8293406	4.320136475	19.6581
14000	0	452.2925415	5.05576158	24.20747
16000	0	451.7753287	4.592978814	22.10519
18000	0	451.7908343	5.428788557	26.08045
20000	0	451.7621275	6.345432711	27.00905
2000	5	451.3035272	1.393026524	12.35589
4000	5	452.0271968	2.238901794	16.20084
6000	5	452.8837096	3.12748679	19.97324
8000	5	452.7653704	3.905799924	23.60855
10000	5	451.6319025	5.192820151	26.65552
12000	5	451.8293406	4.376164819	24.91306
14000	5	452.2925415	5.121370702	29.52162
16000	5	451.7753287	4.652562477	27.39196
18000	5	451.7908343	5.49924814	31.41894
20000	5	451.7621275	6.428016962	32.3595
2000	10	451.3035272	1.410819105	17.44989
4000	10	452.0271968	2.267531759	21.34412
6000	10	452.8837096	3.167515365	25.16491
8000	10	452.7653704	3.955814991	28.84687
10000	10	451.6319025	5.25955689	31.93282

12000	10	451.8293406	4.432193163	30.16801
14000	10	452.2925415	5.186979823	34.83577
16000	10	451.7753287	4.71214614	32.67872
18000	10	451.7908343	5.569707723	36.75743
20000	10	451.7621275	6.510601214	37.70995
2000	15	451.3035272	1.428611686	22.54389
4000	15	452.0271968	2.296161725	26.48741
6000	15	452.8837096	3.20754394	30.35659
8000	15	452.7653704	4.005830058	34.0852
10000	15	451.6319025	5.326293629	37.21011
12000	15	451.8293406	4.488221507	35.42297
14000	15	452.2925415	5.252588945	40.14992
16000	15	451.7753287	4.771729803	37.96548
18000	15	451.7908343	5.640167307	42.09592
20000	15	451.7621275	6.593185465	43.06041
2000	20	451.3035272	1.446404267	27.63789
4000	20	452.0271968	2.32479169	31.6307
6000	20	452.8837096	3.247572515	35.54827
8000	20	452.7653704	4.055845124	39.32352
10000	20	451.6319025	5.393030369	42.48741
12000	20	451.8293406	4.544249851	40.67793
14000	20	452.2925415	5.318198066	45.46406
16000	20	451.7753287	4.831313465	43.25225
18000	20	451.7908343	5.710612817	47.43434
20000	20	451.7621275	6.675381762	48.40972
2000	25	451.3035272	1.464196848	32.73189
4000	25	452.0271968	2.353421655	36.77399
6000	25	452.8837096	3.28760109	40.73994
8000	25	452.7653704	4.105860191	44.56185
10000	25	451.6319025	5.45965715	47.76437
12000	25	451.8293406	4.600278195	45.93289
14000	25	452.2925415	5.382469704	50.77195
16000	25	451.7753287	4.89078712	48.53842
18000	25	451.7908343	5.777789141	52.75732
20000	25	451.7621275	6.752237048	53.74017
2000	30	451.3035272	1.481989429	37.82589
4000	30	452.0271968	2.382051621	41.91727
6000	30	452.8837096	3.327629665	45.93162
8000	30	452.7653704	4.155202821	49.7963
10000	30	451.6319025	5.520614076	53.02261
12000	30	451.8293406	4.654953806	51.18144
14000	30	452.2925415	5.441617519	56.05504

16000	30	451.7753287	4.946456424	53.80618
18000	30	451.7908343	5.841006433	58.06129
20000	30	451.7621275	6.825814051	59.05599
2000	35	451.3035272	1.49978201	42.91989
4000	35	452.0271968	2.410681586	47.06056
6000	35	452.8837096	3.365898751	51.11545
8000	35	452.7653704	4.198894758	55.0032
10000	35	451.6319025	5.578425589	58.26455
12000	35	451.8293406	4.704789493	56.40803
14000	35	452.2925415	5.500256021	61.3354
16000	35	451.7753287	4.99979304	59.06278
18000	35	451.7908343	5.904220088	63.36524
20000	35	451.7621275	6.89939061	64.3718
2000	40	451.3035272	1.517574591	48.01389
4000	40	452.0271968	2.43640347	52.18949
6000	40	452.8837096	3.398864576	56.27395
8000	40	452.7653704	4.241561472	60.20523
10000	40	451.6319025	5.636236032	63.50649
12000	40	451.8293406	4.754378135	61.63348
14000	40	452.2925415	5.558894443	66.61576
16000	40	451.7753287	5.053129533	64.31938
18000	40	451.7908343	5.967433663	68.6692
20000	40	451.7621275	6.972967127	69.68761
2000	0	501.6897596	1.536429891	8.094973
4000	0	502.3024294	2.464387216	12.33583
6000	0	503.1027233	3.446299939	16.50007
8000	0	502.992436	4.311471008	20.52602
10000	0	501.927375	5.740065377	23.92051
12000	0	502.1040825	4.837877314	21.98509
14000	0	502.533583	5.66126388	27.09981
16000	0	502.0378807	5.145400805	24.73864
18000	0	502.0395282	6.073824899	29.21754
20000	0	501.9978654	7.11329159	30.26375
2000	5	501.6897596	1.556291591	13.19967
4000	5	502.3024294	2.496290531	17.4956
6000	5	503.1027233	3.490962954	21.71394
8000	5	502.992436	4.367378452	25.79223
10000	5	501.927375	5.814791331	29.23068
12000	5	502.1040825	4.90060078	27.27014
14000	5	502.533583	5.734713273	32.45141
16000	5	502.0378807	5.212133299	30.05948
18000	5	502.0395282	6.152637777	34.59665

20000	5	501.9978654	7.205864453	35.65634
2000	10	501.6897596	1.576153291	18.30437
4000	10	502.3024294	2.528193846	22.65537
6000	10	503.1027233	3.535625968	26.92782
8000	10	502.992436	4.423285897	31.05844
10000	10	501.927375	5.889517285	34.54086
12000	10	502.1040825	4.963324246	32.55519
14000	10	502.533583	5.808162667	37.80301
16000	10	502.0378807	5.278865793	35.38032
18000	10	502.0395282	6.231450655	39.97576
20000	10	501.9978654	7.298437315	41.04892
2000	15	501.6897596	1.596014991	23.40908
4000	15	502.3024294	2.560097161	27.81513
6000	15	503.1027233	3.580288982	32.1417
8000	15	502.992436	4.479193341	36.32464
10000	15	501.927375	5.964243239	39.85103
12000	15	502.1040825	5.026047712	37.84024
14000	15	502.533583	5.881612061	43.15461
16000	15	502.0378807	5.345598286	40.70116
18000	15	502.0395282	6.310263533	45.35488
20000	15	501.9978654	7.391008933	46.4415
2000	20	501.6897596	1.615876691	28.51378
4000	20	502.3024294	2.592000476	32.9749
6000	20	503.1027233	3.624951996	37.35558
8000	20	502.992436	4.535100786	41.59085
10000	20	501.927375	6.038969194	45.1612
12000	20	502.1040825	5.088771178	43.12529
14000	20	502.533583	5.954748608	48.50473
16000	20	502.0378807	5.41233078	46.022
18000	20	502.0395282	6.387632369	50.7272
20000	20	501.9978654	7.47974441	51.82236
2000	25	501.6897596	1.63573839	33.61848
4000	25	502.3024294	2.623903791	38.13467
6000	25	503.1027233	3.66961501	42.56946
8000	25	502.992436	4.59100823	46.85706
10000	25	501.927375	6.110911412	50.46348
12000	25	502.1040825	5.151363105	48.40962
14000	25	502.533583	6.023096965	53.83213
16000	25	502.0378807	5.477530384	51.33526
18000	25	502.0395282	6.459194584	56.07177
20000	25	501.9978654	7.562805707	57.17826
2000	30	501.6897596	1.65560009	38.72318

4000	30	502.3024294	2.655807106	43.29443
6000	30	503.1027233	3.714277997	47.78334
8000	30	502.992436	4.643658642	52.10624
10000	30	501.927375	6.176577147	55.73948
12000	30	502.1040825	5.209587458	53.67395
14000	30	502.533583	6.08869418	59.14569
16000	30	502.0378807	5.537609846	56.62395
18000	30	502.0395282	6.529846517	61.41195
20000	30	501.9978654	7.645219569	62.53176
2000	35	501.6897596	1.67546179	43.82788
4000	35	502.3024294	2.687710406	48.4542
6000	35	503.1027233	3.75420112	52.97558
8000	35	502.992436	4.691336302	57.33181
10000	35	501.927375	6.241261358	61.0099
12000	35	502.1040825	5.265099505	58.92585
14000	35	502.533583	6.154291459	64.45924
16000	35	502.0378807	5.597310029	61.91085
18000	35	502.0395282	6.600498409	66.75213
20000	35	501.9978654	7.727633378	67.88527
2000	40	501.6897596	1.69532349	48.93258
4000	40	502.3024294	2.714273765	53.58743
6000	40	503.1027233	3.790835137	58.15157
8000	40	502.992436	4.73899642	62.5573
10000	40	501.927375	6.305945432	66.28032
12000	40	502.1040825	5.32061159	64.17775
14000	40	502.533583	6.219888747	69.77279
16000	40	502.0378807	5.657010218	67.19775
18000	40	502.0395282	6.671150292	72.0923
20000	40	501.9978654	7.810047172	73.23878
2000	0	551.4652509	2.601675096	13.94526
4000	0	551.1364655	3.555577499	17.60656
6000	0	550.8805994	4.642349429	22.15961
8000	0	550.4881616	6.145187467	28.36366
10000	0	550.3077749	6.322458738	29.68802
12000	0	549.8787502	6.718681595	30.60942
14000	0	549.6343665	7.885392349	37.2698
16000	0	549.5148635	7.545543416	36.4983
18000	0	549.2228792	8.04844489	37.31125
20000	0	548.8705438	8.789798696	38.80037
2000	5	551.4652509	2.635403907	19.12615
4000	5	551.1364655	3.60167262	22.83491
6000	5	550.8805994	4.702554782	27.44708

8000	5	550.4881616	6.224941611	33.73174
10000	5	550.3077749	6.40449475	35.07319
12000	5	549.8787502	6.805847231	36.00638
14000	5	549.6343665	7.98774948	42.75312
16000	5	549.5148635	7.643460808	41.97143
18000	5	549.2228792	8.152855343	42.79481
20000	5	548.8705438	8.904217199	44.30325
2000	10	551.4652509	2.669132718	24.30704
4000	10	551.1364655	3.647767742	28.06326
6000	10	550.8805994	4.762759942	32.73453
8000	10	550.4881616	6.304704781	39.09967
10000	10	550.3077749	6.486499103	40.45813
12000	10	549.8787502	6.892995069	41.4031
14000	10	549.6343665	8.089441778	48.23274
16000	10	549.5148635	7.741131852	47.44301
18000	10	549.2228792	8.256546711	48.27505
20000	10	548.8705438	9.016226888	49.79918
2000	15	551.4652509	2.70286153	29.48794
4000	15	551.1364655	3.693862863	33.29161
6000	15	550.8805994	4.822962251	38.02185
8000	15	550.4881616	6.384484083	44.46733
10000	15	550.3077749	6.568461477	45.84276
12000	15	549.8787502	6.980098909	46.79939
14000	15	549.6343665	8.185250689	53.68489
16000	15	549.5148635	7.834334477	52.89301
18000	15	549.2228792	8.354672736	53.72989
20000	15	548.8705438	9.120698049	55.26667
2000	20	551.4652509	2.736590341	34.66883
4000	20	551.1364655	3.739957961	38.51993
6000	20	550.8805994	4.883159386	43.30891
8000	20	550.4881616	6.462266309	49.82529
10000	20	550.3077749	6.647062871	51.21178
12000	20	549.8787502	7.063107439	52.177
14000	20	549.6343665	8.276733828	59.11609
16000	20	549.5148635	7.922017396	58.31695
18000	20	549.2228792	8.448559559	59.16484
20000	20	548.8705438	9.222434493	60.71915
2000	25	551.4652509	2.770319159	39.84972
4000	25	551.1364655	3.78605289	43.74808
6000	25	550.8805994	4.942983431	48.59349
8000	25	550.4881616	6.532562353	55.14787
10000	25	550.3077749	6.718844409	56.54845

12000	25	549.8787502	7.140235839	57.52788
14000	25	549.6343665	8.368189532	64.54715
16000	25	549.5148635	8.009602808	63.74043
18000	25	549.2228792	8.542424039	64.59971
20000	25	548.8705438	9.324171609	66.17161
2000	30	551.4652509	2.804048239	45.03049
4000	30	551.1364655	3.831772046	48.97404
6000	30	550.8805994	4.995847631	53.8452
8000	30	550.4881616	6.600943531	60.46112
10000	30	550.3077749	6.78982718	61.88095
12000	30	549.8787502	7.217191448	62.87771
14000	30	549.6343665	8.459645078	69.97819
16000	30	549.5148635	8.097188637	69.16393
18000	30	549.2228792	8.636286727	70.03457
20000	30	548.8705438	9.425909395	71.62405
2000	35	551.4652509	2.836532162	50.20389
4000	35	551.1364655	3.869383293	54.16122
6000	35	550.8805994	5.045672911	59.08227
8000	35	550.4881616	6.669324704	65.77437
10000	35	550.3077749	6.860809686	67.21345
12000	35	549.8787502	7.29414632	68.22752
14000	35	549.6343665	8.55110057	75.40922
16000	35	549.5148635	8.184780529	74.58757
18000	35	549.2228792	8.730158188	75.46952
20000	35	548.8705438	9.527627129	77.07652
2000	40	551.4652509	2.859777656	55.32628
4000	40	551.1364655	3.904736255	59.33627
6000	40	550.8805994	5.095498173	64.31934
8000	40	550.4881616	6.737705442	71.08763
10000	40	550.3077749	6.931793051	72.54595
12000	40	549.8787502	7.371102117	73.57734
14000	40	549.6343665	8.642500837	80.84025
16000	40	549.5148635	8.272335126	80.01145
18000	40	549.2228792	8.82390242	80.90428
20000	40	548.8705438	9.629022905	82.52827
2000	0	583.942507	3.114417405	16.51878
4000	0	583.3364377	4.619428845	22.29185
6000	0	582.9467612	6.714814161	28.80869
8000	0	582.6500518	7.105983978	34.43
10000	0	582.4174251	8.5374022	39.3267
12000	0	582.5214063	9.276142668	42.17916
14000	0	582.101154	10.67611709	49.7099

16000	0	581.7796193	11.10013086	51.08405
18000	0	581.8336929	11.87351414	52.98566
20000	0	581.7173105	10.99151453	50.34403
2000	5	583.942507	3.154853805	21.73336
4000	5	583.3364377	4.679385325	27.58132
6000	5	582.9467612	6.801972997	34.1823
8000	5	582.6500518	7.198225495	39.87636
10000	5	582.4174251	8.648289506	44.83638
12000	5	582.5214063	9.395682513	47.72085
14000	5	582.101154	10.80312869	55.30123
16000	5	581.7796193	11.2309649	56.68491
18000	5	581.8336929	12.01196176	58.60478
20000	5	581.7173105	11.12105181	55.94309
2000	10	583.942507	3.195290205	26.94793
4000	10	583.3364377	4.739341386	32.87068
6000	10	582.9467612	6.889116717	39.55563
8000	10	582.6500518	7.290448515	45.32227
10000	10	582.4174251	8.754629038	50.32585
12000	10	582.5214063	9.508672077	53.23293
14000	10	582.101154	10.92646758	60.87457
16000	10	581.7796193	11.35959695	62.27702
18000	10	581.8336929	12.15015584	64.22172
20000	10	581.7173105	11.24900763	61.52962
2000	15	583.942507	3.235726605	32.16251
4000	15	583.3364377	4.79929645	38.15977
6000	15	582.9467612	6.976237759	44.92858
8000	15	582.6500518	7.378515387	50.74619
10000	15	582.4174251	8.852653485	55.7763
12000	15	582.5214063	9.615335739	58.71695
14000	15	582.101154	11.04980265	66.4481
16000	15	581.7796193	11.48823396	67.86947
18000	15	581.8336929	12.28834009	69.83897
20000	15	581.7173105	11.37699534	67.11643
2000	20	583.942507	3.276163006	37.37709
4000	20	583.3364377	4.859250258	43.44852
6000	20	582.9467612	7.059053115	50.28558
8000	20	582.6500518	7.458216394	56.13058
10000	20	582.4174251	8.948650612	61.21708
12000	20	582.5214063	9.721768771	64.19983
14000	20	582.101154	11.17314255	72.02197
16000	20	581.7796193	11.61687944	73.46249
18000	20	581.8336929	12.42650227	75.45664

20000	20	581.7173105	11.50501831	72.70356
2000	25	583.942507	3.316589643	42.59136
4000	25	583.3364377	4.918348524	48.73391
6000	25	582.9467612	7.133696697	55.60198
8000	25	582.6500518	7.536298428	61.50674
10000	25	582.4174251	9.044646834	66.658
12000	25	582.5214063	9.828211061	69.68292
14000	25	582.101154	11.29650822	77.59644
16000	25	581.7796193	11.74542943	79.05583
18000	25	581.8336929	12.56424231	81.07346
20000	25	581.7173105	11.63289722	78.29061
2000	30	583.942507	3.356997204	47.80504
4000	30	583.3364377	4.968069965	53.97263
6000	30	582.9467612	7.206670591	60.90924
8000	30	582.6500518	7.614383941	66.88299
10000	30	582.4174251	9.140641813	72.0991
12000	30	582.5214063	9.934669441	75.16638
14000	30	582.101154	11.4196314	83.1702
16000	30	581.7796193	11.87363347	84.64776
18000	30	581.8336929	12.70159559	86.6886
20000	30	581.7173105	11.76036934	83.87606
2000	35	583.942507	3.38889353	52.97253
4000	35	583.3364377	5.014551351	59.18967
6000	35	582.9467612	7.279646347	66.21654
8000	35	582.6500518	7.692476356	72.25941
10000	35	582.4174251	9.236802125	77.54113
12000	35	582.5214063	10.04118833	80.65079
14000	35	582.101154	11.5424892	88.74311
16000	35	581.7796193	12.00163319	90.23926
18000	35	581.8336929	12.83876334	92.30373
20000	35	581.7173105	11.88767777	89.4608
2000	40	583.942507	3.41478943	58.1064
4000	40	583.3364377	5.061032778	64.40674
6000	40	582.9467612	7.352628084	71.52395
8000	40	582.6500518	7.77071766	77.637
10000	40	582.4174251	9.333269326	82.98524
12000	40	582.5214063	10.14749981	86.13464
14000	40	582.101154	11.66534553	94.31662
16000	40	581.7796193	12.13074876	95.83563
18000	40	581.8336929	12.98214472	97.93726
20000	40	581.7173105	12.01580535	95.0473
2000	0	659.7617776	4.772001616	26.15342

4000	0	659.3519406	7.822138486	37.61825
6000	0	658.6208801	11.3465023	52.38802
8000	0	658.2643291	12.60903936	59.39421
10000	0	658.1658359	13.75385746	62.43885
12000	0	658.1388321	15.47418822	69.57254
14000	0	658.3612362	16.69849667	78.97209
16000	0	657.8171484	17.81052772	84.66931
18000	0	657.8253304	17.30439954	82.66323
20000	0	657.6008797	17.88135389	82.09955
2000	5	659.7617776	4.834027089	31.49366
4000	5	659.3519406	7.923798774	43.10703
6000	5	658.6208801	11.47293069	57.96593
8000	5	658.2643291	12.75131446	65.04748
10000	5	658.1658359	13.90892159	68.13911
12000	5	658.1388321	15.65142723	75.36917
14000	5	658.3612362	16.89157179	84.88399
16000	5	657.8171484	18.01639561	90.65039
18000	5	657.8253304	17.50462815	88.62283
20000	5	657.6008797	18.08861622	88.05386
2000	10	659.7617776	4.896052561	36.83391
4000	10	659.3519406	8.022584462	48.57692
6000	10	658.6208801	11.59699779	63.52907
8000	10	658.2643291	12.8935976	70.70097
10000	10	658.1658359	14.06414206	73.84013
12000	10	658.1388321	15.82857188	81.16593
14000	10	658.3612362	17.08427312	90.79509
16000	10	657.8171484	18.23053509	96.67307
18000	10	657.8253304	17.70877028	94.60119
20000	10	657.6008797	18.29976315	94.02058
2000	15	659.7617776	4.958078033	42.17415
4000	15	659.3519406	8.110154618	53.99248
6000	15	658.6208801	11.72106485	69.09224
8000	15	658.2643291	13.03613171	76.35726
10000	15	658.1658359	14.2200141	79.54563
12000	15	658.1388321	16.00551465	86.96215
14000	15	658.3612362	17.28392317	96.74406
16000	15	657.8171484	18.4651364	102.788
18000	15	657.8253304	17.92908807	100.6543
20000	15	657.6008797	18.52824366	100.0624
2000	20	659.7617776	5.02010289	47.51437
4000	20	659.3519406	8.190624776	59.36622
6000	20	658.6208801	11.84519276	74.6559

8000	20	658.2643291	13.17894761	82.0166
10000	20	658.1658359	14.37560307	85.25057
12000	20	658.1388321	16.18270422	92.76054
14000	20	658.3612362	17.50332436	102.7816
16000	20	657.8171484	18.72456627	109.0203
18000	20	657.8253304	18.17575399	106.8293
20000	20	657.6008797	18.7823933	106.2246
2000	25	659.7617776	5.072761165	52.79087
4000	25	659.3519406	8.219841814	64.76554
6000	25	658.6208801	11.97048077	80.2265
8000	25	658.2643291	13.32169686	87.67648
10000	25	658.1658359	14.53127166	90.95693
12000	25	658.1388321	16.37051771	98.60689
14000	25	658.3612362	17.746135	108.9237
16000	25	657.8171484	18.99433054	115.3029
18000	25	657.8253304	18.43631448	113.0732
20000	25	657.6008797	19.05147406	112.459
2000	30	659.7617776	5.115292928	58.0136
4000	30	659.3519406	8.300237207	70.13931
6000	30	658.6208801	12.09568822	85.79703
8000	30	658.2643291	13.46454499	93.33952
10000	30	658.1658359	14.69230726	96.68259
12000	30	658.1388321	16.57860054	104.5417
14000	30	658.3612362	17.99761415	115.1076
16000	30	657.8171484	19.2641603	121.586
18000	30	657.8253304	18.69813484	119.3245
20000	30	657.6008797	19.32245686	118.703
2000	35	659.7617776	5.157824636	63.23634
4000	35	659.3519406	8.380633078	75.51314
6000	35	658.6208801	12.22148763	91.37213
8000	35	658.2643291	13.61499272	99.03768
10000	35	658.1658359	14.8701638	102.4829
12000	35	658.1388321	16.80380025	110.552
14000	35	658.3612362	18.24909336	121.2914
16000	35	657.8171484	19.53399017	127.8691
18000	35	657.8253304	18.95995535	125.5758
20000	35	657.6008797	19.59343983	124.9471
2000	40	659.7617776	5.200356334	68.45907
4000	40	659.3519406	8.462521684	80.89587
6000	40	658.6208801	12.34944588	96.9567
8000	40	658.2643291	13.78437199	104.8151
10000	40	658.1658359	15.06446116	108.3599

12000	40	658.1388321	17.03237582	116.5778
14000	40	658.3612362	18.50057264	127.4753
16000	40	657.8171484	19.80382012	134.1523
18000	40	657.8253304	19.22177599	131.8271
20000	40	657.6008797	19.86442294	131.1911
2000	0	679.8381029	4.819287633	26.34731
4000	0	679.9105627	7.904818159	37.94282
6000	0	679.8211332	12.65450378	55.13939
8000	0	679.4001351	13.58611598	62.45986
10000	0	679.4781653	15.23032658	69.96982
12000	0	679.1914277	16.40617893	73.26756
14000	0	679.4277618	17.7254308	82.0981
16000	0	679.1519568	18.4320792	87.17804
18000	0	679.3101358	18.18771547	86.78506
20000	0	679.4943687	19.90950453	90.99216
2000	5	679.8381029	4.881936972	31.69013
4000	5	679.9105627	8.007543038	43.43566
6000	5	679.8211332	12.79605674	60.73695
8000	5	679.4001351	13.73904697	68.14701
10000	5	679.4781653	15.40434183	75.75968
12000	5	679.1914277	16.5938772	79.10699
14000	5	679.4277618	17.92999027	88.04589
16000	5	679.1519568	18.64691369	93.19604
18000	5	679.3101358	18.3996812	92.80157
20000	5	679.4943687	20.15745646	97.10958
2000	10	679.8381029	4.94458631	37.03295
4000	10	679.9105627	8.106432626	48.90653
6000	10	679.8211332	12.93744603	66.33132
8000	10	679.4001351	13.89204731	73.83478
10000	10	679.4781653	15.57811349	81.55112
12000	10	679.1914277	16.7813089	84.94563
14000	10	679.4277618	18.13896056	94.01013
16000	10	679.1519568	18.87768875	99.28578
18000	10	679.3101358	18.62661644	98.88763
20000	10	679.4943687	20.42863157	103.3279
2000	15	679.8381029	5.007235648	42.37577
4000	15	679.9105627	8.193637225	54.32222
6000	15	679.8211332	13.07883546	71.92575
8000	15	679.4001351	14.04564956	79.52846
10000	15	679.4781653	15.75171291	87.34256
12000	15	679.1914277	16.96867115	90.78449
14000	15	679.4277618	18.36465706	100.0467

16000	15	679.1519568	19.13377554	105.4867
18000	15	679.3101358	18.87756284	105.0854
20000	15	679.4943687	20.72318302	109.6633
2000	20	679.8381029	5.069891055	47.71845
4000	20	679.9105627	8.274977902	59.69599
6000	20	679.8211332	13.22082987	77.52425
8000	20	679.4001351	14.19905669	85.22195
10000	20	679.4781653	15.92595922	93.13813
12000	20	679.1914277	17.1634068	96.6569
14000	20	679.4277618	18.61654337	106.1991
16000	20	679.1519568	19.40959535	111.7822
18000	20	679.3101358	19.1487346	111.3787
20000	20	679.4943687	21.02686308	116.0487
2000	25	679.8381029	5.121880726	52.98989
4000	25	679.9105627	8.356318716	65.06978
6000	25	679.8211332	13.36282473	83.12557
8000	25	679.4001351	14.35263436	90.9181
10000	25	679.4781653	16.11150053	98.98583
12000	25	679.1914277	17.37639688	102.6086
14000	25	679.4277618	18.88228292	112.4218
16000	25	679.1519568	19.68910442	118.1027
18000	25	679.3101358	19.42493866	117.6971
20000	25	679.4943687	21.33033785	122.4348
2000	30	679.8381029	5.164043423	58.20971
4000	30	679.9105627	8.437659964	70.44363
6000	30	679.8211332	13.50497512	88.72912
8000	30	679.4001351	14.50999468	96.62962
10000	30	679.4781653	16.3189404	104.9247
12000	30	679.1914277	17.61031262	108.6516
14000	30	679.4277618	19.14942948	118.6545
16000	30	679.1519568	19.96861353	124.4231
18000	30	679.3101358	19.70114275	124.0155
20000	30	679.4943687	21.6338126	128.8209
2000	35	679.8381029	5.206206093	63.42954
4000	35	679.9105627	8.519001653	75.81757
6000	35	679.8211332	13.64774325	94.33662
8000	35	679.4001351	14.68354903	102.406
10000	35	679.4781653	16.54076836	110.9282
12000	35	679.1914277	17.85285732	114.7335
14000	35	679.4277618	19.4165761	124.8871
16000	35	679.1519568	20.24812266	130.7435
18000	35	679.3101358	19.97734686	130.3339

20000	35	679.4943687	21.93728733	135.207
2000	40	679.8381029	5.248368757	68.64936
4000	40	679.9105627	8.602026972	81.20129
6000	40	679.8211332	13.80122635	99.98072
8000	40	679.4001351	14.87505351	108.2604
10000	40	679.4781653	16.76507423	116.9428
12000	40	679.1914277	18.09541209	120.8154
14000	40	679.4277618	19.68372273	131.1198
16000	40	679.1519568	20.52763183	137.064
18000	40	679.3101358	20.25355099	136.6523
20000	40	679.4943687	22.24076205	141.5931

## TEZ İZİN FORMU / THESIS PERMISSION FORM

### PROGRAM / PROGRAM

Sürdürülebilir Çevre ve Enerji Sistemleri / Sustainable Environment and Energy Systems

Siyaset Bilimi ve Uluslararası İlişkiler / Political Science and International Relations

İngilizce Öğretmenliği / English Language Teaching

Elektrik Elektronik Mühendisliği / Electrical and Electronics Engineering

Bilgisayar Mühendisliği / Computer Engineering

Makina Mühendisliği / Mechanical Engineering

### YAZARIN / AUTHOR

**Soyadı** / Surname : ..... Odeh .....

**Adı** / Name : ..... Nemer .....

**Programı** / Program : ..... Electrical & Electronics Engineering .....

**TEZİN ADI / TITLE OF THE THESIS** (İngilizce / English) : Using The Neural Network Algorithms  
to Estimate the Thermal Stresses of Power Electronics Devices as Function of Design  
Parameters .....

**TEZİN TÜRÜ / DEGREE:**  **Yüksek Lisans / Master**  **Doktora / PhD**

1. **Tezin tamamı dünya çapında erişime açılacaktır.** / Release the entire work immediately for access worldwide.

2. **Tez iki yıl süreyle erişime kapalı olacaktır.** / Secure the entire work for patent and/or proprietary purposes for a period of two years. \*

3. **Tez altı ay süreyle erişime kapalı olacaktır.** / Secure the entire work for period of six months. \*

**Yazarın imzası / Author Signature** ..... **Tarih / Date** .....

**Tez Danışmanı / Thesis Advisor Full Name:** .....

**Tez Danışmanı İmzası / Thesis Advisor Signature:** .....

**Eş Danışmanı / Co-Advisor Full Name:** .....

**Eş Danışmanı İmzası / Co-Advisor Signature:** .....

**Program Koordinatörü / Program Coordinator Full Name:** .....

**Program Koordinatörü İmzası / Program Coordinator Signature:** .....